Title
Sialylation of lipooligosaccharides in Haemophilus: studies on cytidine 5'-monophosphate n-acetylneuraminc acid synthetase and sialyltransferase

Author
Samuels, Nicole Michelle

Publication Date
2000

Peer reviewed|Thesis/dissertation

Sialylation of Lipooligosaccharides in *Haemophilus*: Studies on Cytidine 5'-Monophosphate N-Acetylneuraminc Acid Synthetase and Sialyltransferase

by

Nicole Michelle Samuels

DISSERTATION

Submitted in partial satisfaction of the requirements for the degree of

DOCTOR OF PHILOSOPHY

in

Pharmaceutical Chemistry

in the

GRADUATE DIVISION

of the

UNIVERSITY OF CALIFORNIA SAN FRANCISCO

Date University Librarian

Degree Conferred: .....

Acknowledgments

First, I would like to thank my research advisor, Professor Brad Gibson, and co-advisor, Professor Susan Miller, for their advice, guidance and patience through my years at UCSF. I would like to extend a special thanks to Lisa Uyechi, Dr. Diane Wong, Lisa Kim-Shapiro, Dr. Kedan Lin, Van Hoang and Dr. Carla Washington for their support and for keeping me sane before my oral exam. I can not forget to thank Dr. Michael Tullius for providing technical information or assistance with lab equipment on numerous occasions as well as for being a good friend. If I could be like Mike! To my biggest cheerleader, thank you Dr. Herschel Wade for being a sounding board for ideas and source of encouragement, especially in the dark days. To the old Gibson group members (Dr. Nancy Phillips, Dr. Connie John, Dr. Susan Chen, Dr. Willie Melaugh and Jeff Engstrom) and the new members (Dr. Birgit Schilling, Dr. Ning Tang, Dr. Karoline Scheffler, Dr. YaJuan Chen and Dr. Dong-Hui Yi), thank you for your friendship and for putting up with my frantic states.

Thanks to our collaborators, Paul Jones and Professor Michael Apicella, for providing the many LOS samples from *H. influenzae*. I am very appreciative of the help I received from Dr. Denes Medzihradszky in the early days. I am also grateful for technical advice from Professor Arnie Falick and Dave Maltby in the mass spectrometry facility. I would also like to acknowledge PerSeptive Biosystems for the generous loan of the Voyager and Voyager-DE mass spectrometers to our laboratory.

I owe a debt of gratitude to my former science teachers, Mrs. Seifert, Dr. Montana, Dr. Weber and Dr. Nagel for reinforcing my scientific foundation, encouraging me to attend graduate school and above all, for being great mentors.

Last but not least, I thank my parents and grandparents for their love and support. I also thank Trish, Evie, Andrea and Pat for their friendship and for lending an ear when I needed to vent. And to the rest of my family, thank you for your words of encouragement.

Collaborations

Chapter 2 is based on a paper written in collaboration with Professor Susan M. Miller: Samuels, N. M., Gibson B. W., and Miller, S. M. (1999). Investigation of the Kinetic Mechanism of Cytidine 5'-Monophosphate N-Acetylneuraminic Acid Synthetase from *Haemophilus ducreyi* With New Insights On Rate-limiting Steps from Product Inhibition Analysis. *Biochemistry* 38 (19), 6195-6203. All the work in this chapter was performed by myself at UCSF.

Chapter 3 is based on a paper to be submitted for publication to *Protein Science*: Samuels, N. M. and Gibson, B. W. (2000). Probing the Active Site Topography and Ligand-Induced Conformational Changes by Limited Proteolysis and Amide Hydrogen Exchange of Cytidine 5'-Monophosphate N-acetylneuraminic Acid Synthetase. All the work in this chapter was performed by myself at UCSF.

Chapter 4 is based on research conducted in collaboration with Dr. Apicella's laboratory at the University of Iowa. The gene cloning and the construction of *H. influenzae* mutants was performed by Paul Jones, a graduate student in Dr. Apicella's laboratory. Paul also grew the bacterial cultures and isolated the bacterial lipooligosaccharides. The mass spectrometric analysis was performed by myself at UCSF.

Sialylation of Lipooligosaccharides in *Haemophilus*: Studies on the Cytidine 5'-Monophosphate N-Acetylneuraminic Acid Synthetase and Sialyltransferase

by

Nicole Michelle Samuels

ABSTRACT

Members of the *Haemophilus* genus synthesize structurally diverse populations lipooligosaccharide (LOS), a large number of which terminate with N-acetylneuraminic acid, commonly known as sialic acid. Although the presentation of similar surface structures has definitively been shown to contribute to the virulence of other mucosal pathogens, studies examining the genes and gene products involved in the biosynthesis of this glycolipid continue to investigate the role of LOS sialylation in the pathogenesis *Haemophilus* organisms.

Recent investigations revealed that *neuA*, which encodes a cytidine 5'-monophosphate N-acetylneuraminic acid (CMP-NeuAc) synthetase, is required for the incorporation of this acidic sugar into LOS manufactured by *Haemophilus ducreyi*, the infectious agent of chancroid. To gain further insights into the mechanism of sialic acid activation by a nucleotide monophosphate, the CMP-NeuAc synthetase from *H. ducreyi* was evaluated by steady state kinetic analysis. These studies demonstrated that the enzyme obeys a sequential ordered kinetic mechanism, where CTP is the first substrate bound and CMP-NeuAc is the second product released. To map the surface topography, CMP-NeuAc

synthetase was probed by limited proteolysis and amide hydrogen isotopic exchange. Several regions of the enzyme were dramatically protected from enzymatic cleavage and amide hydrogen exchange upon the binding of selected ligands and therefore inferred to reside in the active site or undergo ligand-induced changes in conformation.

The second gene required for LOS sialylation in *H. ducreyi*, *lst*, encodes a sialyltransferase, which has significant homology to the HI0871 (*siaA*) gene product in *Haemophilus influenzae*. To ascertain the function of *siaA* in *H. influenzae* type B, the most prevalent cause of childhood bacterial meningitis, the gene was deleted in two strains by insertional mutagenesis and the subsequent glycolipid products were analyzed by mass spectrometry. Isogenic mutant strains lacking a functional SiaA failed to produce sialylated LOS glycoforms present in the parental strains, however, retained the capacity to produce novel species terminating with one or more N-acetylneuraminic acids. *H. influenzae* was found to express a second sialyltransferase in addition to SiaA with different substrate specificity. In addition, the structures of several LOS glycoforms expressed in the parental strains were elucidated with electrospray tandem mass spectrometry.

List of Abbreviations

Abe	abequose
ACTH	adrenocorticotropic hormone
BSA	bovine serum albumin
CD4	T (thymus-derived) lymphocyte cell differentiation antigen
CDT	cytolethal distending toxin
CID	collision-induced dissociation
CMP-NeuAc	cytidine 5'-monophosphate N-acetylneuraminic acid
CTP	cytidine 5'-triphosphate
Da	daltons
DNA	deoxyribonucleic acid
D_2O	deuterium oxide
DTT	dithiothreitol
EDTA	ethylenediaminetetraacetic acid
ESI	electrospray ionization mass spectrometry
Fru	fructose
Gal	galactose
GalNAc	N-acetylgalactosamine
Glc	glucose
Glc1,6DP	α-D-glucose-1,6-diphosphate
GlcNAc	N-acetylglucosamine
Hep	L-*glycero*-D-*manno*-heptose or D-*glycero*-D-*manno*-heptose
Hex	hexose
HexNAc	N-acetylhexosamine
Hib	*Haemophilus influenzae* type b
HIV	Human Immunodeficiency Virus
HPLC	high performance liquid chromatography
kDa	kilo Daltons
KDO	2-keto-3-deoxy-D-manno-octulosonic acid
LC	liquid chromatography
LOS	lipooligosaccharide
LPS	lipopolysaccharide
M	molar
$(M+nH)^{n+}$	multiply charged protonated ion
MALDI-MS	matrix assisted laser desorption ionization mass spectrometry
Man	mannose
ManANAc	2-acetamido-2-deoxy-mannose uronic acid
ManNAc	N-acetylmannosamine

Me-O-NeuAc	2-O-methyl-β-D-N-acetylneuraminic
$MgCl_2$	magnesium chloride
MOMP	major outer membrane protein
MOPS	3-[N-morpholino]propanesulfonic acid
M_r	molar mass
MS	mass spectrometry
MS/MS	tandem mass spectrometry
m/z	mass to charge ratio
NAD^+	β-nicotinamide adenine dinucleotide
$NADP^+$	β-nicotinamide adenine dinucleotide phosphate
NADPH	β-nicotinamide adenine dinucleotide phosphate reduced form
NeuAc	N-acetylneuraminic acid, sialic acid
NMR	nuclear magnetic resonance spectroscopy
NTHi	nontypable *Haemophilus influenzae*
OD	optical density
O-LOS	O-deacylated lipooligosaccharide
OMP	outer-membrane protein
ORF	open reading frame
OS	oligosaccharide
P	phosphate
PAGE	polyacrylamide gel electrophoresis
PBS	phosphate buffered saline
PEA	phosphoethanolamine
PEP	phospho(enol)pyruvate
P_i	phosphate
PP_i	pyrophosphate
PPEA	2-aminoethyl diphosphate
PSD	post-source decay
RCF	relative centrifugal force
Rha	rhamnose
Rib	ribose
RPM	revolutions per minute
SDS	sodium dodecyl sulfate
TFA	trifluoroacetic acid
TOF	time-of-flight mass analyzer
Tricine	N-(tris-(hydroxymethyl)-methyl)-glycine
Tris	tris(hydroxymethyl)aminomethane
UDPG	uridine 5'-diphosphoglucose
UV	ultraviolet light

Table of Contents

List of Tables

List Of Figures

Chapter 3.

Chapter 4.

CHAPTER 1.

Overview of Virulence Factors in *Haemophilus* and Sialylation of Lipooligosaccharides

1.1 HAEMOPHILUS

Members of the *Haemophilus* genus are small, pleomorphic, Gram-negative coccobacilli with fastidious growth requirements (Kilian 1985). By definition, the species of *Haemophilus* (blood-loving) require hemin (factor X), nicotinamide adenine dinucleotide (factor V) or both for growth in culture, however this requirement is not restricted to this genus. As members of the *Pasteurellaceae* family, species of *Haemophilus* colonize the mucosal surface of the respiratory and genital tracts, causing local and systemic disease. The proceeding discussion will focus on two strict human pathogens found among this genus, *Haemophilus ducreyi* and *Haemophilus influenzae*.

1.1.1 Haemophilus ducreyi

Haemophilus ducreyi was originally described as a compact, streptobacillary rod with rounded ends by Auguste Ducrey in 1889 (Ducreyi 1889). The pathogen was then identified as the etiological agent of the venereal disease, chancroid or soft chancre, which is characterized by cutaneous erosion or ulceration(Morse 1989). Due to the inability to culture the organism in vitro, serial cutaneous inoculations of the forearms of infected individuals were performed to isolate the infectious agent (Ducreyi 1889). A major advance in the ability to directly isolate *H. ducreyi* from lesions was the development of selective medium consisting of an enriched chocolate agar containing vancomycin to inhibit the

growth of Gram-positive bacteria (Hammond et al. 1978; Hannah and Greenwood 1982). Although various medium formulations have been used, it is generally accepted that GC agar base (GC-HgS) containing hemoglobin, fetal bovine serum, Iso Vitale X and vancomycin combined with Mueller-Hinton agar (MH-HB) containing chocolatized horse blood, Iso Vitale X and vancomycin is optimal for the isolation of *H. ducreyi* from clinical specimens (Trees and Morse 1995).

Chancroid is one of several genital ulcerative diseases common throughout the world, including syphilis, genital herpes, lymphogranuloma venereum and donovanosis (Brown et al. 1999). Although chancroid is an uncommon sexually transmitted disease in the United States, the disease is particularly common in African, Asian, and Latin American countries (Ortiz-Zepeda et al. 1994). Chancroid has received renewed attention following the association between genital ulcer diseases and the transmission of the human immunodeficiency virus (HIV) (Dickerson et al. 1996; Wasserheit 1992). Most of the data identifying genital ulcerative disease as a significant risk factor in the transmission of HIV come from studies performed in Zaire and Kenya, where chancroid is the prevalent cause of genital ulcer disease (Jessamine and Ronald 1990; Plummer et al. 1985). Although not fully understood, one mechanism by which chancroid is proposed to enhance the dissemination and transmission of HIV is by increased shedding of the virus through the ulcer (Kreiss et al. 1989; Plummer et al. 1990). In the second, the ulcer may serve as a portal for acquiring the virus, as ulceration disrupts the natural epithelial barriers and recruits HIV-susceptible cells, CD4 T lymphocytes (Spinola et al. 1996). The correlation between HIV and genital ulcer disease underscores the importance of the prevention and effective treatment of chancroid. Although *H. ducreyi* is vulnerable to various classes of antibiotics, antimicrobial resistance to tetracycline, ampicillin, and amoxicillin have been reported worldwide (Schmid 1997; Trees and Morse 1995).

1.1.2 Haemophilus influenzae

Haemophilus influenzae is a non-motile facultative anaerobe, characterized by an absolute requirement for supplemental NAD^+ and a source of heme for growth under aerobic conditions. Despite the fact that strains of *H. influenzae* are metabolically and morphologically similar, the clinical symptoms evoked by this pathogen are very distinct and dependent on the presence or absence of capsular polysaccharides. *H. influenzae* is subdivided into encapsulated (typable) and unencapsulated (nontypable) groups. Typable isolates bear capsules of one of six structurally and antigenically distinct compositions, denoted as types a-f (Kroll and Booy 1996).

Although both typable and nontypable *H. influenzae* cause infection, the presence of capsular polysaccharides in general renders the pathogen more invasive and apt to cause systemic disease, in particular *H. influenzae* type b (Hib) (Lee 1987; Parke 1987). Historically, Hib was the principal agent of childhood bacterial meningitis, in addition to causing other serious diseases such as epiglotitis, septic arthritis, and pneumonia. In the past decade, the advent of conjugated vaccines, partially composed of the type b capsular polysaccharide, has led to a substantial decline in the incidence of childhood bacterial meningitis (Peltola 2000). However, Hib vaccines do not protect against nontypable strains of *H. influenzae*.

Various strains of nontypable *H. influenzae* (NTHi) are part of the normal flora of the upper respiratory tract in humans (Murphy and Apicella 1987; Rao et al. 1999). Albeit NTHi isolates are generally less virulent and rarely associated with systemic infection, these pathogens remain the most common cause of acute otitis media (Giebink 1989; Roberts et al. 1986). NTHi strains also account for diseases of the upper respiratory system such as community acquired pneumonia (Murphy and Apicella 1987), acute or chronic sinusitis and the exacerbation of chronic bronchitis (Murphy and Sethi 1992). NTHi strains are vulnerable to ampicillin, however, resistance to β-lactam containing antibiotics is becoming

increasingly common (Barry et al. 1994). As pneumonia due to NTHi infections remains a significant cause of childhood mortality and morbidity in developing nations, the design of effective vaccines against these pathogens would not only reduce the incidence of infection but also eliminate the sole dependence on antibiotic therapies (Kyd and Cripps 1999); (Monto 1989).

1.2 TISSUE CULTURE AND ANIMAL MODELS

To evaluate the initial step in the pathogenesis of *H. influenzae* infections, host-pathogen interactions involved in bacterial colonization have been investigated *in vitro* using various cell types from respiratory tissues including cultured lung cells (Van Schilfgaarde et al. 1995), bronchial epithelial cells (Riise et al. 1994), and nasopharyngeal and buccal epithelial cells (Harada et al. 1990). Factors influencing the capacity of *H. influenzae* to adhere to and damage the epithelium of an intact respiratory mucosa have also been examined in human organ cultures, *in vitro* model systems that simulate physiological conditions better (Jackson et al. 1996; Read et al. 1991). The establishment of animal models of *H. influenzae* infections has great utility in assessing the virulence factors essential for pathogenesis of and potential protective ability of candidate vaccines against pulmonary infection, otitis media, and meningitidis. For studying host-pathogen interactions in the lower respiratory tract, mice and rats have been used to evaluate clearance of NTHi from the lungs (Foxwell et al. 1998). Whereas the chinchilla model of otitis media is most frequently used for studying the progression of middle and inner ear inflammation by virtue of its human-like auditory capabilities and low susceptibility to naturally occurring middle ear infections that are common to guinea pigs and rabbits (Giebink 1999). Experimental meningitis has been produced in mice, rabbits and primates, however, infant rats have become the most commonly used animal model for studying early pathogenic

events of bacterial meningitidis, including nasopharyngeal colonization, mucosal invasion, intravascular survival and meningeal invasion (Koedel and Pfister 1999).

A variety of cell lines have been employed to evaluate the initial events in the pathogenesis of chancroid, interactions of *H. ducreyi* with the outer and inner layers of the skin, the epidermis and dermis respectively. The pathogen has been shown to attach to and invade epidermal cells from human foreskins (Totten et al. 1994; Trees and Morse 1995) and more specifically, shown to adhere to keratinocytes, the principle cell type of the epidermis (Brentjens et al. 1994). To elicit ulcer formation, *H. ducreyi* ultimately gains access to the dermal layer of the skin; the nature of this host-pathogen interaction has been investigated *in vitro* using human foreskin fibroblasts, the principle cell type of the dermis (Lammel et al. 1993). Although tissue culture assays with cells of genital origin allow for the evaluation of factors affecting host cell adherence and invasion, intradermal animal models utilizing rabbits and mice have been frequently used to evaluate factors affecting abscess formation and ulceration *in vivo* (Trees and Morse 1995). Contrary to observations for the rabbit model, pustules and ulcers similar to those seen in human infections have been reported for the mouse model, however more importantly, the lesions produced in both animal models were not produced specifically by viable organisms (Campagnari et al. 1991). In an effort to develop a better animal model of *H. ducreyi* infections, Purcell described a temperature dependent rabbit model for experimental chancroid, where rabbits are housed at lower temperatures (15 to 17 °C) to satisfy the requirements of a viable bacterial inoculum and bacterial replication for necrotic formation (Purcell et al. 1991). A major limitation of the intradermal animal injection systems is inadvertent delivery of bacteria into the dermis and subcutaneous tissues, which bypasses the presumed natural portal of entry through the breaks in the epithelium. A safe and reliable model of *H. ducreyi* infection in humans was reported whereby volunteers are inoculated using a multitest applicator on abraded skin of the upper arm, which introduces viable bacteria to both the epidermis and dermis (Spinola et al. 1994; Spinola et al. 1996). Subjects

developed papular lesions that evolved into pustules resembling the natural disease, from which viable bacteria were isolated. The human challenge model should prove useful in studying interactions of *H. ducreyi* with human skin, however, pustule formation is not allowed to progress to painful ulcers in the subjects and therefore these types of studies are limited to the evaluation of early stages of chancroid pathogenesis.

1.3 VIRULENCE FACTORS

Microorganisms possess virulence factors which contribute to their pathogenicity or the ability to cause disease. Generally, multiple virulence factors are required by pathogenic bacteria to attach to host cells, invade target cells, evade host defenses and damage host tissues (Jacques and Paradis 1998). A popular strategy for assessing the roles of proposed virulence determinants in bacterial pathogenesis has been the generation of mutant strains by the random or directed insertion of transposable elements into genes under investigation. To dissect the contributions of inactivated gene products, the variants are then evaluated using *in vivo* and *in vitro* model systems to permit the correlation between the loss or gain of a specific function with the virulence of the organism. Additional insights into those factors essential for the virulence of *Haemophilus* pathogens may provide novel targets for chemotherapeutic intervention.

1.3.1 Pili

Adhesion to host surfaces, an initial event of bacterial colonization, is governed by specific interactions between adhesins presented on the surface of the pathogen and the complementary host cell ligand (Jacques and Paradis 1998). Members of the *Haemophilus* genus have evolved pili (fimbriae), or filamentous surface appendages, which facilitate the association of bacteria with epithelial surfaces and therefore prevent the removal of the

organism by natural cleansing mechanisms (Gilsdorf et al. 1997; Stull et al. 1984). Pili have been shown to mediate the adherence of *H. influenzae* to buccal and bronchial epithelial cells, but not to human nasal epithelial cells or human tracheal fibroblasts, suggesting that only certain respiratory cell types possess receptors for pili (Gilsdorf et al. 1996). Through the employment of gene deletion methods, the *hifA*, *hifE* and *hifF* genes of the Hib fimbrial gene cluster were shown to be required for the adherence of the bacterium to oropharyngeal epithelial cells and human erythrocytes carrying the blood group AnWj antigen, the proposed host receptor for fimbriae (Van Alphen et al. 1991; Van Ham et al. 1995). The *hifA* gene of *H. influenzae* encodes the major structural unit of the pilus and shows significant sequence similarity to the major structural subunits of pili expressed by *E. coli*, *K. pneumoniae*, *B. pertussis* and *S. marcescens* (Gilsdorf et al. 1997). The mutagenesis of *hifA* was shown to abrogate the expression of the pilus (St. Geme et al. 1996) and significantly diminish adherence to human buccal epithelial cells and nasal colonization of yearling rhesus monkeys by isogenic non-piliated mutants (Weber et al. 1991).

The *H. ducreyi* pili was shown to be predominantly composed of a novel class of pilin monomer sharing homology with *E. coli* Dps and *T. pallidum* antigen TpF1 or 4D (Brentjens et al. 1996). An isogenic mutant strain of *H ducreyi* 35000HP lacking a functional *ftpA*, the gene encoding the 24 kDa pilin monomer, bound to laminin, collagen and fibronectin as well as the parental strains (Bauer and Spinola 1999). The authors concluded that the major pilin subunit was not required for the adherence to extracellular matrix proteins, although a contributing role in conjunction with other adhesins could not be ruled out.

1.3.2 Outer Membrane Proteins

The outer membranes of Gram-negative bacteria are impregnated with proteins, a number of which are pore-forming transmembrane channels called porins. Among the few outer-membrane proteins (OMPs) characterized from *H. ducreyi* are a novel 28 kDa lipoprotein (Hiltke et al. 1996) and an 18 kDa protein sharing extensive homology with P6 from *H. influenzae* and PAL from *E. coli* (Spinola et al. 1996). The major outer membrane protein (MOMP) from *H. ducreyi*, a 44 kDa species, is homologous to OmpA proteins from members of the *Enterobacteriaceae*, *Neisseriaceae* and *Pasteurellaceae* families (Klesney-Tait et al. 1997; Spinola et al. 1993; Weiser and Gotschlich 1991). Disruption of the *momp* gene rendered isogenic mutants of *H. ducreyi* susceptible to normal human serum in contrast to the parental strain, illustrating at least one mechanism by which MOMP contributes to the virulence of *H. ducreyi* (Hiltke et al. 1999). However, recent studies revealed that MOMP is not required for pustule formation by *H. ducreyi* in the human model of infection (Throm et al. 2000).

The outer membrane of NTHi is composed of approximately twenty proteins, with four to six proteins accounting for most of the content (Kyd and Cripps 1999). Although there is strain to strain variability in the OMP composition, several proteins have been proposed as potential vaccine antigens. Among the highly conserved leading candidates are P6, a 16 kDa lipoprotein (Nelson et al. 1991), P4, a 28-30 kDa surface-exposed lipoprotein (Green et al. 1991), protein D, a 42 kDa protein with an affinity for binding IgD (Akkoyunlu et al. 1991) and a group of high molecular weight proteins ranging in mass from 120 to 125 kDa (Barenkamp and St. Geme 1996). Recently, the immunization of rats with recombinant OMP26 was found to significantly enhance bacterial clearance following pulmonary challenge with *H. influenzae*, demonstrating this 26 kDa outer membrane protein is a suitable vaccine candidate against NTHi infection (Kyd and Cripps 1998).

1.3.3 Lipooligosaccharides (LPS) and Lipopolysaccharides (LOS)

Unlike eukaryotic cells and Gram-positive bacteria, Gram-negative bacteria are encompassed by an outer membrane containing lipopolysaccharide (LPS) (Raetz 1990), (Rietschel et al. 1994). This amphipathic lipid is the most abundant component of the outer membrane and serves as a barrier to heavy metals, lipid-disrupting agents and lytic enzymes. In general, LPS from enteric bacteria are comprised of a membrane-anchoring lipid A moiety and a relatively conserved inner core containing heptose and KDO (Raetz 1990) (Figure 1.1). Diversity of LPS structures is achieved by varying the composition and number of hexoses in the outer core and the number and types of O-antigen repeating units at the non-reducing terminus (Figure 1.1). Numerous endotoxic activities such as mitogenicity, pyrogenicity, platelet aggregation, and cytokine activation have been attributed to enterobacterial LPS, where the lipid A moiety is responsible for many of these responses (Westphal et al. 1983). *H. ducreyi* and *H. influenzae* are characterized by the presence of truncated LPS or lipooligosaccharides (LOS), which are similar to those produced by other mucosal pathogens. In general, the overall architectures are similar. However, LOS lack O-antigens and tend to have more intricate branching patterns compared to LPS (Griffiss et al. 1988; Hood et al. 1999; Kahler and Stephens 1998; Mandrell and Apicella 1993). The structural features of LOS will be discussed in further detail in the proceeding section.

Biological studies have supported the functional role of LOS as a determinant for virulence in the pathogenesis of *H. ducreyi* and *H. influenzae*. Besides inducing intradermal abscesses in the rabbit model (Campagnari et al. 1991), LOS has also been shown to mediate the adherence to human foreskin fibroblasts and keratinocytes and the invasion of keratinocytes by *H. ducreyi* (Alfa and DeGagne 1997; Gibson et al. 1997). Furthermore, LOS from virulent strains of *H. ducreyi* were found to have a higher hexose:KDO ratio compared to avirulent strains (Odumeru et al. 1987), the composition of which was found to dictate the susceptibility of *H. ducreyi* to killing by complement-

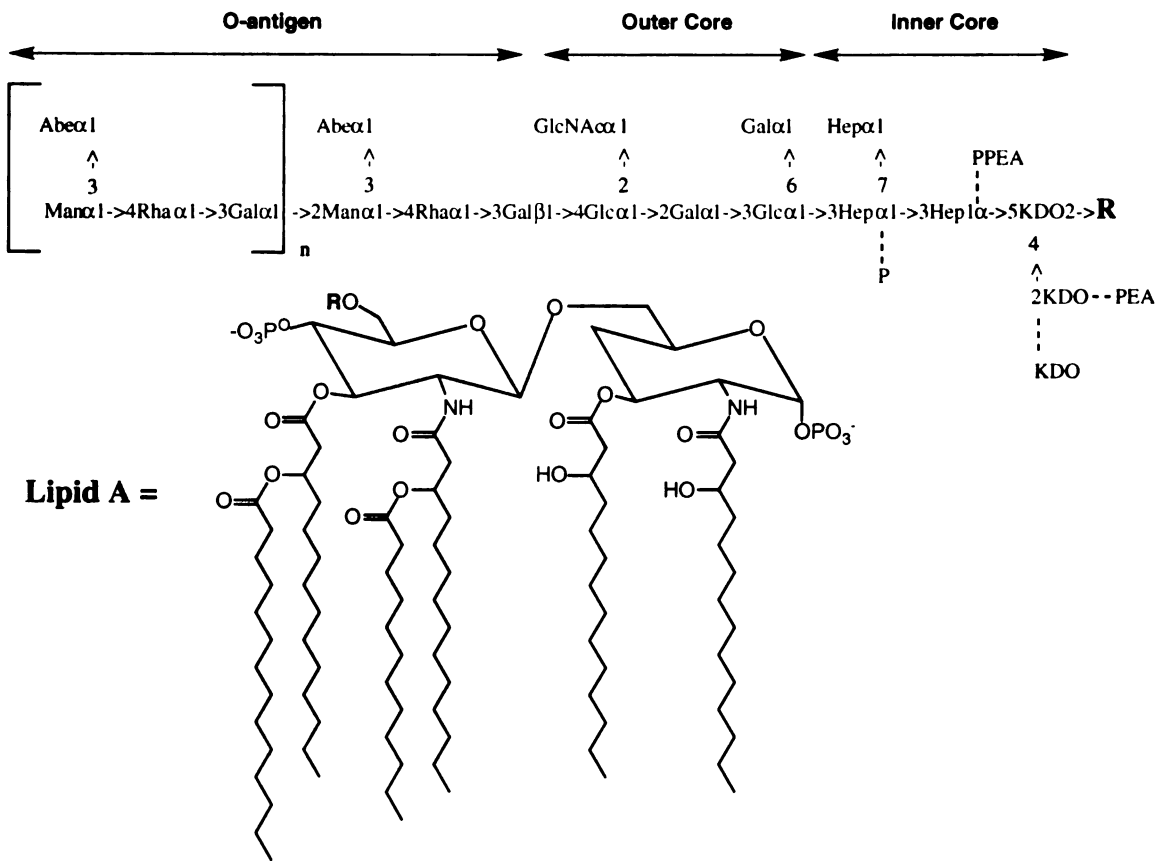

Figure 1.1 Structure of LPS from *Salmonella typhimurium*. Structure containing a representative O-antigen (type B) and one of several possible Lipid A forms.

mediated activities of human serum (Odumeru et al. 1985). The relative size of LOS was also found to correlate with the virulence of Hib, where parental strains possessing smaller glycoforms produced bacteremia at very low frequencies while isogenic variants possessing larger glycoforms were significantly more virulent (Kimura and Hansen 1986). Moreover, differences in the susceptibility of Hib to complement-mediated bactericidal activity of normal rat serum were associated with differences in the electrophoretic mobility of isolated LOS on SDS-polyacrylamide gels (Gilsdorf and Ferrieri 1986). These data indicate LOS may facilitate bacterial adhesion to host cells, tissue destruction and the evasion of host immune defenses, thereby playing multiple roles at various stages in the pathogenesis of *Haemophilus* species.

1.3.4 Hemolysin

One putative virulence factor in the pathogenesis of *H. ducreyi* is a secreted hemolysin (Holland et al. 1990; Totten et al. 1995). The expression of hemolysin in *H. ducreyi* requires the transcription of two adjacent genes, *hhdA* and *hhdB*, which presumably encode the secretion/activation protein (HhdB) and the structural hemolysin protein (HhdA), which share homology with the family of pore-forming toxins including hemolysins from *S. marcescens*, *E. tarda* and *P. mirabilis* (Braun et al. 1992; Palmer and Munson 1995). These cytolysins are known to lyse eukaryotic cells by producing defined pores in the plasma membrane and represent potent weapons with which invading microbes damage the host cells. Although the *H. ducreyi* cytolysin has been designated a hemolysin due to its hemolytic activity towards horse erythrocytes, human erythrocytes are quite resistant to hemolysis and therefore do not appear to be the primary target (Palmer et al. 1994; Palmer and Munson 1995). In functional studies, hemolysin was found to exhibit toxicity against cell types relevant to chancroid infections including human foreskin epithelial cells, human foreskin fibroblasts, macrophages, T (thymus-derived) cells and B (bursa-derived) cells

(Alfa et al. 1996; Palmer et al. 1996; Wood et al. 1999). Furthermore, hemolysin expression was demonstrated to enhance the invasion of human epithelial cells by *H. ducreyi* 10-fold compared to a control strain. Recently, human subjects were inoculated with an isogenic mutant constructed by deleting the *hhdB* gene to evaluate the role of hemolysin *in vivo* (Palmer et al. 1998). In this study it was concluded that hemolysin does not play a role in pustule formation or the ability of *H. ducreyi* to replicate in lesions. However due to the limitations of this model system, the role of hemolysin in later stages such as ulceration, immune system avoidance and transmission of infection could not be evaluated .

1.3.5 Cytotoxin

Separate from its hemolytic activity, *H. ducreyi* also produces a cytotoxin shown to have a cytopathic effect on human T (thymus-derived) cells and several epithelial cell lines (Gelfanova et al. 1999; Purven and Lagergard 1992). The soluble cytotoxic activity in *H. ducreyi* culture supernatant was demonstrated to be the result of the activity of a homolog of the cytolethal distending toxin (CDT) expressed by enteric bacteria (Cope et al. 1997). The cytotoxin is chromosomally encoded by three genes, *cdtA*, *cdtB*, and *cdtC*, the products of which possess 24-51% identity to the CdtABC proteins from *E. coli*. As monoclonal antibodies to the *H. ducreyi* CdtC protein were shown to neutralize CDT activity *in vitro*, the *cdtC* gene product was concluded to be responsible for the expression of the cytotoxic activity. In recent studies, culture supernatant from CdtC deficient mutants failed to kill both Hela epithelial cells and HaCaT keratinocytes (Stevens et al. 1999). Nonetheless, the isogenic mutant was as virulent as the wild type strain as judged by the retained capacity to cause necrotic lesions and survive in the skin of rabbits. The authors concluded that the expression of CDT could be involved in the development of ulcers, however, may not be essential for the survival of *H. ducreyi* in the rabbit model.

1.3.6 Capsular Polysaccharides

The virulence factor of prime importance to *H. influenzae* is the presence of a capsule. Of the six structurally and antigenically distinct forms, types a, b, c and f contain phosphodiester linkages while types d and e contain mannuronic acid (Eagan et al. 1982; Jennings 1983) (Table 1.1). All capsular polysaccharides are high molecular weight polymers of linear repeating disaccharides, with the exception of type e. In general, capsular polysaccharides confer resistance to complement-dependent killing and phagocytosis, thereby providing a selective advantage for bacteria in the bloodstream (Moxon and Kroll 1990). Although less frequent, various encapsulated strains of *H. influenzae* have demonstrated the potential to cause systemic infection in rats, however, the presence of type b capsular polysaccharides was required for invasiveness and the induction of persistent bacteremia (Moxon and Vaughn 1981). Moreover, type b capsular polymer has been shown to increase the virulence by rendering the pathogen resistant to clearance from the bloodstream in rats (Weller et al. 1977). Therefore, the expression of the polyribosylribitol phosphate (PRP) capsule provides Hib unique virulence characteristics and is an important determinant for the ability to colonize the nasopharynx, disseminate within the blood stream and invade the central nervous system.

1.4 LIPOOLIGOSACCHARIDES (LOS)

1.4.1 Lipooligosaccharide (LOS) Structure

In an effort to further understand functional contribution of LOS to the virulence of mucosal pathogens, LOS from numerous wild type sources have been structurally characterized by mass spectrometric, multidimensional NMR and chemical analyses

Table 1.1 Structure of *Haemophilus influenzae* capsular polysaccharides

Type	Composition
a	->4) -β- Glc1 -> 4-ribitol -5- (phosphate->
b	->3) -β- Rib1 -> 1-ribitol -5- (phosphate->
c	->4) -β- GlcNAc1 -> 3αGal -1- (phosphate-> 3 ^ | OAc
d	->4)β-GlcNAc1->3βManANAc-(1-> 6 ^ | R R= L-Serine L-Alanine L-Threonine
e	->3)β-GlcNAc1->4βManANAc-(1->
e	->3)β-GlcNAc1->4βManANAc-(1-> 3 ^ | 2βFru
f	->3)β-GalNAc1->4αGalNAc-(1-phosphate-> 3 ^ | OAc

Ribose (Rib) and fructose (Fru) are in the furanose ring form; glucose (Glc), galactose (Gal), N-acetylglucosamine (GlcNAc), and 2-acetamido-2-deoxy-mannose uronic acid (ManANAc) are in pyranose form.

(Cotter et al. 1987; Gibson et al. 1997; Griffiss et al. 1988; Kahler and Stephens 1998; Kulshin et al. 1992; Rahman, 1998; Wakarchuk et al. 1998) (Figure 1.2). Generally, *Haemophilus* and *Neisseria* LOS consist of a fairly conserved lipid A anchor consisting of a hexa-acyl diphosphoryl-N-acetylglucosamine disaccharide modified by O-and N-linked fatty acids. A complex oligosaccharide, the second portion of the LOS molecule, is comprised of a heptose and KDO containing core, from which variable branches extend. Between separate genera, the number of heptose and KDO monosaccharides vary slightly, as well as the degree of substitution by phosphate, phosphoethanolamine (PEA), 2-aminoethyl diphosphate (PPEA), acetate and phosphorylcholine. The PEA and phosphate content have been demonstrated to fluctuate for a single strain under different growth conditions. Although phosphorylcholine has been detected on the LOS from multiple strains of *H. influenzae*, this modification has not yet been observed in *H. ducreyi*, *N. meningitidis* and *N. gonorrhoeae* (Kolberg et al. 1997).

Haemophilus and *Neisseria* pathogens are characterized by the capacity to decorate the surface of their outer membranes with heterogeneous populations of LOS (Gibson et al. 1993; Hood et al. 1999; Mandrell and Apicella 1993; Melaugh et al. 1994; Pavliak et al. 1993; Phillips et al. 1992; Phillips et al. 1993; Rahman et al. 1998; Schweda et al. 1995; Wakarchuk et al. 1998; Yamasaki et al. 1991; Yamasaki et al. 1993) (Figure 1.3). For the most part, structural diversity is achieved by varying the composition of the oligosaccharide branches, which extends 2 to 7 sugars from a core heptose. In addition, these mucosal pathogens produce an array of LOS structures by varying the number of oligosaccharide branches and assembling truncated biosynthetic intermediates. Mass spectrometric analysis of a collection of LOS from nontypable and typable strains of *H. influenzae* highlights the diversity achieved by extending the branch oligosaccharides from a single or all 3 heptoses contained within the core. Although all structures from *H. ducreyi* determined to date contain a one oligosaccharide branch emanating from a single core heptose, multiply branched LOS have also been observed in species from *Neisseria*. Characterization of the

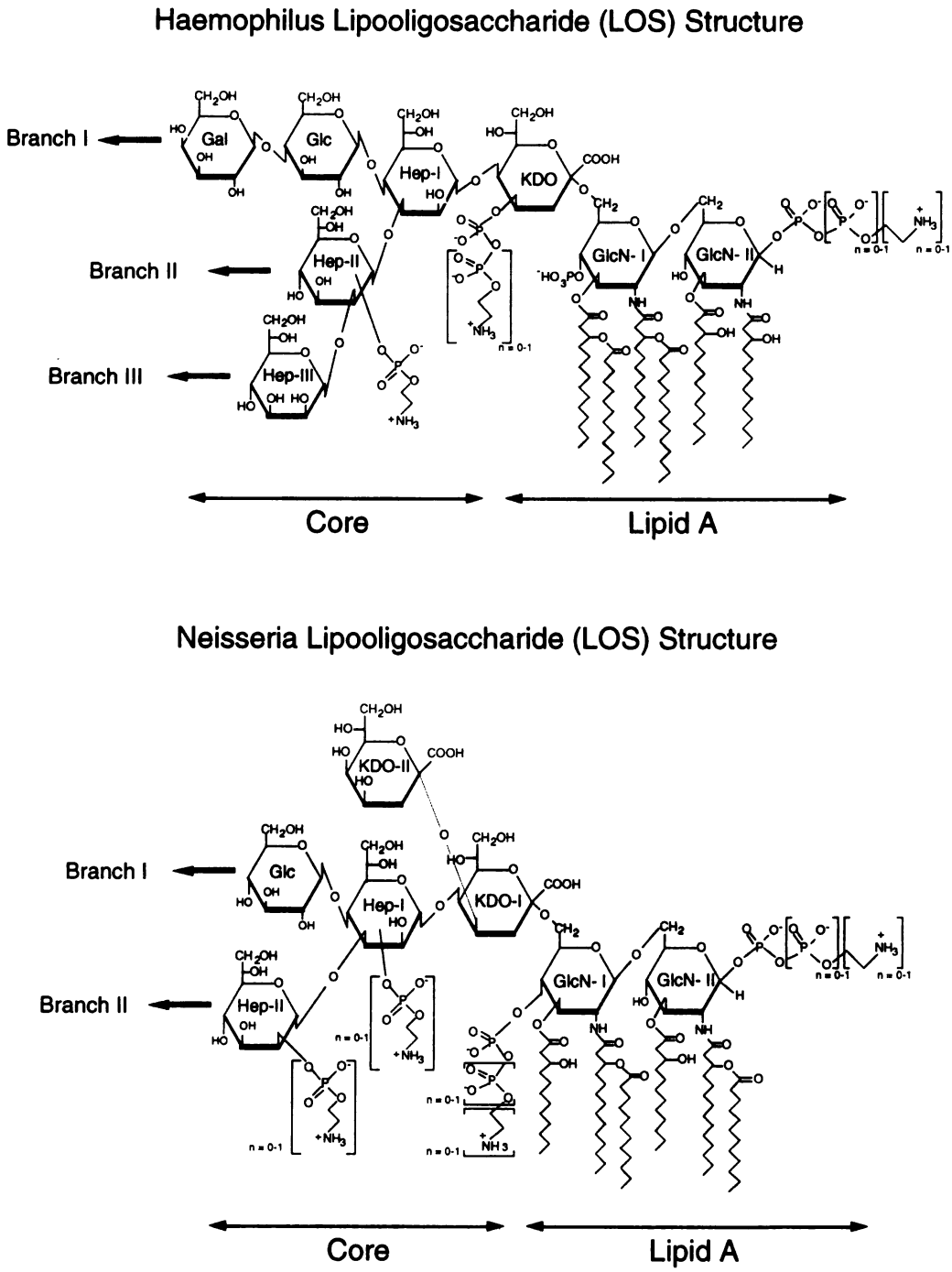

Figure 1.2 General structure of LOS from *Haemophilus* and *Neisseria.* Arrows indicate positions of further oligosaccharide branch extensions.

Figure 1.3 Structures of LOS from various strains of *N. gonorrhoeae*, *N. meningitidis*, *H. ducreyi* and *H. influenzae*

N. gonorrhoeae

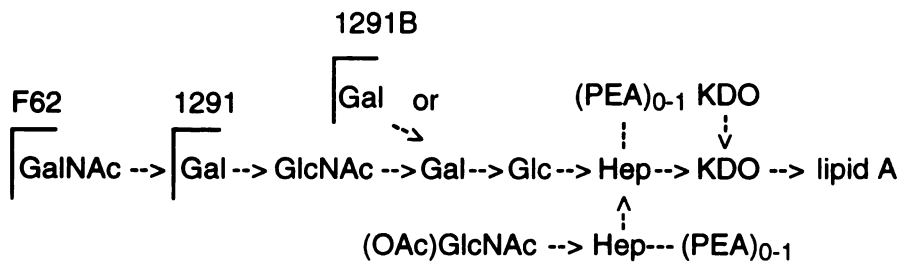

N. meningitidis

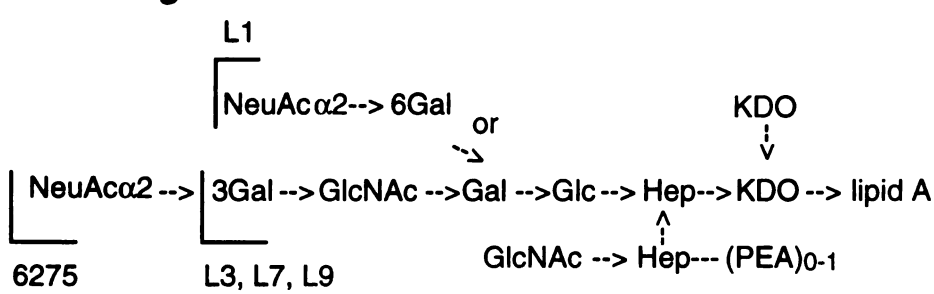

H. ducreyi

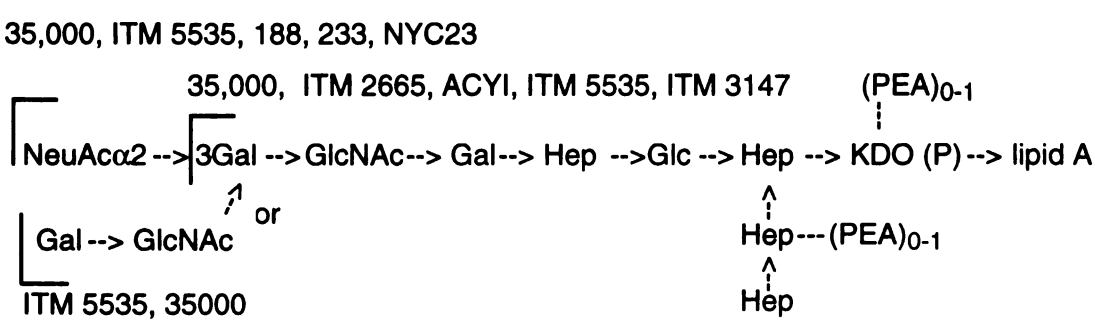

H. influenzae

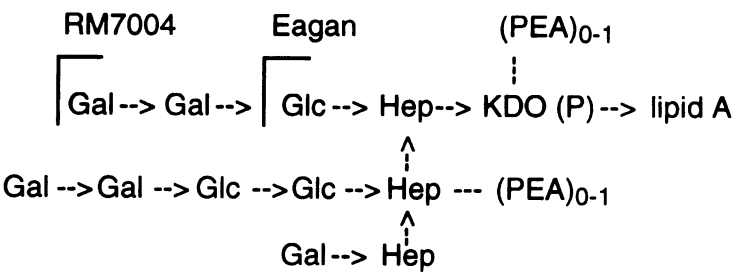

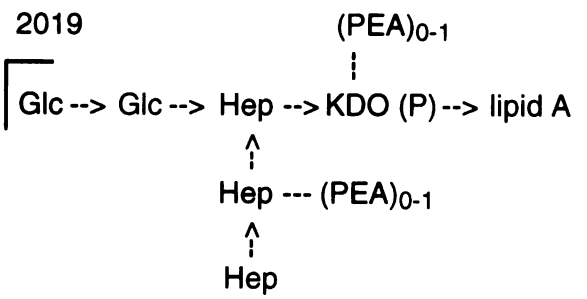

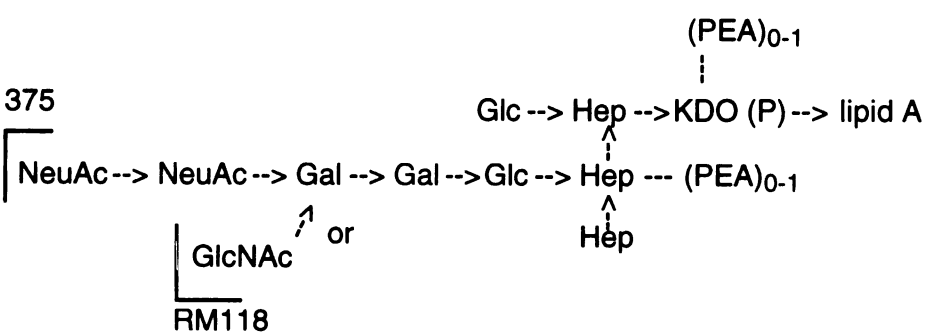

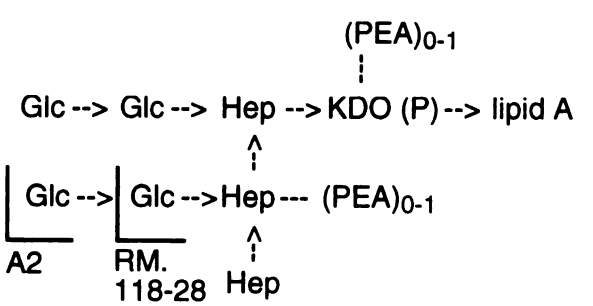

LOS from *H. ducreyi* strain 35000 revealed a heterogeneous population comprised of truncated and elongated analogs of the major glycoform (Melaugh et al. 1992; Melaugh et al. 1994). The mature glycoform was found to be modified with an N-acetylneuraminic acid, where the non-reducing N-acetyllactosamine was identified as the acceptor site. LOS terminating with N-acetylneuraminyl-N-acetyllactosamine have also been detected in *N. meningitidis*, *H. influenzae* and *N. gonorrhoeae* (Mandrell et al. 1990; Mandrell et al. 1992; Melaugh et al. 1996; Pavliak et al. 1993; Phillips et al. 1993; Yamasaki et al. 1993). Furthermore, LOS structures from *H. ducreyi* strain 35000 were derived from competing biosynthetic pathways which extended the major glycoform with an N-acetylneuraminic acid or an additional N-acetyllactosamine (Melaugh et al. 1994).

1.4.2 Phase Variation

Inter- and intra-strain heterogeneity not only reflects the generation of incomplete products along the LOS biosynthetic pathway but, also genetically controlled variation in some species of *Haemophilus* and *Neisseria*. In *H. influenzae*, a major influence on LOS heterogeneity is a specific genetic mechanism that promotes the gain and loss of antigenic epitopes or phase variation, through contingency genes (Moxon et al. 1994). Three loci required for phase variation of specific LOS oligosaccharide epitopes, *lic1*, *lic2*, and *lic3*, have been identified in *H. influenzae* (Weiser et al. 1990). These chromosomal loci are characterized by repeats of the tetranucleotide 5'-CAAT-3' in the first open reading frame where the loss or gain of copies of this repeat during replication results in frame-shifting of the reading frame with respect to the start codons, switching gene expression on or off. Although the function of *lic3* is unknown, *lic1* and *lic2* are responsible for the expression of phosphorylcholine (Weiser et al. 1989; Weiser et al. 1997) and the digalactoside [αGal(1-4)βGal] epitopes (High et al. 1993; Weiser et al. 1990) in LOS, respectively. The addition of phosphorylcholine to the LOS was shown to correlate with an increase in the pathogen's

ability to persist on mucosal surfaces, whereas loss of the phenotype correlated with the ability to cause invasive infection by evading C-reactive protein mediated activation of complement (Weiser et al. 1998). Furthermore, the presence of the digalactoside on the LOS, an epitope also found on human glycolipids, conferred resistance to killing by naturally acquired antibodies and complement present in human serum (Weiser and Pan 1998). Therefore, phase variation of the LOS provides *H. influenzae* a reversible mechanism to present distinct oligosaccharide epitopes in an effort to adapt to different host environments during certain stages of infection.

1.4.3 Biosynthetic Genes and Gene Products

In an effort to evaluate the contribution of LOS to the virulence of the *Haemophilus* species, various LOS biosynthetic genes have been inactivated by insertional deletion methods to produce isogenic mutants expressing modified structures. In the NTHi strain 2019, mutation of the *htrB* gene encoding a lipid A acyltransferase results in bacteria expressing a mixture of the major wild type glycoform plus one to two additional hexoses, as well as a lipid A moiety lacking one or two myristic acids and variable levels of substitution with PEA (Lee et al. 1995). While, disruption of the *rfaD* gene encoding an ADP-L-*glycero*-D-*manno*-heptose-6-epimerase led to the production of LOS lacking the entire oligosaccharide portion emanating from the core KDO (Lee et al. 1995; Nichols et al. 1997). Neither mutation affected the capacity of NTHi to colonize or persist in the nasopharynx, initial steps in otitis media pathogenesis, after intranasal challenge of chinchillas. However, in studies examining effects on the later stages of the disease course and its inner ear sequelae following TB injection of bacteria into the inner ear, the disruption of these genes rendered the LOS-deficient mutants less virulent as demonstrated by larger dose requirements for the induction of otitis media and the lack of sustained multiplication in the middle ear (DeMaria et al. 1997).

In similar studies, the effects of disrupting the *losb* gene encoding a D-*glycero*-D-*manno*-heptosyltransferase in *H. ducreyi* strain 35000 were assessed. The production of LOS terminating with single glucose attached to the innermost core heptose resulted in isogenic mutants that exhibited a significant reduction in adherence to and invasion of primary human keratinocytes (Gibson et al. 1997). However, the expression of this truncated LOS did not affect the ability of the *losb* mutant to bind to extracellular matrix proteins (Bauer et al. 1998; Spinola et al. 1990) and resist the bactericidal activity of normal human serum (Hiltke et al. 1999) when compared to the parental strains. Furthermore, the *losb* mutant proved to be as virulent as the wild type by retaining the capacity to produce dermal lesions in rabbits (Stevens et al. 1997) and pustules in human subjects (Young et al. 1999). The role of the full-length LOS was further evaluated following the disruption of genes encoding a phospho-heptose isomerase (*gmhA*) (Bauer et al. 1998) and heptosyltransferase II (*waaF*) (Bauer et al. 1999). The *waaF* and *gmhA* mutants produce even deeper truncations of the LOS, expressing structures consisting of lipid A, KDO and three core heptoses or just lipid A and KDO, respectively. Contrary to the observations with the *losb* mutant (Gibson et al. 1997), the complete loss of the variable oligosaccharide branch alone or in addition to core heptoses rendered *waaF* and *gmhA* mutants less virulent in the rabbit model. Collectively, these studies may indicate the LOS oligosaccharide branch is most important for the encounter of *H. ducreyi* with keratinocytes, the principal cell type of the outermost sheet of the epidermis. As artificial inoculation of rabbits or humans introduce mutant bacteria to the dermis and lower portions of the skin, the interactions between LOS and components of the epidermis, an initial interaction in the natural route for infection, may be minimized. Therefore, the mutant bacteria could appear as virulent as the parental strain. Moreover, truncation of the LOS past a certain point may begin to significantly diminish the contribution of LOS to the virulence of *H. ducreyi*, especially in the later stages of infection.

1.5 SIALIC ACID

Sialic acids constitute a family of 36 naturally occurring derivatives of the nine-carbon sugar, N-acetylneuraminic acid (NeuAc), most commonly referred to as sialic acid (Schauer 1982; Schauer et al. 1995). Reported modifications include acetyl esterification or phosphorylation of hydroxyl groups and N-acetyl or N-glycolyl substitution at the amino group of neuraminic acid. Various sialic acid derivatives are found in higher organisms, however only N-acetylneuraminic acid has been observed in *H. ducreyi* and *H. influenzae* to date. Sialic acids are most frequently α-glycosidically linked to galactose or N-acetylgalactosamine and rarely to N-acetylglucosamine or another sialic acid. When present, sialic acid is most often the terminal residue in glycoconjugates, and therefore is an important regulator of cellular and molecular interactions (Kelm and Schauer 1997).

1.5.1 Biological Roles of Sialic Acid

Sialic acid is found in a multitude of mammalian glycolipids and glycoproteins where it frequently serves as a mediator of cell-cell recognition, cell differentiation and various receptor-ligand interactions (Kelm and Schauer 1997). This acidic sugar has a dual role in molecular interactions, in which it may function as a recognition determinant or to mask recognition sites. The recognition of sialylated ligands by selectins has been shown to control the capturing of leukocytes from the bloodstream and homing to the vessel wall at the site of inflammation (Vestweber and Blanks 1999). Conversely, the anti-recognition properties of sialic acid have been well demonstrated by its ability to mask galactose from interactions with specific receptors on hepatocytes and macrophages. For example, the recognition of desialylated glycoproteins and erythrocytes by the asialoglycoprotein receptor and the galactose particle receptor respectively, have been shown to result in their rapid removal from the bloodstream (Kelm and Schauer 1997). However, in some instances

pathogenic microorganisms have been demonstrated to exploit surface bound sialic acid as a recognition determinant for anchoring onto the surface of host cells. Hemagglutinin-fusion proteins on the surface of the influenza A and B viruses are known to bind to sialic acid containing glycoconjugates on the surface of host cells; an interaction essential for infection (Kelm and Schauer 1997). Furthermore, the attachment of *H. influenzae* to human respiratory epithelial cells has been shown to involve the recognition of endogenous sialylated glycosphingolipids of the host cells by bacterial adhesions (Kawakami et al. 1998).

Although the occurrence of the acidic sugar in bacterial glycoconjugates is quite rare, the presentation of peripheral sialic acid is a common tactic employed to buffer microbes from the onslaught of host defense mechanisms. Perhaps the best example of sialylated glycoconjugates contributing to virulence is the concealment of bacteria in capsular polysaccharides containing sialic acid (Bitter-Suermann 1993). Encapsulation in either homopolymers of sialic acid or heteropolymer of sialic acid with other sugars contributes to the virulence of pathogenic bacteria in two way. First, polysialic acid has been shown to confer bacterial resistance to complement-mediated killing and phagocytosis (Hammerschmidt et al. 1994; Moxon and Kroll 1990). Secondly, bacteria camouflaged in polymers of α-2,8 linked sialic acid, which are chemically and immunologically identical to the polysaccharide constituent of the mammalian neural cell adhesion molecule, fail to evoke the production of autoantibodies (Bitter-Suermann 1993; Reglero et al. 1993). Therefore, pathogens equipped with polysialic acid capsules are capable of causing invasive disease by neutralizing the innate (antigen nonspecific) immune response through concealment in a highly negatively charged coating and by deceiving the adaptive (antigen specific) immune response by molecular mimicry (Bitter-Suermann 1993).

1.5.2 Sialic Acid Metabolism

In mammalian cells, free sialic acid is synthesized in the cytosol by the condensation of phospho(enol)pyruvate (PEP) with N-acetylmannosamine-6-phosphate by the NeuAc-9-phosphate synthetase (Kelm and Schauer 1997) (Figure 1.4). The NeuAc-9-phosphate is subsequently dephosphorylated by the NeuAc-9-phosphatase, to liberate the free monosaccharide. Although the pathway for the biosynthesis of sialic acid in *Haemophilus* has not yet been established, a NeuAc synthetase has been shown to produce sialic acid from the condensation of N-acetylmannosamine (ManNAc) and PEP in *E. coli*, *N. meningitidis* and *C. jejuni* (Ferrero et al. 1996; Linton et al. 2000; Masson and Holbein 1983). The *E. coli* K1 enzyme has been purified to homogeneity and shown to couple ManNAc exclusively to PEP *in vitro* (Vann et al. 1997). However, other research groups have shown the NeuAc lyase to synthesize sialic acid through the coupling of pyruvate and ManNAc *in vitro*. The lyase encoded by the *nanA* gene was shown to be necessary for the utilization of ManNAc as a sole carbon source for good growth and therefore has been proposed to have an important catabolic role in the detoxification of the monosaccharide in the host environment (Plumbridge and Vimr 1999; Vimr and Troy 1985). Recent data from our laboratory has suggested that in *H. ducreyi*, sialic acid is imported directly from the extracellular environment and is not synthesized from ManNAc (Schilling et al. 2000).

The pathway for sialylation appears to be conserved in all organisms and involves two steps, the activation and transfer of sialic acid (Figure 1.4). In the first step, CMP-NeuAc synthetase catalyzes the activation of the anomeric hydroxyl group in sialic acid by formation of an ester linkage in CMP-NeuAc, which then serves as the substrate for the attachment of sialic acid to an acceptor by sialyltransferases. Currently, nine gene sequences from bacterial sources have been identified as or postulated to be CMP-NeuAc synthetases, in addition to the human (accession number AAF76203) and the first full mammalian sequence to be reported from mice (Münster et al. 1998). Four regions within

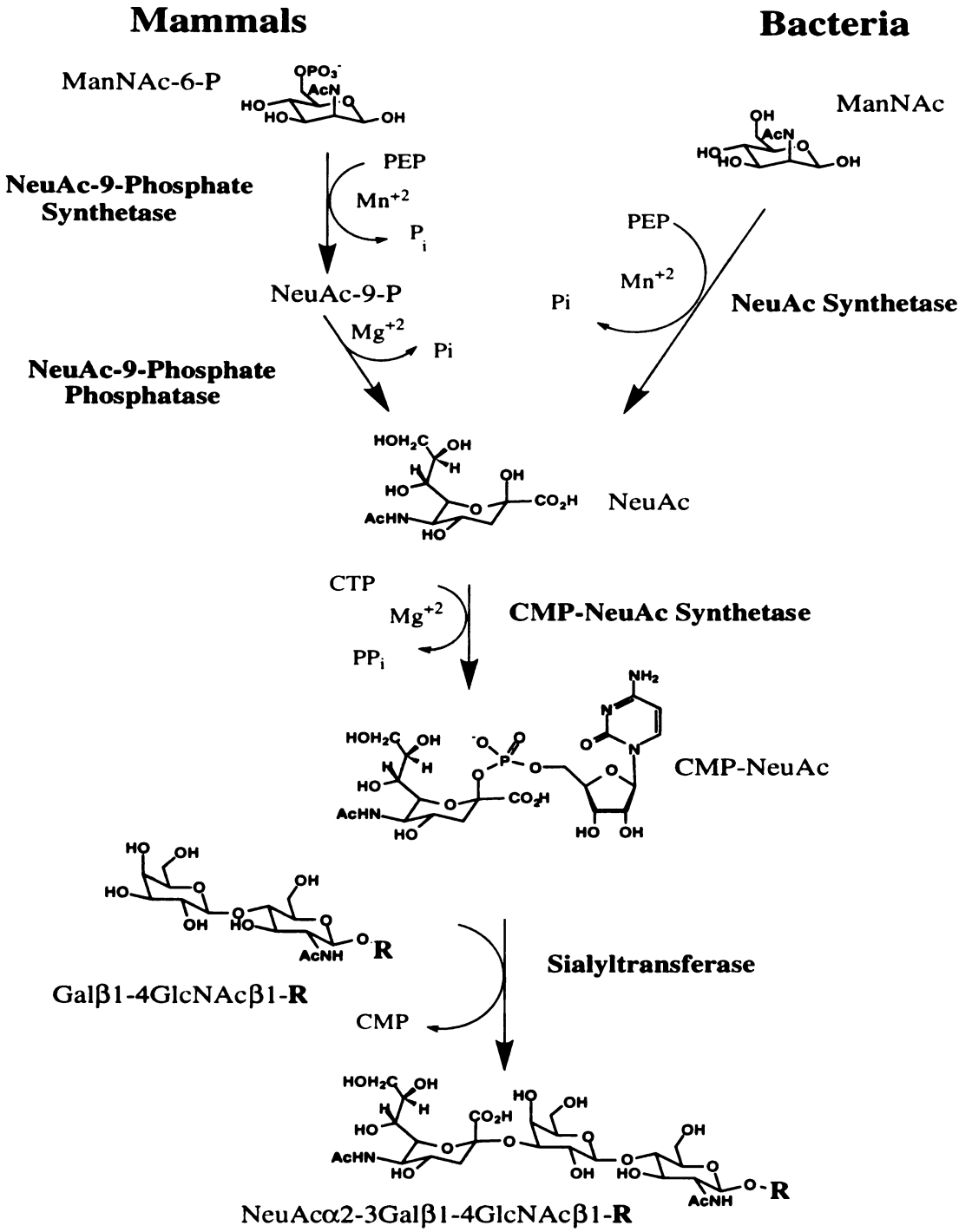

Figure 1.4 Biosynthetic pathways for sialic acid-containing glycoconjugates in mammals and some bacteria. In the final enzymatic step, sialic acid is transferred to the 3'-position of a representative oligosaccharide containing a non-reducing terminal N-acetyllactosamine.

the N-terminal portion of the mouse sequence are highly conserved in bacterial CMP-NeuAc synthetases, providing evidence for an ancestral relationship between the sialylation pathways in bacterial and animal cells. Conversely, unsuccessful attempts to clone prokaryotic sialyltransferases utilizing nucleic acid probes based on the mammalian "sialyl motif" (Datta and Paulson 1997) or complete mammalian genes, gave the first indication of the lack of homology between prokaryotic and eukaryotic sialyltransferases. The *lst* gene encoding the α-2,3-sialyltransferase involved in the biosynthesis of LOS from *N. meningitidis* and *N. gonorrhoeae* was cloned, expressed in *E. coli* (Gilbert et al. 1996) and shown to be distinct from the mammalian α-2,3-sialyltransferase and bacterial α-2,8-polysialyltransferase families. Recently, an LOS specific sialyltransferase was identified in *H. ducreyi* and shown to lack homology to other known sialyltransferases (Bozue et al. 1999). Given the importance of this acidic sugar in the modulation of virulence in pathogenic bacteria, the enzymes in the pathway for the synthesis, activation and transfer of sialic acid to LOS represent potential targets for drug development.

1.5.3 Sialylation of Lipooligosaccharides (LOS)

Among pathogenic members of the *Haemophilus* and *Neisseria* genera, sialic acid has been detected in the LOS of a number of strains. Of the LOS structures characterized in detail, sialic acid has been observed linked to the terminal galactose or N-acetylgalactosamine of oligosaccharide branches resembling components of human glycosphingolipids (Mandrell et al. 1992). For example, analyses revealed the terminal trisaccharide Galα1→4Galβ1→4Glc and tetrasaccharide Galβ1→4GlcNAcβ1→3Gal1→4Glc of the LOS from *N. meningitidis* were chemically and antigenically identical to the oligosaccharide portions of ceramide trihexoside (P^k antigen) and paragloboside, precursors of the glycolipid ABH blood group antigens on human erythrocytes (Mandrell and Apicella 1993; Moran et al. 1996). Furthermore, a large

number of the human glycosphingolipids are sialylated, as are the analogous terminal epitopes of the LOS from these bacteria. Therefore, researchers have postulated that expression of LOS crowned with host-like oligosaccharide branches may abet mucosal pathogens in the evasion of immune responses by molecular mimicry or may facilitate adherence to and/or invasion of human cells by exploiting host receptors for glycosphingolipids or sialic acid (Smith et al. 1995).

As a result of increased efforts to define the role of LOS sialylation in the pathogenesis of the species of *Haemophilus* and *Neisseria*, the enzymes catalyzing the activation and transfer of sialic acid have become the focus of much attention. In two cases where the biological consequences of disrupting genes encoding the LOS specific sialyltransferase have been examined, that is, the sialyltransferase deletion mutants of *N. gonorrhoeae* (Bramley et al. 1995) and *N. meningitidis* (Kahler et al. 1998), incorporation of sialic acid into the LOS was found to be critical for the conversion to and/or maintenance of a serum resistant phenotype. Considering that the LOS produced by some members of the *Neisseria* and *Haemophilus* spp. are similar in structure (Gibson et al. 1993; Preston et al. 1996), the sialylation of LOS was anticipated to play an important role in the pathogenesis of *Haemophilus*. In a similar study, the disruption of the gene encoding CMP-NeuAc synthetase in NTHi had little effect on the capacity of the isogenic mutant to attach to and/or invade human epithelial cells or neutrophils (Hood et al. 1999). However, the loss of the sialylation phenotype rendered NTHi susceptible to the lethal effects of normal human serum. Therefore, sialylation of LOS in NTHi is a major virulence factor influencing the survival of the pathogen within the host. Recently, both sialyltransferase and CMP-NeuAc synthetase deletion mutants of *H. ducreyi* were constructed and shown by mass spectrometry and sugar composition analysis to be devoid of sialylated LOS-glycoforms (Bozue et al. 1999). The evaluation of the *H. ducreyi* sialyltransferase mutant in human challenge studies revealed that the loss of the capacity to sialylate the terminal paragloboside-like LOS epitope did not affect pustule formation (Young et al. 1999). As

this study in human subjects did not permit the examination of the role of LOS sialylation in the later stages of chancroid infections, contributing roles in ulceration, immune system avoidance and transmission of infection could not be excluded.

1.6 SIALYLTRANSFERASE

Based on the specificity for anomeric linkages and composition of acceptor substrates, at least 13 sialyltransferase genes are present in mammalian systems (Tsuji 1996), however only a handful of genes encoding both polysialic acid capsular and LOS-specific sialyltransferases from several bacterial sources have been cloned (Bozue et al. 1999; Gilbert et al. 1996; Weisgerber et al. 1991). The recombinant sialyltransferase from *N. meningitidis* was purified to homogeneity and partially characterized (Gilbert et al. 1997). Although detergents were not required for activity, the membrane associated enzyme was stimulated by $MnCl_2$ or $MgCl_2$ and inhibited by CMP and CDP. The meningococcal enzyme was shown to utilize acceptors containing an α or β configured non-reducing terminal galactose in a variety of glycosidic linkages to a penultimate GlcNAc, Gal or Glc. As expected, the enzyme displayed the highest apparent k_{cat}/K_m value for oligosaccharides containing the lacto-N-neotraose epitope, Galβ1$\rightarrow$4GlcNAcβ1$\rightarrow$3Galβ1$\rightarrow$4Glc, a mimetic of the nonreducing terminus of the natural substrate (Rest and Mandrell 1995; Smith et al. 1995).

1.7 CYTIDINE 5'-MONOPHOSPHATE N-ACETYLNEURAMINIC ACID (CMP-NeuAc) SYNTHETASE

Prior to the transfer of sialic acid to LOS, a cytidine 5'-monophosphate N-acetylneuraminic acid synthetase activates the acidic sugar by transforming the monosaccharide into the donor form, CMP-NeuAc (Kean 1991). A number of CMP-

NeuAc synthetases have been isolated from both animal (Rodriguez-Aparicio et al. 1992; Schauer et al. 1980; Schmelter et al. 1993) and bacterial (Haft and Wessels 1994; Vann et al. 1987; Warren and Blacklow 1962) sources, yet, only the enzymes from *H. ducreyi* (Tullius et al. 1996), *N. meningitidis* (Ganguli et al. 1994) and *E. coli* (Liu et al. 1992; Shames et al. 1991) have been expressed in their recombinant forms and purified. In general, CMP-NeuAc synthetases have optimal pH ranges of 8-10 and require divalent metals for catalytic activity. Although CMP-NeuAc synthetases exclusively utilize CTP as the nucleotide substrate, the enzymes from *H. ducreyi* and a few animal tissues have been shown to consume N-glycolylneuraminic acid, in addition to the natural substrate, sialic acid (Kean 1991; Rodriguez-Aparicio et al. 1992; Tullius et al. 1996).

1.8 RESEARCH GOALS

The incorporation of N-acetylneuraminic acid into LOS has been shown to aid species of *Neisseria* in the evasion of host defense mechanisms (Rest and Mandrell 1995; Smith et al. 1995) however, the role of sialic acid-containing LOS in the pathogenesis of *Haemophilus* remains unresolved. In an effort understand the contributions of LOS sialylation to the virulence of *Haemophilus* pathogens, we have focused our investigations towards identifying genes and characterizing gene products involved in the biosynthesis of the glycolipid. Prior studies from our laboratory have demonstrated that the *neuA* gene encodes a cytidine 5'-monophosphate N-acetylneuraminic acid (CMP-NeuAc) synthetase that is essential for the expression of sialic acid-containing LOS in *H. ducreyi* (Bozue et al. 1999). This enzyme has been over-expressed in *E. coli* and purified to homogeneity, affording large quantities for the initiation studies aimed at the characterization of this potential chemotherapeutic target (Tullius et al. 1996). To this end, Chapter 2 describes the determination of the kinetic mechanism of the *H. ducreyi* CMP-NeuAc synthetase by steady state kinetic analysis and the prediction of the rate-limiting step in k_{cat} by the rigorous

examination of product inhibition constants. Chapter 3 describes studies probing the surface topography of CMP-NeuAc synthetase by limited proteolysis and amide hydrogen isotopic exchange techniques in an effort to gain insights into the nature of the active site of the enzyme.

A second gene (*lst*), encoding a novel sialyltransferase, was also previously demonstrated to be required for the sialylation of LOS in *H. ducreyi* (Bozue et al. 1999). To date, sialyltransferase activity has not been detected in *H. influenzae* by *in vitro* assays, however, *lst* was found to have significant homology to the *siaA* gene in *H. influenzae*. Chapter 4 describes efforts to determine the function of the hypothetical protein (SiaA), in the biosynthesis of sialylated LOS by deleting *siaA* gene and characterizing of LOS produced by isogenic mutant strains by mass spectrometry.

CHAPTER 2.

Investigation of the Kinetic Mechanism of Cytidine 5'-Monophosphate N-Acetylneuraminic Acid Synthetase from *Haemophilus ducreyi* With New Insights On Rate-limiting Steps from Product Inhibition Analysis

2.1 INTRODUCTION

Cytidine 5'-monophosphate N-acetylneuraminic acid (CMP-NeuAc) synthetase is a central enzyme in the biosynthetic pathway producing sialic acid containing lipooligosaccharide (LOS), a virulence factor for *Haemophilus ducreyi.* The cloning of the *neuA* gene and the over-expression of the gene product has allowed for the acquisition of large quantities of pure protein for the initiation of basic biochemical studies (Tullius et al. 1996). Although several CMP-NeuAc synthetases have been partially characterized, there has been no detailed kinetic analysis of any to provide a framework for rational drug design.

This chapter describes efforts to determine the kinetic mechanism of the CMP-NeuAc synthetase from *H. ducreyi* via steady state kinetic analysis. Examination of double reciprocal plots of the substrate initial velocity kinetic data revealed a sequential mechanism, requiring the formation of a ternary complex before the release of either product. To resolve the order of substrate addition to and product release from CMP-NeuAc synthetase, the initial velocity was measured as a function of the two products, CMP-NeuAc and pyrophosphate (PP_i). As a final step to establish the order of substrate additions, the sialic acid analog 2-O-methyl-β-D-N-acetylneuraminic acid (Me-O-NeuAc) was found to be a competitive inhibitor versus NeuAc and an noncompetitive inhibitor versus CTP, exhibiting a K_i of 64.5 ± 15.5 μM. Collectively, these data are consistent with an ordered Bi-Bi kinetic mechanism where CTP is bound before NeuAc and PP_i is released before CMP-

NeuAc with the following kinetic constants: k_{cat}, 1.8 ± 0.2 sec^{-1}; K_{mCTP}, 10.6 ± 1.2 μM; K_{mNeuAc}, 76.3 ± 7.8 μM; K_{ia}, 44.6 ± 6.8 μM. Furthermore, a methodical analysis of the kinetic expressions for the observable constants from the resulting ordered Bi-Bi mechanism showed that variation in the magnitude of apparent product inhibition constants can be used to predict rate-limiting steps in the reaction.

2.2 MATERIALS AND METHODS

2.2.1 Materials

MOPS, $MgCl_2$, DTT, BSA, NeuAc, CTP, CMP-NeuAc, PP_i, UDPG, $NADP^+$, α-D-glucose-1,6-diphosphate, glucose-6-phosphate dehydrogenase, phosphoglucomutase and uridine-5'-diphosphoglucose pyrophosphorylase were all purchased from Sigma Chemicals. Me-O-NeuAc was purchased from GlycoTech.

2.2.2 Methods

2.2.2.1 *Preparation of CMP-NeuAc Synthetase*

The expression and purification of CMP-NeuAc synthetase from *H. ducreyi* was previously described (Tullius et al. 1996). The enzyme was stored at 4 °C as an ammonium sulfate suspension. For assays using the anion exchange HPLC method described below, stock solutions of CMP-NeuAc synthetase were made by dilution of the ammonium sulfate suspension with assay buffer containing 200 mM MOPS, pH 7.1, 200 mM NaCl, 20 mM $MgCl_2$ and 1 mg/mL BSA. However, for the enzyme-coupled fluorescence assay described below, the ammonium sulfate suspension of CMP-NeuAc synthetase was desalted prior to use, by applying it to a Bio-Silect SEC-250 guard column (Biorad; 50 × 7.8 mm) and eluting with 200 mM MOPS, pH 7.1, containing 200 mM NaCl. The total protein

concentration of each enzyme preparation was quantitated using the extinction coefficient ε_{280} of 0.40 mL mg^{-1} cm^{-1} determined from amino acid analysis on a sample of enzyme of defined A_{280}.

2.2.2.2 *Anion Exchange HPLC Assay*

The rate of production of CMP-NeuAc was monitored by single-point measurements as previously described with slight modifications (Tullius et al. 1996). Briefly, 90 µL of the premixed substrates are preincubated at 25 °C for 2 minutes prior to the addition of 10 µL of diluted CMP-NeuAc synthetase, resulting in final conditions of 200 mM MOPS, pH 7.1, 20 mM $MgCl_2$, 20 mM NaCl, 0.1 mg/mL BSA. The final concentration of CMP-NeuAc synthetase was 0.71 nM for all experiments except for the dead-end inhibition study with NeuAc as the variable substrate, where it was 1.1 nM. For each enzyme concentration, limits for the duration of the initial linear phase were determined by measuring the initial velocity at multiple time points for the reactions where both substrates were either at the lowest or highest concentrations used in the full study, and also for the two reactions where one substrate was at its lowest and the other at its highest concentration. At appropriate times, reactions were terminated by addition of 20 µL of 300 mM ammonium formate, pH 3.5, followed by immediate freezing on dry ice. The frozen reaction mixture was thawed just prior to analysis by anion exchange chromatography using a nucleotide analysis column (Vydac; 4.6 × 50 mm) with elution by a gradient of 35 mM to 500 mM ammonium formate, pH 3.5. The amount of CMP-NeuAc at each time point was determined by integration of its peak area measured at 280 nm using Mac Integrator I™ software (Rainin).

2.2.2.3 *Enzyme-Coupled Fluorescence Assay*

As an alternative assay for some of the product inhibition studies, CMP-NeuAc synthetase activity was monitored continuously by coupling the production of PP_i to the

reduction of $NADP^+$ via a series of three auxiliary enzymes (Figure 2.1) (Passonneau 1993). The coupling enzymes, their substrates, CTP, NeuAc and CMP-NeuAc, as a product inhibitor, were premixed (360 µL) and preincubated at 25 °C for 2 minutes prior to initiation of the reaction by addition of CMP-NeuAc synthetase (40 µL). Optimal conditions were determined to be: 200 mM MOPS, pH 7.1, 1 mM UDPG, 0.5 mM $NADP^+$, 5 µM α-D-glucose-1,6-diphosphate (to activate phosphoglucomutase), 20 mM NaCl, 20 mM $MgCl_2$, 3 U/mL UDPG pyrophosphorylase (yeast), 8 U/mL phosphoglucomutase (rabbit muscle), 5 U/mL glucose-6-phosphate dehydrogenase (yeast), 0.1 mM DTT, 0.1 mg/mL BSA, 70.2 nM CMP-NeuAc synthetase in 400 µL total volume. Prior to use, the ammonium sulfate suspension of phosphoglucomutase was exchanged into 200 mM MOPS, pH 7.1, containing 1 mM DTT, using a Microcon-10 microconcentrator (Amicon). The rate of NADPH formation was measured by following the increase in fluorescence (λ_{ex} = 340 nm, slit width 15 nm; λ_{em} = 450 nm, slit width 20 nm) using an LS 50B luminescence spectrometer (Perkin Elmer). Under these conditions, the instrument response was found to be linear from 62 nM to 8 µM NADPH. Initial velocities were determined from the slope of the linear portion of the progress curve following the addition of CMP-NeuAc synthetase to the preincubated reaction mixture. The linear portion typically lasted from 40 to 150 seconds, and corresponded to less than 5% conversion of the substrate (in lowest concentration) to product in each case.

To verify the substrates and products of CMP-NeuAc synthetase did not effect the activity of the auxiliary enzymes, the initial velocity of the coupled assay system was measured following the addition of buffer alone (200 mM MOPS, pH 7.1), 100 µM CTP, 1.5 mM Me-O-NeuAc or 0.5 mM CMP-NeuAc. The reaction was initiated with 25 µM pyrophosphate in place of CMP-NeuAc synthetase. The final conditions were identical to those above with the exception of 0.35 mM NADP+, 0.1 mM α-D-glucose-1,6-diphosphate and 0.7 mM UDPG.

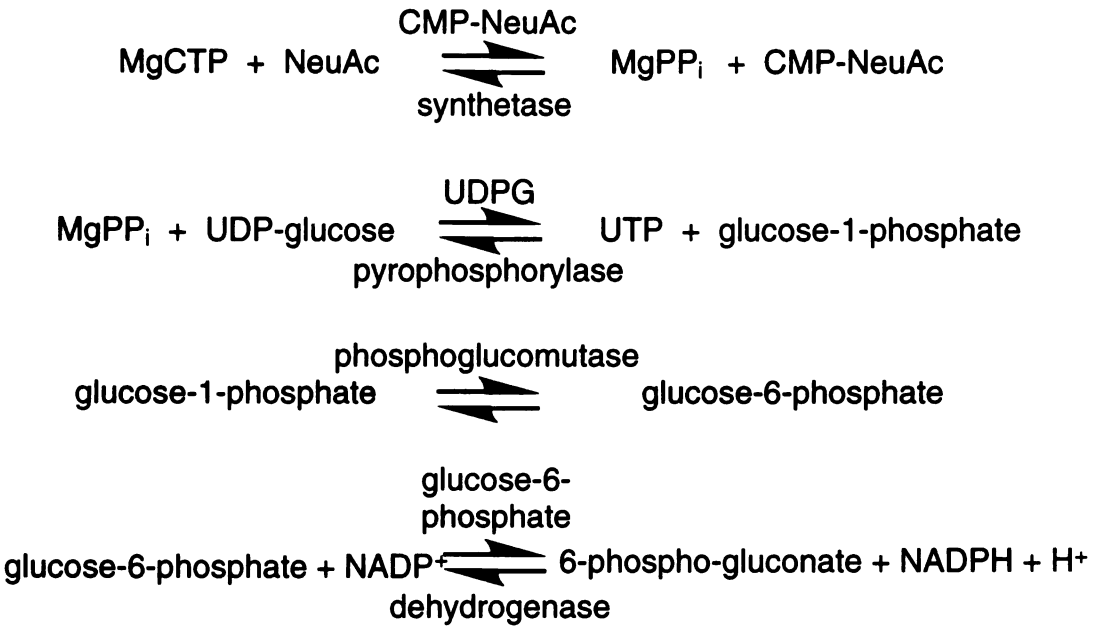

Figure 2.1 Enzyme-coupled fluorescence assay for the measurement of PP_i.

To assure the substrates and products of the coupled assay did not effect the activity of CMP-NeuAc synthetase, the initial velocity of the enzyme was measured in the presence of individually added reagents (200 μM DTT, 1.0 mM UDPG, 10 μM UTP, 100 μM glucose 1,6 diphosphate, 0.5 mM NADP+ or 10 μM NADPH). In separate experiments, the concentration of one substrate was held constant at a limiting concentration (10 μM CTP or 50 μM NeuAc) while maintaining the other constant at maximal concentration (1 mM NeuAc or 100 μM CTP). Reactions with CMP-NeuAc synthetase proceeded for 30 minutes under conditions identical to those above and the production of CMP-NeuAc was monitored by the anion exchange HPLC assay. The final concentration of CMP-NeuAc synthetase was held constant at 0.43 nM.

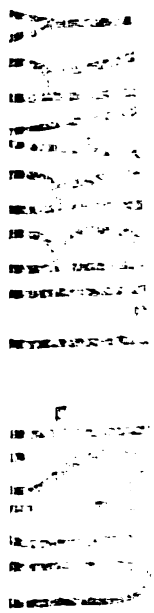

2.2.2.4 *Substrate Initial Velocity Analysis*

The discontinuous anion exchange HPLC assay was used to obtain initial velocity data at varied concentrations of both substrates. CTP was varied from 12.5 to 100 μM as the concentration of NeuAc was varied from 62.5 μM to 1.0 mM to yield a 5 × 5 matrix. In each reaction, no more than 11% of the substrate in lowest concentration was converted to product. Each data point represents the mean of three separate trials (Figure 2.5).

2.2.2.5 *Product Inhibition Analysis*

The inhibition behavior of each product with respect to each substrate was determined by measuring initial velocities in the presence of a constant concentration of one substrate, while varying the concentration of the other substrate and the appropriate product, PP_i or CMP-NeuAc. For studies of PP_i as an inhibitor, production of CMP-NeuAc was measured using the anion exchange HPLC assay. Conversely, for studies of CMP-NeuAc as an inhibitor, the generation of PP_i was measured indirectly by the enzyme-coupled assay (Figure 2.1). Assay conditions were as described above with the exception of the addition of the chosen product inhibitor to the assay premix prior to the

addition of CMP-NeuAc synthetase. Under these conditions, no more than 8% of the substrate in lowest concentration was converted to product. Each data point represents the average of at least two separate trials (Figures 2.6 and 2.7).

2.2.2.6 *Dead-End Inhibition Analysis*

To examine the inhibition behavior of Me-O-NeuAc with respect to each substrate, initial velocities were measured in the presence of a constant concentration of one substrate, while varying the concentration of the other substrate and the inhibitor. For both types of reactions, production of CMP-NeuAc was monitored using the anion exchange HPLC assay. Conditions were as described above with the exception of the inclusion of Me-O-NeuAc in the premix prior to the addition of CMP-NeuAc synthetase. Under these conditions, no more than 4% of the substrate in lowest concentration was converted to product. Each data point represents the average of three separate trials (Figure 2.9).

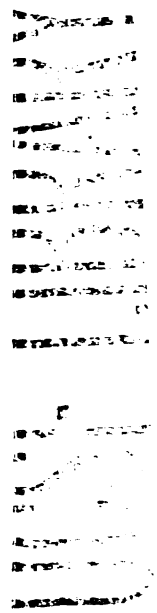

2.2.2.7 *Data Analysis*

All experimental data were fit to rate equations by nonlinear regression analysis using the KinetAsyst software (IntelliKinetics) employing the nomenclature of Cleland (Cleland 1963). Initial velocity data from the substrate kinetics were fit to the rate equation for a ternary complex mechanism (Equation 1).

$$v = V_{max}[A][B]/\{K_{ia}K_{mB} + K_{mA}[B] + K_{mB}[A] + [A][B]\} \quad (1)$$

Data from the product and dead end inhibition studies were fit to Equations 2-4 for competitive, uncompetitive and noncompetitive inhibition, respectively.

$$v = V_{max}[S]/\{K_{mS}(1 + [I]/K_{is}) + [S]\} \quad (2)$$

$$v = V_{max}[S]/\{K_{mS} + [S](1 + [I]/K_{ii})\} \quad (3)$$

$$v = V_{max}[S]/\{K_{mS}(1 + [I]/K_{is}) + [S](1 + [I]/K_{ii})\} \quad (4)$$

For the above equations, the following designations hold: v, velocity; V_{max}, maximal velocity; K_{ia}, dissociation constant for the first substrate; K_{mX}, Michaelis constant for the designated substrate X; K_{is}, slope inhibition constant; K_{ii}, intercept inhibition constant; I, inhibitor concentration; S, the varied substrate in the inhibition experiments. Double reciprocal plots of the data were created with Kaleidagraph (Synergy Software) using the kinetic constants obtained from the KinetAsyst analysis.

2.3 RESULTS AND DISCUSSION

2.3.1 Development of Enzyme Coupled Assay

The comprehensive evaluation of the kinetic mechanism of CMP-NeuAc synthetase required the use of separate reaction assays to monitor the generation of each product. In the first, the initial velocity of the enzyme was monitored by the direct quantitation of CMP-NeuAc by anion exchange HPLC (Tullius et al. 1996). The second assay was employed to measure the initial rate of CMP-NeuAc synthetase continuously by coupling the generation of pyrophosphate (PP_i) to the reduction of $NADP^+$ with three auxiliary enzymes (Passonneau 1993). However, before the enzyme coupled system could be adopted for the study of CMP-NeuAc synthetase, all reagents were tested for potential inhibitory effects and the concentrations of the substrates and auxiliary enzymes were optimized for maximal activity. Initially, the reaction of CMP-NeuAc synthetase was exclusively monitored in the presence of individually added reagents (Figure 2.2). Whether the CTP or NeuAc was the limiting substrate, the reagents of the coupled assay did not alter the activity of CMP-NeuAc

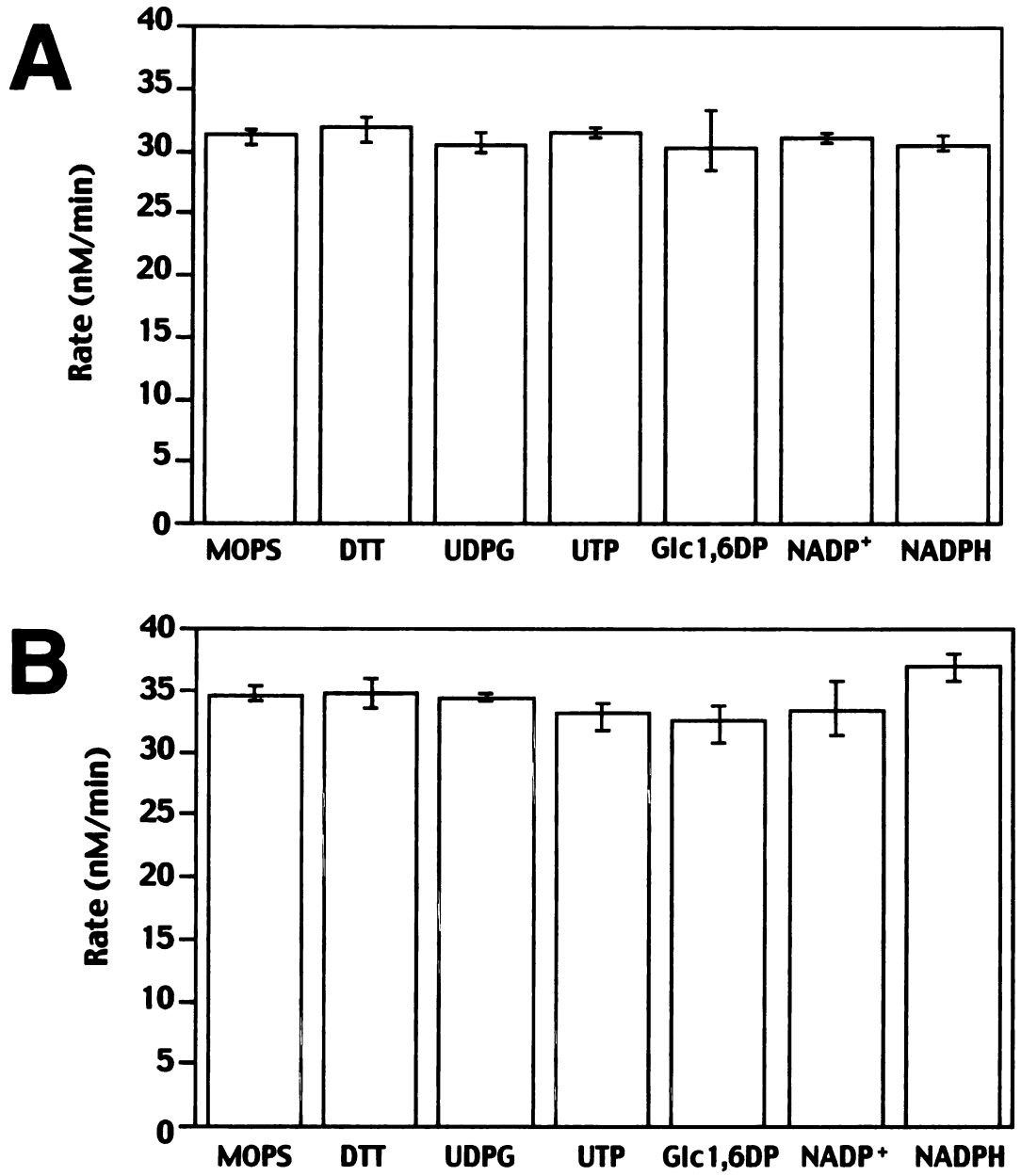

Figure 2.2 Effects of the enzyme coupled assay reagents on the activity of CMP-NeuAc synthetase. Initial Velocity Measurements of CMP-NeuAc Synthetase with (A) 100 μM CTP and 50 μM NeuAc or (B) 10 μM CTP and 1.0 mM NeuAc. The enzyme was assayed in the presence of buffer alone (200 mM MOPS, pH 7.1), 200 μM DTT, 1.0 mM UDPG, 10 μM UTP, 100 μM glucose 1,6 diphosphate, 0.5 mM NADP+ or 10 μM NADPH.

synthetase. Next, we assessed the effects of CTP, NeuAc and CMP-NeuAc on the activities of the auxiliary enzymes (Figure 2.3). When the reagents were held constant at the highest concentrations used in subsequent product inhibition studies, the coupling enzymes were not significantly affected by the substrates and product of CMP-NeuAc synthetase. In control experiments to confirm that the reaction of CMP-NeuAc synthetase was the rate-limiting step of the enzyme coupled assay, the rate of NADPH generation was found to be proportional to the final concentration of CMP-NeuAc synthetase up to 140 nM (Figure 2.4). On the whole, linking the production of pyrophosphate to the fluorescent cofactor, NADPH, by a series of auxiliary enzymes has easily permitted sensitive measurements of the initial velocity of CMP-NeuAc synthetase.

2.3.2 Bisubstrate Initial Velocity Data

As the first step in defining the kinetic mechanism, we have evaluated the pattern of variation in the initial velocity as a function of both substrates. Velocities were measured for a 5×5 matrix of CTP and NeuAc concentrations and the data were displayed in double reciprocal plots (Figure 2.5) for initial analysis of the pattern. The intersecting lines evident in the data indicate a mechanism with formation of a ternary enzyme-substrate complex (E•A•B) before the release of either product. However, the order of substrate binding and product release cannot be discerned from these data alone, since the presence of intersection points to the left of the y-axis in *both* plots is consistent with several random- and preferred-order mechanisms. Thus, the data were initially fit to a form of eq. 1 in which the term $K_{ia} \bullet K_{mB}$ is simply designated K_{ab} to obtain values for k_{cat}, K_{mCTP} and K_{mNeuAc}, summarized in Table 2.1. The data do rule out obligatory ordered mechanisms (A followed by B) in which the first substrate (A) binds in a rapid equilibrium step, since this behavior gives an intersection of the lines in the 1/v versus 1/[B] plot *on* the y-axis.

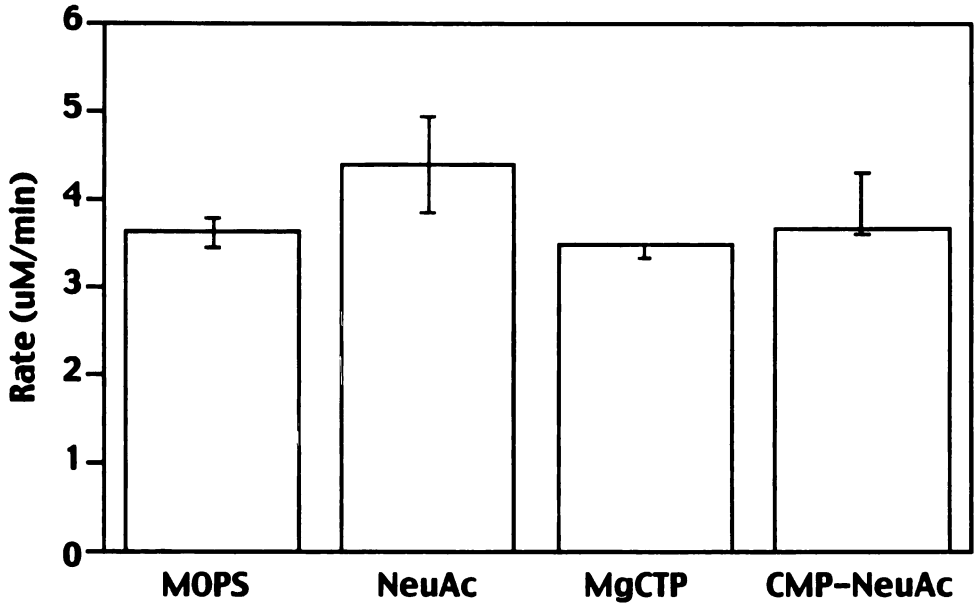

Figure 2.3 Effects of sialic acid, CTP and CMP-NeuAc on the activities of the coupling enzymes. The initial rate of NADPH production was measured following the addition of buffer alone (200 mM MOPS, pH 7.1), 1.5 mM NeuAc, 100 μM CTP or 0.5 mM CMP-NeuAc.

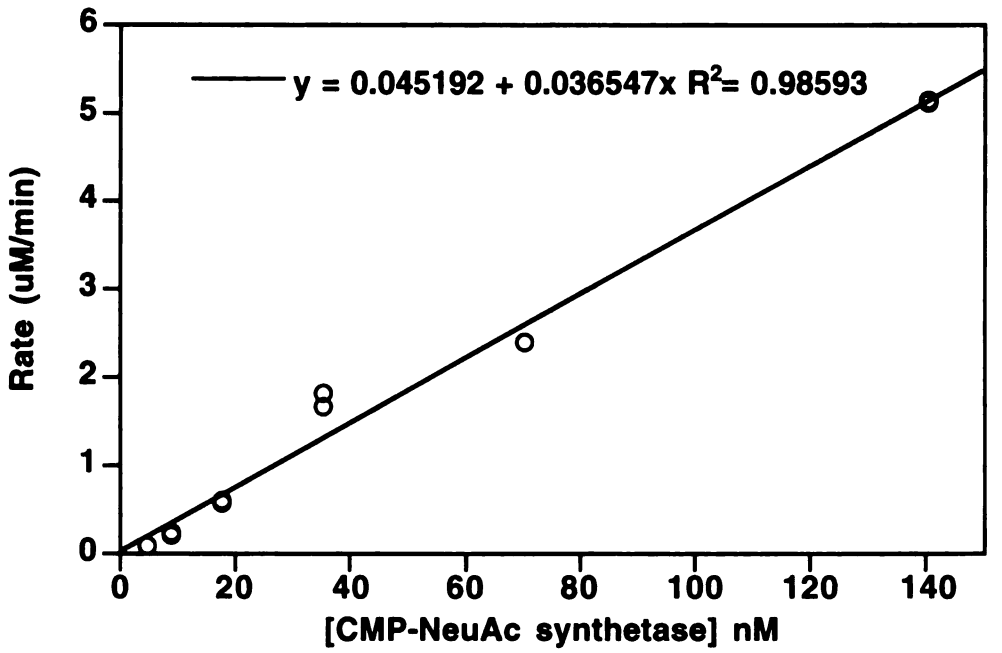

Figure 2.4 Dependence of the rate of NADPH production on the final concentration of CMP-NeuAc synthetase. CTP and NeuAc were held at 100 μM and 1.5 mM, respectively, while the concentration of CMP-NeuAc synthetase was varied from 4.39 - 140.4 nM.

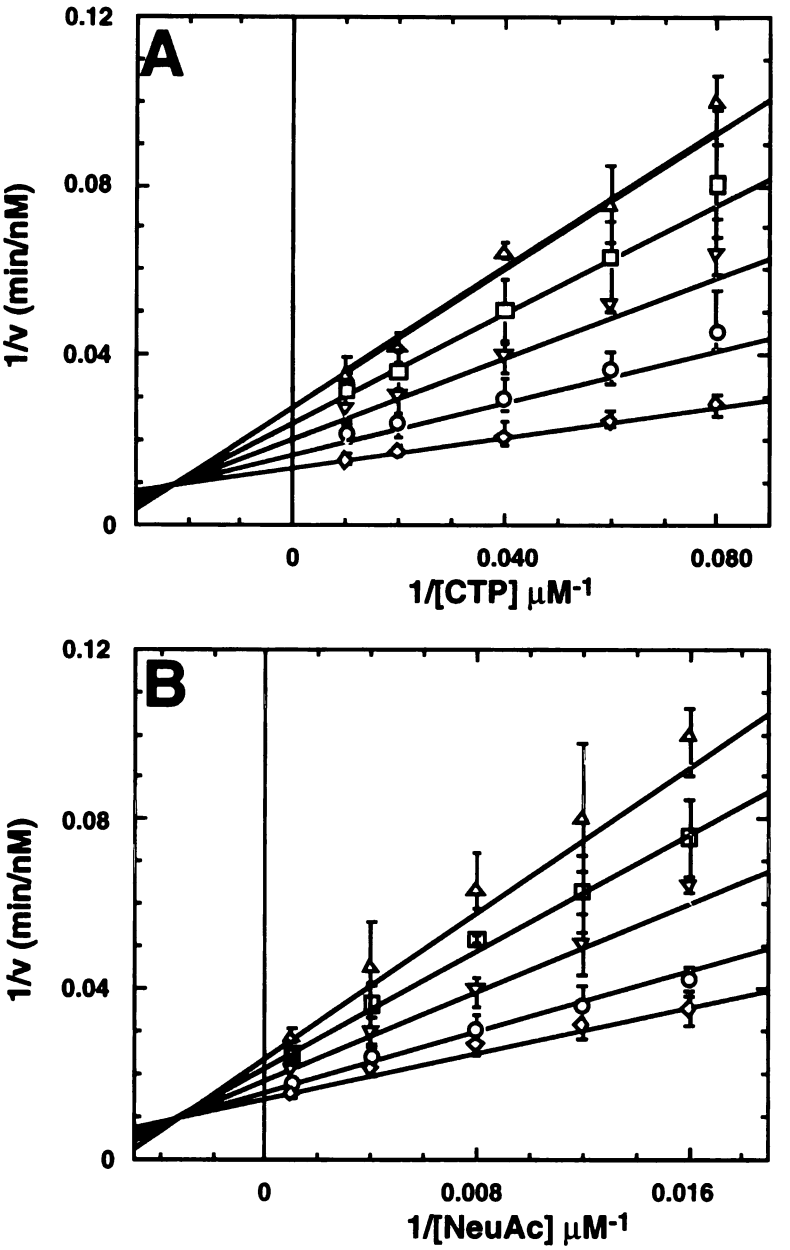

Figure 2.5 Initial velocity patterns for CMP-NeuAc synthetase. (A) Double reciprocal plot with CTP as the varied substrate (12.5 - 100 μM) with fixed NeuAc concentrations of (Δ) 62.5 μM, (❑) 83.3 μM, (∇) 125 μM, (○) 250 μM, (◊) 1.0 mM. (B) Double reciprocal plot with NeuAc as the varied substrate (62.5 - 1000 μM) with fixed CTP concentrations of (Δ) 12.5 μM, (❑) 16.6 μM, (∇) 25 μM, (○) 50 μM, (◊) 100 μM.

Table 2.1 Kinetic constants for CMP-NeuAc synthetase

Substrate	K_m (μM)	k_{cat} (sec^{-1})	K_{ia} (μM)
CTP	10.6 ± 1.2	1.8 ± 0.2	44.6 ± 6.8[a]
NeuAc	76.3 ± 7.8	_	_

[a] Based on determination of the order of substrate addition below.

2.3.3 Product Inhibition Data

In order to eliminate some of the possible pathways for substrate binding and product dissociation, we examined the ability of each product to inhibit the apparent steady-state constants for each substrate, apparent k_{cat} and apparent k_{cat}/K_m, at fixed concentrations of the other substrate. Which constants are affected depends on three characteristics of the kinetic mechanism: (1) whether the chemical conversion is reversible, (2) the point(s) of product binding relative to the point of binding for each substrate, and (3) the concentration of the nonvaried substrate. To make accurate predictions of the expected patterns of inhibition, we first examined the reversibility of the chemical conversion. In previous studies of the CMP-NeuAc synthetase from *N. meningitidis* (Warren and Blacklow 1962), no reversal of the reaction was detected when an indirect chemical assay was used to monitor loss of CMP-NeuAc, nor when a charcoal binding assay was used to monitor exchange of (^{32}P)-PP_i into CTP during normal turnover. We reexamined this question for the enzyme from *H. ducreyi* using our HPLC assay to directly monitor formation of CTP. Analysis of time points from a reaction run under identical conditions as for the forward reaction, but with a higher concentration of CMP-NeuAc synthetase (56.8 nM), and 0.75 mM CMP-NeuAc and 3 mM PP_i, instead of CTP and NeuAc, clearly showed the time-dependent formation of CTP (data not shown). The estimated turnover number for this single set of conditions is 0.62 s^{-1}, only 3-fold lower than the k_{cat} value determined for the forward reaction under the same conditions (1.8 s^{-1}, Table 2.1). Thus, the reaction appears to be freely reversible, and the product inhibition data should follow patterns for a chemically reversible reaction.

As with all types of inhibitors, products are classified as competitive inhibitors if increasing concentrations decrease the apparent k_{cat}/K_m for the varied substrate, uncompetitive if they decrease the apparent k_{cat}, and noncompetitive if they decrease both. The patterns are easily evaluated as increases in the slopes (apparent K_m/k_{cat}), the intercepts

(apparent $1/k_{cat}$), or both, respectively, for lines in double reciprocal plots of 1/v versus 1/substrate obtained at increasing concentrations of product (and a constant concentration of the second substrate). Double reciprocal plots displaying the inhibition behavior of PP_i and CMP-NeuAc versus both substrates are shown in Figures 2.6 and 2.7, respectively, and the associated patterns and inhibition constants derived from fits of the data to eqs. 2 - 4 are summarized in Table 2.2. Comparison of the full set of patterns for all four substrate/product pairs with predicted sets of patterns at both saturating and sub-saturating concentrations of the nonvaried substrate for a wide variety of mechanisms allows us to rule out random mechanisms and limit the possible obligatory-order mechanisms to the two shown in Figure 2.8 (Segel 1975). For the Bi-Bi ordered sequential mechanism, competitive inhibition is observed for the first substrate/last product pair as they directly compete for binding to free enzyme. Thus, in this mechanism CTP would be the first bound substrate and CMP-NeuAc, the last dissociating product. In contrast, competitive inhibition is observed in the Iso Theorell-Chance mechanism in Figure 2.8 for the second substrate/first product pair, since the interconversion of the binary enzyme-substrate and enzyme-product complexes is an equilibrium process limited only by the second order rate constants for binding of the second substrate and first product. Thus, CTP and CMP-NeuAc would be the internal pair in this mechanism.

2.3.4 Dead-End Inhibition Data

The opposite order of substrate binding and product release predicted for the two mechanisms of Figure 2.8 provides an avenue for distinction between the two using either direct binding assays or kinetic analysis of the pattern of inhibition by a structural homolog of one of the substrates (Fromm 1995). With our kinetic assays well in hand, we chose to examine the pattern of inhibition by the sialic acid analog Me-O-NeuAc, which has previously been shown to be a competitive inhibitor (with respect to NeuAc) of the

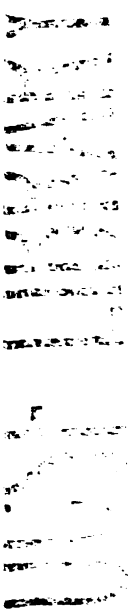

Figure 2.6 Product inhibition by $MgPP_i$... (A) versus NeuAc as varied substrate (0.075 - 3.0 mM), with fixed concentrations of (Δ) 0, (❑) 0.5, (O) 1.0, and (◊) 2.0 mM PP_i. CTP was held constant at 100 μM. (B) ...versus CTP as varied substrate (15 - 150 μM), with fixed concentrations of (Δ) 0, (❑) 0.5, and (O) 1.0 mM PP_i. NeuAc was held constant at 300 μM. (C) ...versus CTP as varied substrate (12.5 - 100 μM), with fixed concentrations of (Δ) 0, (❑) 1.0, and (O) 2.0 mM PP_i. NeuAc was held constant at 2.0 mM. For all three plots, the lines were generated using constants obtained from fits of the data to eq. 4 for noncompetitive inhibition. For comparison, the data in panel (C) were also fit to the uncompetitive model (eq. 3); however, calculation of an F_X value (Bevington 1969) from the variances for the two fits showed that inclusion of the extra variable in the noncompetitive model gave a better fit at the 99% confidence level.

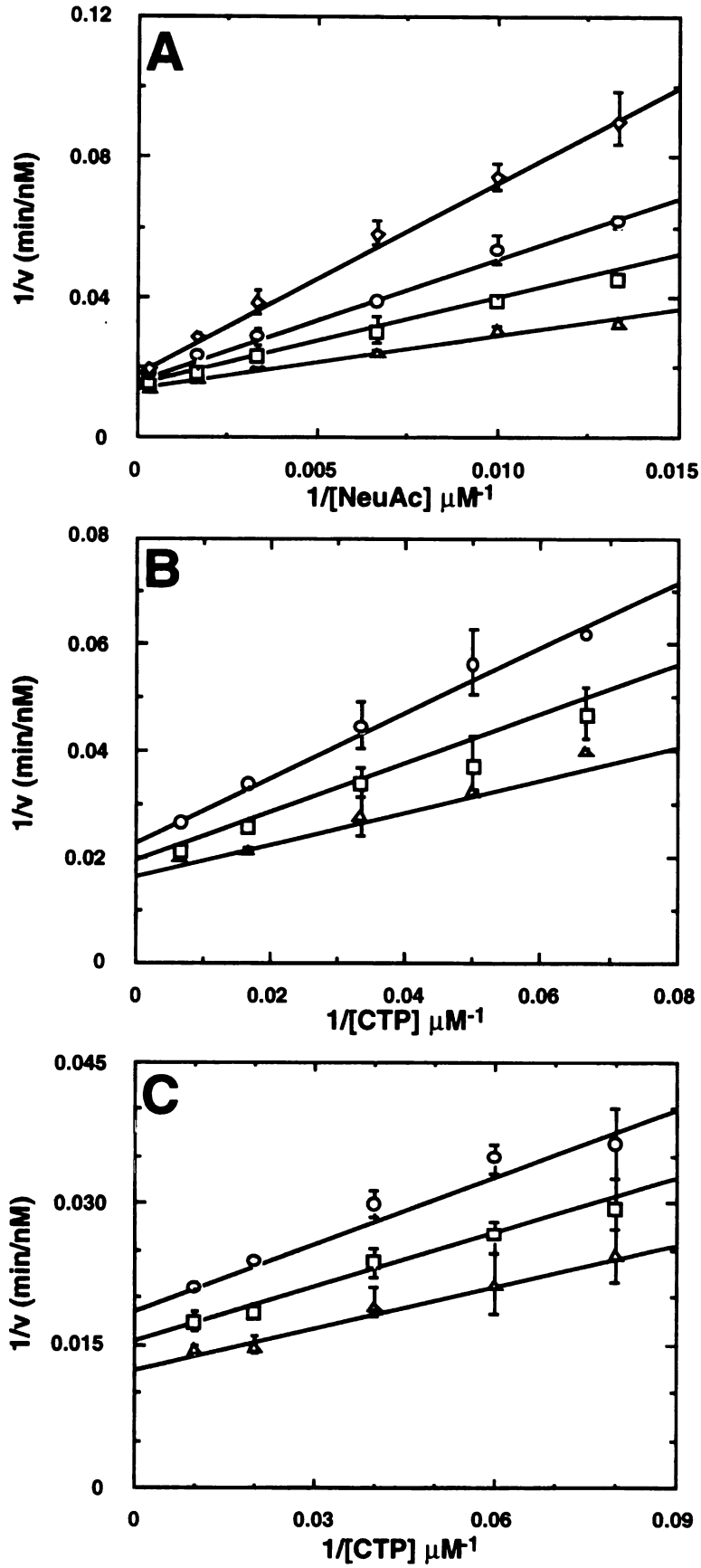
A
0.12
0.08
0.04
0
1/v (min/nM)
0
0.005
0.010
0.015
1/[NeuAc] μM-1
B
0.08
0.06
0.04
0.02
0
1/v (min/nM)
0
0.02
0.04
0.06
0.08
1/[CTP] μM-1
C
0.045
0.030
0.015
0
1/v (min/nM)
0
0.03
0.06
0.09
1/[CTP] μM-1

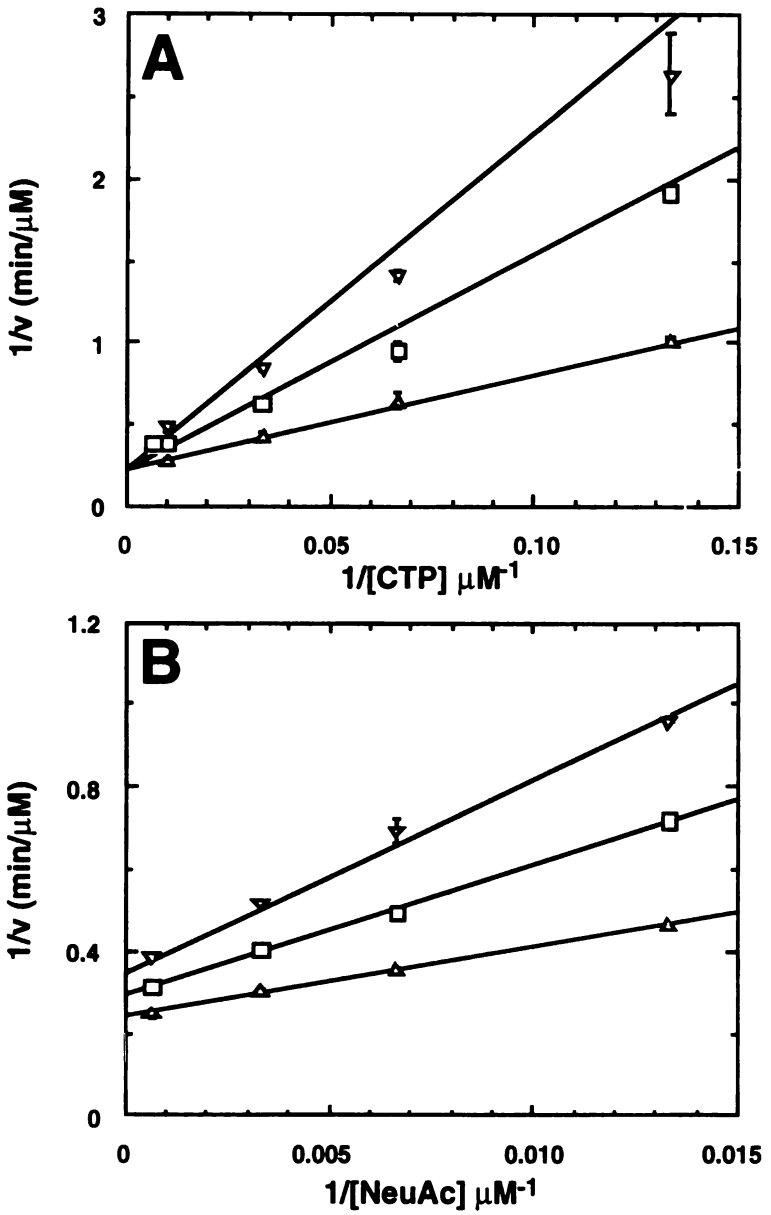

Figure 2.7 Product inhibition by CMP-NeuAc... (A) versus CTP as varied substrate (7.5 - 150 μM), with fixed concentrations of (Δ) 0, (❑) 16, and (∇) 32 μM CMP-NeuAc. NeuAc was held constant at 1.5 mM. Lines were generated using constants obtained from a fit of the data to eq. 2 for competitive inhibition. (B) versus NeuAc as varied substrate (0.075 - 1.5 mM), with fixed concentrations of (Δ) 0, (❑) 16, and (∇) 32 μM CMP-NeuAc. CTP was held constant at 150 μM. Lines were generated using constants obtained from a fit of the data to eq. 4 for noncompetitive inhibition.

Table 2.2 Product inhibition patterns and constants for CMP-NeuAc synthetase[a]

Inhibitor	Varied Substrate	Constant Substrate	Pattern	K_{is}	K_{ii}
PP_i	NeuAc	CTP (100 μM)	NC	0.77 ± 0.10 mM	6.70 ± 1.25 mM
PP_i	CTP	NeuAc (300 μM)	NC	1.00 ± 0.30 mM	2.56 ± 0.60 mM
PP_i	CTP	NeuAc (2.0 mM)	NC	3.06 ± 1.07 mM	4.20 ± 0.70 mM
CMP-NeuAc	NeuAc	CTP (150 μM)	NC	18.8 ± 2.0 μM	70.5 ± 5.6 μM
CMP-NeuAc	CTP	NeuAc (1.5 mM)	C	12.5 ± 1.7 μM	_

[a] Experimental conditions are as described in Materials and Methods. The errors reported for the inhibition constants are the standard errors for the fits to the corresponding rate equations. C, competitive; NC, noncompetitive; K_{ii} and K_{is}, intercept and slope inhibition constants, respectively.

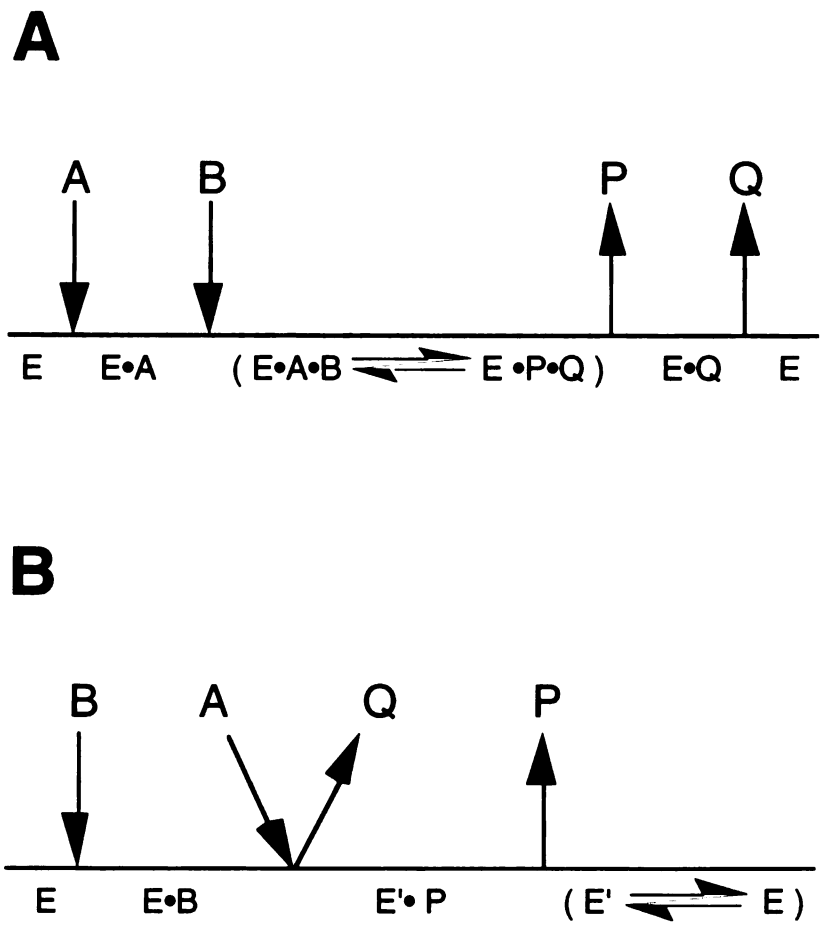

Figure 2.8 Potential kinetic mechanisms for CMP-NeuAc synthetase. (A) Ordered Bi-Bi Mechanism. (B) Iso Theorell-Chance Mechanism. A = CTP, B = NeuAc, P = PP_i, Q = CMP-NeuAc

CMP-NeuAc synthetase from *E. coli* (K_i of 2.5 mM, (Schmid et al. 1988)). Clearly, competitive inhibition with respect to NeuAc is expected for both mechanisms. The distinction lies in the expected pattern with respect to CTP. Binding of the inhibitor after CTP (to E•CTP) in the Bi-Bi mechanism will affect only the apparent k_{cat}, thereby giving an uncompetitive pattern, while binding before CTP (to E) provides a reversible link at subsaturating NeuAc, thereby giving a noncompetitive pattern for the Iso Theorell-Chance mechanism. As shown in Figure 2.9, Me-O-NeuAc does indeed exhibit a competitive inhibition pattern with respect to NeuAc, confirming that they bind to the same enzyme form. The fit of the initial velocity data to the equation for competitive inhibition (eq. 2) yields a dissociation constant K_{is} of 64.5 ± 15.5 μM. Conversely, when NeuAc is held constant, increasing concentrations of Me-O-NeuAc give rise to an uncompetitive inhibition pattern versus CTP (Figure 2.9), consistent with the downstream binding of Me-O-NeuAc relative to CTP predicted for the Bi-Bi mechanism.

2.3.5 Relative Magnitudes of Some Microscopic Constants from Inhibition Data

The minimal kinetic mechanism for the *H. ducreyi* CMP-NeuAc synthetase consistent with the combined results is shown in Figure 2.10, together with expressions for several of the observed kinetic constants in terms of the individual rate constants and equilibrium constants within this scheme. Because of the complexity of the expressions, the initial velocity data alone provide little information regarding rate-limiting steps or the magnitudes of internal equilibrium steps. However, an examination of the expressions for the inhibition constants obtained in this study shows that analysis of the magnitudes and trends in these values provides some insight into the relative magnitudes of a few of the microscopic constants in the mechanism.

Consider first the expressions for the apparent K_{iiPPi} constants as a function of the nonvaried substrate concentration (Figure 2.10). In each expression, the right-hand factor is

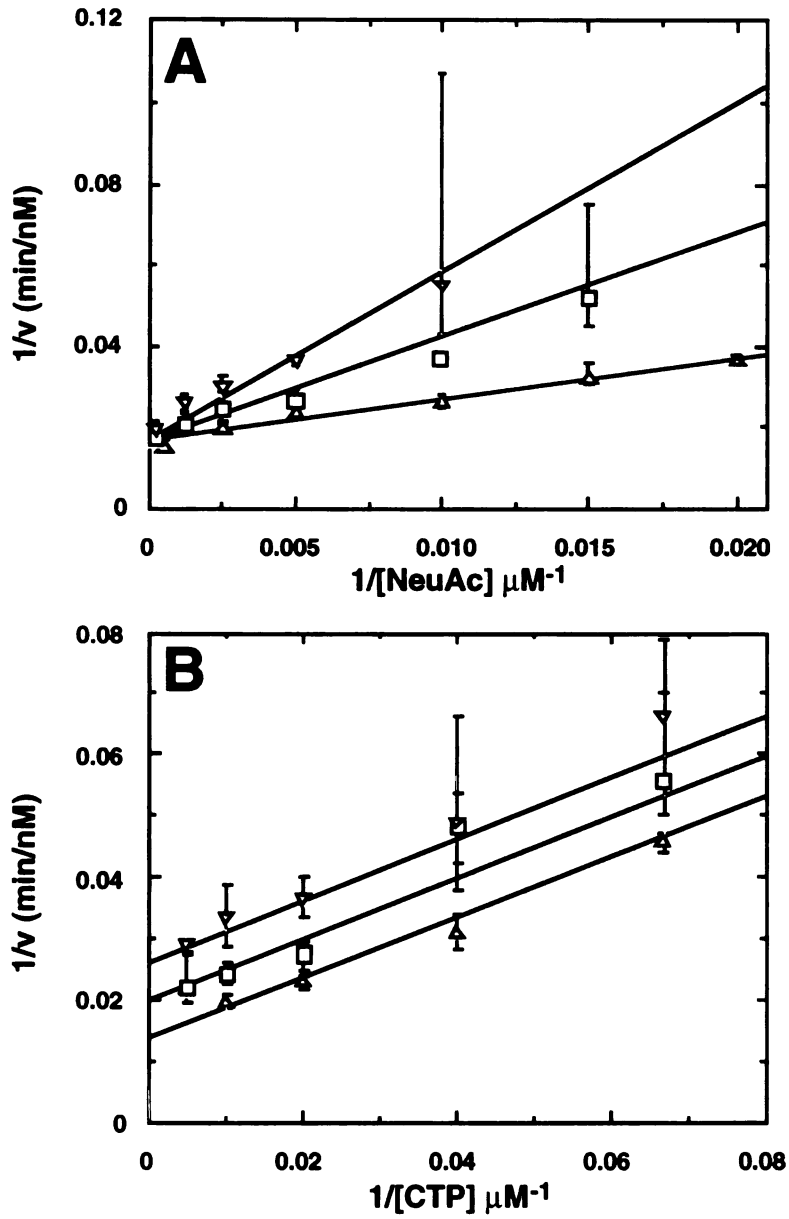

Figure 2.9 Inhibition of CMP-NeuAc synthetase by Me-O-NeuAc. (A) Double reciprocal plot with NeuAc as the varied substrate (50 - 4000 μM) at fixed Me-O-NeuAc concentrations of (Δ) 0 μM, (❑) 100 μM, (∇) 200 μM. CTP was held constant at 300 μM. The K_i was generated from the fit of the data to eq. 2 for competitive inhibition. (B) Double reciprocal plot with CTP as the varied substrate (15 - 200 μM) at fixed Me-O-NeuAc concentrations of (Δ) 0 μM, (❑) 125 μM, (∇) 250 μM. NeuAc was held constant at 300 μM. The data were fit to eq. 3 for uncompetitive inhibition.

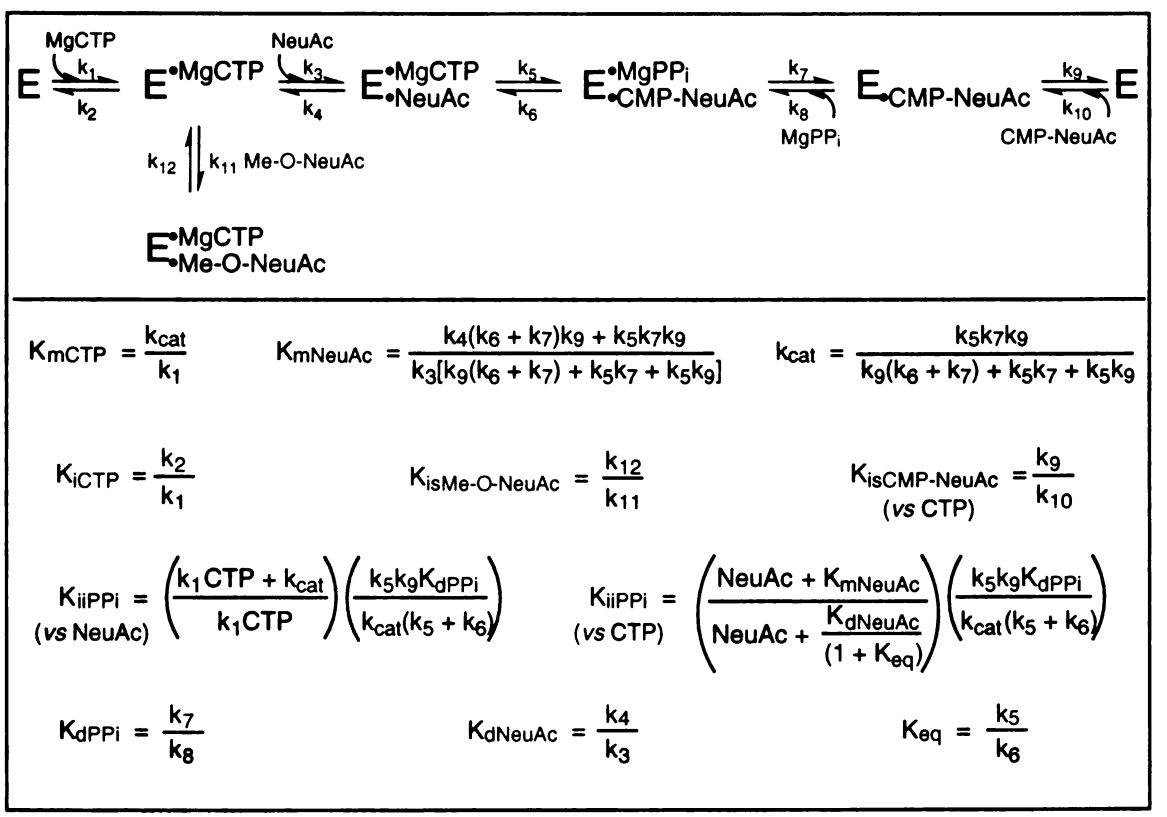

Figure 2.10 Minimal kinetic mechanism for CMP-NeuAc synthetase and expressions for observed kinetic constants.

the limiting value that would be observed when both substrates are fully saturating, while the other factor describes the expected trend in the apparent value as the concentration of the fixed substrate is varied. Comparison of these latter factors shows that while K_{iiPPi} versus NeuAc will always decrease to the limiting value as [CTP] increases, K_{iiPPi} versus CTP may *decrease* or *increase* to the limiting value as [NeuAc] increases, depending on the relative magnitudes of K_{mNeuAc} and the term $[K_{dNeuAc}/(1 + K_{eq})]$. If K_{mNeuAc} is smaller, K_{iiPPi} increases as [NeuAc] increases; if K_{mNeuAc} is larger, K_{iiPPi} decreases as [NeuAc] increases; and if the terms are equal, K_{iiPPi} is independent of [NeuAc]. By substitution of the values for k_{cat}, k_1 ($= k_{cat}/K_{mCTP}$, Figure 2.10), and [CTP] into the expression for the apparent K_{iiPPi} versus NeuAc in Figure 2.10, we estimate the limiting value for K_{iiPPi} to be 6.1 ± 1.7 mM. Comparison of this value with the data for K_{iiPPi} versus CTP in Table 2.2 shows an increase in the apparent value toward this limiting value as [NeuAc] increases, indicating that $K_{mNeuAc} < [K_{dNeuAc}/(1 + K_{eq})]$ and likewise that $K_{mNeuAc} < K_{dNeuAc}$. Analysis of the expression for K_{mNeuAc} in Table 2.3 indicates that the direction of this relationship is directly dependent on which step is rate limiting in k_{cat}. When the chemical step, k_5 is rate-limiting, $K_{mNeuAc} \geq K_{dNeuAc}$, and when dissociation of PP_i, k_7 is rate-limiting, $K_{mNeuAc} = [K_{dNeuAc}/(1 + K_{eq})]$. The only condition where K_{mNeuAc} can be less than $[K_{dNeuAc}/(1 + K_{eq})]$ is when k_9 is significantly rate-limiting. In addition, the observation of $K_{mNeuAc} < K_{dNeuAc}$ also indicates that the rate constant for dissociation of NeuAc, k_4, must be greater than the rate-limiting dissociation of product (Klinman and Matthews 1985). *Thus, the trend observed in the K_{iiPPi} data strongly suggests that dissociation of CMP-NeuAc, k_9, is the major rate-limiting step in this reaction and that $k_4 > k_9$.*

Another analysis supporting the conclusion that k_9 is significantly rate-limiting comes from a comparison of the rate constants for association and dissociation of CTP (k_1, k_2) with minimal estimates of the values for association and dissociation of CMP-NeuAc (k_9, k_{10}) derived from the observed equilibrium dissociation constant $K_{isCMP\text{-}NeuAc}$ (Figure 2.10, Table 2.2). From the expressions for K_{mCTP} and K_{iCTP} (which is extracted from the

Table 2.3 Simplified expressions for k_{cat} and K_{mNeuAc} for different rate-limiting steps in k_{cat}

rate-limiting step	k_{cat} =	K_{mNeuAc} =
all steps similar	$\frac{k_5 k_7 k_9}{k_3(k_5 + k_7) + k_5 k_7 + k_5 k_9}$	$\frac{k_4(k_6 + k_7)k_9 + k_5 k_7 k_9}{k_3[k_9(k_6 + k_7) + k_5 k_7 + k_5 k_9]}$
$k_5 << k_7, k_9$	$\frac{k_5 k_7}{k_5 + k_7}$	$K_{dNeuAc} + \frac{k_5 k_7}{k_3(k_6 + k_7)}$
$k_7 << k_5, k_9$	$\frac{K_{eq} k_7}{(1 + K_{eq})}$	$\frac{K_{dNeuAc}}{(1 + K_{eq})}$
$k_9 << k_5, k_7$	k_9	$\frac{k_9\{k_4[(k_6/k_7) + 1] + k_5\}}{k_3 k_5}$

initial velocity data as K_{ia} in eq. 1), we calculate values for k_1 and k_2 of 1.7×10^5 M^{-1} s^{-1} and 7.6 s^{-1}, respectively. By comparison, if dissociation of CMP-NeuAc is completely rate-limiting in k_{cat}, that is $k_9 \approx 1.8$ s^{-1}, the minimal value for the association rate constant for CMP-NeuAc, k_{10} is 1.4×10^5 M^{-1} s^{-1}, a value remarkably close to that of k_1 and consistent with the substantial retention of the CTP structure in CMP-NeuAc. If k_9 were not at least partially rate-limiting, the values for both k_9 and k_{10} would be at least 10-fold larger than these minimal values, and hence, larger than the rate constants for CTP binding, which seems less likely considering the increased bulk and number of potential hydrogen bonding interactions in the structure of CMP-NeuAc compared with CTP. Thus the data provide a self-consistent indication that the dissociation of CMP-NeuAc is significantly rate-limiting in the forward reaction.

One additional piece of information that falls out of the product and dead-end inhibition data is that the magnitude of K_{dNeuAc} is somewhat larger than the corresponding dissociation constant measured for the highly similar analog Me-O-NeuAc. Rearrangement of the expression for K_{iiPPi} versus CTP, and substitution of the limiting and measured values yields the relationship $K_{dNeuAc}/K_{mNeuAc} = (1 + K_{eq})(10 \pm 6)$, which translates into $K_{dNeuAc}/K_{isMe\text{-}O\text{-}NeuAc} \approx (1 + K_{eq})(10 \pm 6)$ since K_{mNeuAc} (~ 76 μM) ≈ $K_{isMe\text{-}O\text{-}NeuAc}$ (~ 64 μM). This indicates that the analog binds at least (10 ± 6)-fold more tightly than the substrate to the E•CTP complex, but the disparity could be substantially larger if the internal equilibrium of the chemical conversion step lies far to the right ($K_{eq} \geq 1$). Thus, it is of interest to consider what factors could enhance the binding of Me-O-NeuAc versus NeuAc and to what extent. Referring to the structure of β-NeuAc in Figure 1.4, the only difference between it and Me-O-NeuAc is the replacement of the hydrogen on the reactive anomeric oxygen by a methyl group. Three properties change as a result of this replacement: (1) the steric bulk at the reactive oxygen, (2) the solvation of -OH versus -OR, and (3) the ability to anomerize. Because it increases the steric bulk at the reactive center, the methyl group might be expected to decrease the binding affinity of the analog rather than increasing it.

However, if the active site can accommodate the extra bulk, the methyl group could enhance the affinity to a small extent since the -OMe should require less desolvation than the -OH group upon binding to the active site; desolvation of the -OH would be expected since this group, in its deprotonated state, acts as a nucleophile in the reaction. Although this has not been shown explicitly for the *H. ducreyi* enzyme, retention of the ^{18}O label in the anomeric hydroxyl upon conversion of 2-[^{18}O]-β-NeuAc to CMP-NeuAc has been demonstrated using the *E. coli* enzyme (Ambrose et al. 1992). The third property altered by the presence of the methyl group is the stability of the β-configuration at the anomeric carbon. The Me-O-analog is a stable β-glycoside, while NeuAc is a hemiketal that can undergo anomerization. Once again however, this should only increase the K_{dNeuAc} versus the $K_{isMe\text{-}O\text{-}NeuAc}$ by a minor amount, since at equilibrium, approximately 93% of the NeuAc is present as the correct β-anomer (Ambrose et al. 1992). With only these two small factors expected to enhance the affinity of the analog versus the substrate for the enzyme, it seems unlikely that the affinities for the two would differ by much more than an order of magnitude. This then leads to the prediction that the internal equilibrium constant for the chemical conversion step, K_{eq}, does not deviate too far from a value of one, a common result found for many enzymes.

2.3.6 Relationship to Other CMP-NeuAc Synthetases

Having established a mechanism for the *H. ducreyi* CMP-NeuAc synthetase, one would like to know whether this mechanism is conserved throughout the larger CMP-NeuAc synthetase family and whether specific members of this family can be considered as appropriate targets for drug design. Since the biosynthetic pathways leading to the synthesis of sialic acid-containing glycoconjugates in both prokaryotes and eukaryotes require the formation of CMP-NeuAc as the activated sugar donor, the feasibility of developing inhibitors that selectively target, for example, CMP-NeuAc synthetase from

pathogenic bacteria over the human host's enzyme, will require the existence of some notable differences in their properties. Despite the limited information regarding the kinetic and mechanistic properties of this enzyme family, at least a couple of comparisons can be made. Examination of alignments of seven of the eleven reported gene sequences reveals two subgroups, proteins approximately 225 amino acids in length, including those from pathogenic strains of *Haemophilus* and *Neisseria* spp. and proteins over 400 amino acids in length, including those from *E. coli*, *Streptococcus agalactiae*, and *Campylobacter coli* (Tullius et al. 1996), but perhaps most importantly, the first full mammalian sequence to be reported from mouse (Münster et al. 1998). Complete conservation of several residues in the whole family, including a lysine (K19) identified in the CTP binding site of the *H. ducreyi* enzyme (Tullius et al. 1999) suggests similar chemical mechanisms of catalysis in the two groups. However, the observation of micromolar K_m values for the smaller enzymes (Samuels et al. 1999; Tullius et al. 1996; Warren and Blacklow 1962) compared with millimolar values reported for some of the larger enzymes (Haft and Wessels 1994; Liu et al. 1992; Vann et al. 1993), as well as the 64 μM $K_{isMe\text{-}O\text{-}NeuAc}$ value reported here for the *H. ducreyi* enzyme versus a value of 2.5 mM for the *E. coli* enzyme (Schmid et al. 1988), suggests that there may be exploitable kinetic differences between these groups of enzymes. In addition, the cellular location of the bacterial versus the mammalian enzymes may provide a further selective advantage, since the bacterial enzymes are cytoplasmic, while the mammalian enzymes are located in the nucleus (Münster et al. 1998). These observations, together with the kinetic picture developed in this work provide a framework for further investigation of this group of enzymes.

CHAPTER 3.

Probing the Active Site Topography and Ligand-Induced Conformational Changes by Limited Proteolysis and Amide Hydrogen Exchange of Cytidine 5'-Monophosphate N-acetylneuraminic Acid Synthetase

3.1 INTRODUCTION

In the previous chapter, steady state kinetic analyses of CMP-NeuAc synthetase demonstrated that the enzyme catalyzes the activation of sialic acid by a sequential ordered kinetic mechanism, where CTP is bound before NeuAc and CMP-NeuAc is released after pyrophosphate (Samuels et al. 1999). Currently, no crystal structure is available for any member of this enzyme family. Therefore, an aim of this study was to gain additional insight into structural aspects of CMP-NeuAc synthetase and potentially reveal the origin of its sequential ligand associations and dissociations. The current chapter describes the employment of mass spectrometric approaches to evaluate the effects of ligand binding on the limited proteolysis and amide hydrogen exchange of CMP-NeuAc synthetase in an effort to identify regions of the active site and to detect potential ligand-induced changes in protein conformation. Under limiting conditions, proteolysis preferentially occurs in areas with increased segmental mobility and hence, is likely to explore highly exposed surface loops, domain linkers, and/or flexible hinges in proteins (Fontana et al. 1986; Hubbard 1998). In contrast, amide hydrogen exchange has the capacity to explore all solvent accessible surfaces of a native protein (Englander et al. 1985; Smith et al. 1997; Woodward et al. 1982; Zhang and Smith 1993). The combination of these powerful techniques with matrix assisted laser desorption ionization (MALDI) mass spectrometry provided a

sensitive probe of the global structure and dynamics of CMP-NeuAc synthetase as well as an easy means to spatially resolve segments of the backbone influenced by ligand binding.

More specifically, variations in the proteolytic fragmentation patterns and the extent of deuterium exchange of CMP-NeuAc synthetase as a result of binding CMP-NeuAc alone, MgCTP and/or the competitive inhibitor, Me-O-NeuAc were evaluated. In all, combinations of the ligands retaining features of the nucleotide at minimum significantly hindered the general proteolysis of CMP-NeuAc synthetase by trypsin and endoproteinase Glu-C. However, the combined presence of the nucleotide and sugar were required to detect a measurable decline in the global exchange of backbone amides of CMP-NeuAc synthetase as well. Several regions of the protein protected from amide exchange and proteolysis upon ligand binding were identified and mapped to the equivalent segments of the three dimensional structure for the capsule-specific cytidine 5'-monophosphate 2-keto-3-deoxyoctonate (CMP-KDO) synthetase from *E. coli*, a member of a sugar-activating family of enzymes related to CMP-NeuAc synthetases (Jelakovic et al. 1996). In addition, these data suggest the occurrence of an ligand-induced change in the conformation of CMP-NeuAc synthetase leading to a more compact structure with a reduced solvent accessible surface.

3.2 MATERIALS AND METHODS

3.2.1 Materials

ACTH(1-24), CTP, CMP-NeuAc, MOPS, $MgCl_2$, pepsin (porcine mucosa) and trypsin (sequencing grade) and SDS-PAGE ultra low molecular weight markers were purchased from Sigma Chemicals. Endoproteinase Glu-C (sequencing grade) was purchased from Boehringer Mannheim. Me-O-NeuAc was purchased from Glyco-Tech. 3,5-Dimethoxy-4-hydroxy-cinnamic acid, α-cyano-4-hydroxycinnamic acid and deuterium

oxide (100 atom %D) were purchased from Aldrich. Capillary Zone Electrophoresis peptide standard kit, P6 SEC gel, sample buffer, running buffer and SDS-PAGE ready gels were purchased from Bio-Rad. TFA was purchased from Pierce. Fast Stain was purchased from Zoion Biotech and SepPak Plus C18 Cartridges were obtained from Waters.

3.2.2 Methods

3.2.2.1 *Preparation and Digestion of CMP-NeuAc Synthetase*

The over-expression in *E. coli* and purification of CMP-NeuAc synthetase has been previously described (Tullius et al. 1996). The enzyme was desalted into 100 mM MOPS pH 7.5 with a P6 gel filtration column, lyophilized and stored at -10 °C. Prior to use, the protein was reconstituted in water to yield 21.1 mg/mL CMP-NeuAc synthetase in 200 mM MOPS pH 7.5. Aliquots of the concentrated enzyme were complexed with various combination of ligands, at a ten-fold excess of their final concentrations, in 200 mM MOPS pH 7.5 for 15 minutes at room temperature. Following a dilution of the pre-complexed CMP-NeuAc synthetase (15 µL) into water (135 µL), an aliquot (16.5 µL) of 10-X protease in 20 mM MOPS pH 7.5 was added to separate microcentrifuge tubes containing various combinations of the ligands to yield the following conditions: 1.33 mg/mL CMP-NeuAc synthetase, 0.9 mM Me-O-NeuAc, 450 µM CTP, 135 µM CMP-NeuAc, 18 mM $MgCl_2$, 20 mM MOPS pH 7.5 with 27 µg/mL trypsin or 111 µg/mL endoproteinase Glu-C. CMP-NeuAc synthetase was digested at 25 °C up to 90 minutes.

3.2.2.2 *SDS-PAGE Analysis of Proteolytic Fragments*

For the analysis of the proteolytic fragments of CMP-NeuAc synthetase, reactions were terminated by mixing 7 µL of digested protein with 14 µL of Tris-Tricine sample buffer and boiling for 5 minutes. Proteolytic digests (10-15 µL/lane) were resolved on

16.5% Tris-Tricine ready gels at 100 mV for 135 minutes. All gels were fixed with a solution of 45% methanol/10 % acetic acid and visualized with Fast Stain.

3.2.2.3 *MALDI Mass Spectrometric Analysis of Proteolytic Fragments*

Aliquots of the digestion reaction were terminated by combining the digested protein with an equal volume of 0.20 % TFA. 0.5 µL of quenched protein was mixed with 0.5 µL of 20 mg/mL sinapinic acid in acetonitrile:ethanol:0.1 % TFA (1:1:1, v/v/v)on a MALDI target. All data were acquired on a PerSeptive Biosystems Voyager-DE time-of-flight linear mass spectrometer in the positive ion mode. Mass spectra were smoothed twice by a 19 point Savitsky-Golay function and average masses were assigned by centroiding the top 30% of the peak heights. All mass spectra were calibrated both externally and internally with the singly and doubly charged molecular ions for the native CMP-NeuAc synthetase. The sequences of all proteolytic fragments of CMP-NeuAc synthetase were determined based on average masses measured by MALDI mass spectrometry and the specificity of the individual proteases.

3.2.2.4 *Preparation of Pre-Complexed CMP-NeuAc Synthetase*

An ammonium sulfate suspension of the enzyme was desalted into 100 mM MOPS pH 7.1 with a P6 gel filtration column. Individual aliquots of the desalted enzyme were lyophilized and stored at -10 °C. Prior to use, CMP-NeuAc synthetase was reconstituted in water to yield a 21.1 mg/mL solution in 200 mM MOPS pH 7.1. Next, the concentrated enzyme solution was diluted with buffer containing selected ligands and equilibrated for 10 minutes at room temperature prior to exchange in D_2O. For studies with unliganded CMP-NeuAc synthetase, only 200 mM MOPS was added.

3.2.2.5 *Deuterium Exchange of CMP-NeuAc Synthetase*

The strategies employed throughout this study are outlined in Figure 3.1. Isotopic exchange of amide hydrogens was initiated by the dilution of 4 μL of the unliganded or precomplexed enzyme into 36 μL of 100 % atom D_2O. The final conditions for the exchange reaction were: 1.48 μg/μL CMP-NeuAc synthetase in 20 mM MOPS with a combination of 1.0 mM Me-O-NeuAc, 20 mM $MgCl_2$, 500 μM CTP or 150 μM CMP-NeuAc in 90% D_2O. For analysis at the protein level, 10 μL of the exchanged protein was mixed with 10 μL of 0.12% TFA on ice. Immediately, 2 μL of the acidified protein was mixed with 8 μL of 20 mg/mL 3,5-dimethoxy-4-hydroxy-cinnamic acid in ethanol:acetonitrile:0.1% TFA on ice. For analysis at the peptide level, the exchange reaction was terminated and proteolysis initiated in one step by mixing 10 μL of exchanged protein (1.48 μg/μL) with 10 μL of 3.86 μg/μL pepsin in 0.12% TFA that had been chilled on ice. Following a 1 minute digestion, 2 μL of the peptide mixture was mixed with 8 μL of 20 mg/mL α-cyano-4-hydroxycinnamic acid in ethanol:acetonitrile:0.10 % TFA (1:1:1, v/v/v) on ice. Whether analyzing the whole protein or digest, 1 μL of each acidified solution containing matrix was spotted on a MALDI target (at room temperature) and dried within 10 seconds and promptly analyzed by mass spectrometry. Mass spectra of all peptide samples were acquired within an average of 7 minutes after the deposition of the matrix containing solution on the MALDI target, whereas analysis of protein samples averaged 15 minutes.

3.2.2.6 *Total Deuterium Exchange and In-Exchange of CMP-NeuAc Synthetase*

To determine the maximal number of deuteriums solely retained in backbone amides ($N_{observed}$), it was necessary to measure both $N_{100\%}$ and $N_{In\text{-}Exchange}$ (Equation 2). Figure 3.2 illustrates the sites expected to undergo isotopic exchange during each control experiment. To determine the total number of hydrogens capable of isotopic exchange ($N_{100\%}$), CMP-NeuAc synthetase (1.64 μg/μL) was incubated in 100 atom % D_2O in 20 mM MOPS for

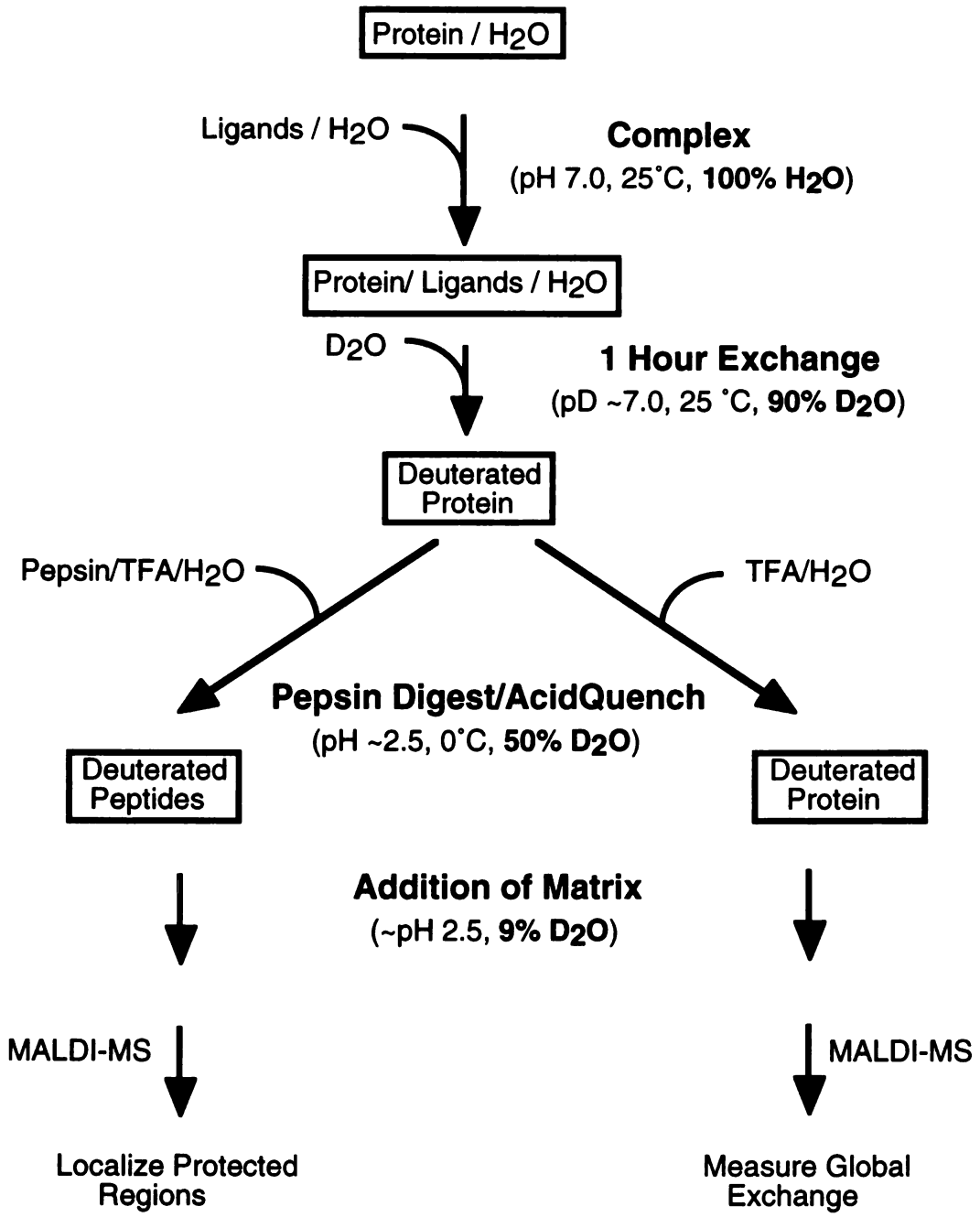

Figure 3.1 Diagram of the amide hydrogen exchange protocol for the measurement of deuterium incorporated into CMP-NeuAc synthetase and the peptic digestion products.

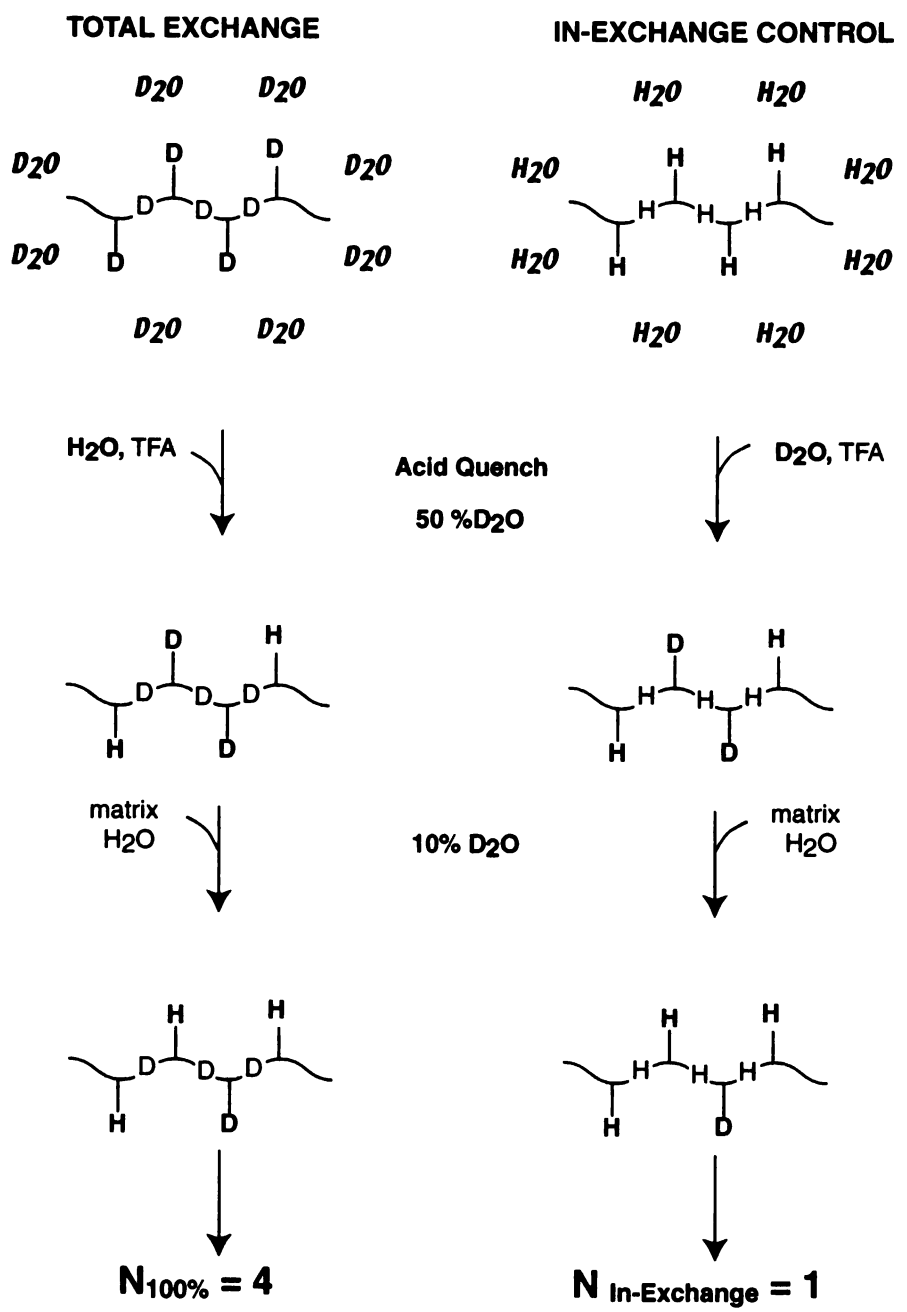

Figure 3.2 Comparison of locations and quantity of deuteriums incorporated into CMP-NeuAc synthetase during total exchange and in-exchange experiments. In this example, a total 4 deuteriums are retained in both C_α amides and side chain groups of the protein following complete exchange. However, the in-exchange control revealed the portion of deuterium exclusively incorporated into residue side chains during manipulations at low pH in the presence of residual D_2O.

68 hours at 55 °C. The completely exchanged enzyme was mixed with an equal volume of an ice cold solution of 0.12 % TFA, prior to combining with matrix, adhering to the same condition as above. To quantitate the number of deuteriums exchanged into the protein during the acid quench and matrix mixing steps ($N_{In\text{-}Exchange}$), the enzyme was instead reconstituted in 20 mM MOPS in water and quenched with 0.12 % TFA in D_2O (100 atom % D) and immediately analyzed by mass spectrometry.

In analogous control experiments, $N_{100\%}$ and $N_{In\text{-}Exchange}$ were also determined for each peptide of the pepsin digest. Ideally, $N_{100\%}$ could be measured for an individual peptide derived from the digestion of CMP-NeuAc synthetase that had been completely exchanged under harsh conditions, however, the denatured enzyme is not efficiently digested by pepsin. Therefore, a solution containing the predigested CMP-NeuAc synthetase was prepared and completely exchanged by the following protocol. A chilled solution of 1.48 mg/mL CMP-NeuAc synthetase in 20 mM MOPS pH 7.1 was digested on ice with an equal volume of 0.80 mg/mL pepsin in 0.12 % TFA on ice for 5 minutes. The resulting peptides were quickly loaded onto a chilled Sep-Pak Plus C18 cartridge and washed with ice-cold 0.10 % TFA, then eluted with 90 % acetonitrile containing 0.10 % TFA. Following an initial lyophilization, the peptide mixture was repeatedly dissolved in water and lyophilized to remove residual TFA. The predigested CMP-NeuAc synthetase was reconstituted in 100 atom % D D_2O containing 20 mM MOPS and exchanged for 6.5 hours at 85 °C. To mimic the exact condition during the digestion of the enzyme, the fully exchanged mixture of peptides was mixed with an equal volume of an ice-cold solution of 0.12 % TFA and incubated on ice for 1 minute, prior to addition of the matrix and analysis by MALDI-MS. To determine the average number of deuteriums exchanged into each peptide solely during the pepsin digestion and matrix mixing steps ($N_{In\text{-}Exchange}$), predigested CMP-NeuAc was instead reconstituted in 20 mM MOPS in water and quenched with 0.12 % TFA in 100 atom %D D_2O.

3.2.2.7 *MALDI Mass Spectrometric Analysis of Exchanged CMP-NeuAc Synthetase and Peptide Mixture*

To quantitate the number of amide hydrogens incorporated into CMP-NeuAc synthetase and its digestion products, samples were analyzed on a PerSeptive Biosystems Voyager DE MALDI time-of-flight mass spectrometer in the positive ion mode. All mass spectra were smoothed 1-2 times with a 19 point Savitsky-Golay function and calibrated externally with 2 points using undeuterated CMP-NeuAc synthetase or a mixture of angiotensin II and ACTH(1-24) with one exception. The mass spectrum of the protein digest was calibrated internally using the average calculated masses of peptides that had been previously sequenced by MALDI-PSD (M_r = 819.0, 1073.3, 1414.7, 1698.0, 2494.1 and 3020.7 Da) to obtain accurate mass measurements (M_r, Table 3.1). Average masses of were assigned by centroiding the top 30% of the peak height of unresolved isotopic clusters. The total number of deuteriums incorporated into CMP-NeuAc synthetase and the peptic peptides was calculated using Equations 1 and 2, where $M_{0\%}$ is the average mass with natural isotopic distributions, M_t is the average mass following deuterium exchange for t minutes, $M_{100\%}$ is the average mass following the complete exchange of all hydrogens bonded to heteroatoms, and $M_{InExchange}$ is the average mass after the in-exchange of deuterium exclusively into side chain groups.

Equation 1 $$N_t = M_t - M_{0\%}$$

Equation 2 $$N_{observed} = M_{100\%} - M_{In\ Exchange}$$

Each measurement is the average of 2 - 4 separate trials. Peptic peptides of CMP-NeuAc synthetase were identified by direct sequencing with MALDI-PSD on a Voyager Elite and a

Voyager DE STR (PerSeptive Biosystems) or using a combination of the measured mass and the observed specificity of pepsin.

3.3 RESULTS

3.3.1 SDS-PAGE Analysis of Proteolytic Digest of CMP-NeuAc Synthetase

As a first step, the proteolysis of the apo-enzyme by trypsin and endoproteinase Glu-C was monitored as a function of time in an attempt to map the surface of CMP-NeuAc synthetase. Using a 49:1 ratio of CMP-NeuAc synthetase:trypsin, the digestion reaction generated 4 bands ranging from ~14-25 kDa in size over a period of 60 minutes (Figure 3.3A). To obtain additional cleavage sites, the enzyme was also digested with endoproteinase Glu-C and analyzed by SDS-PAGE. With a ratio of CMP-NeuAc synthetase: endoproteinase Glu-C of nearly 12:1, digestion of the intact protein appeared to produce a single fragment of approximately 15 kDa after a 90 minute reaction (Figure 3.4A).

To assess global changes in the digestibility of CMP-NeuAc synthetase attributed to ligand binding, the proteolytic fragments of the free enzyme were compared to those derived from the enzyme complexed with various molecules. Under the chosen experimental conditions, the concentration of each ligand was at least 10-fold in excess of its respective dissociation constant, and therefore the active site of CMP-NeuAc synthetase was saturated (Samuels et al. 1999). SDS-PAGE analysis revealed that the addition of the sugar analog alone resulted in digestion patterns identical to those from the apo-enzyme (Figure 3.3B). Conversely, the presence of CMP-NeuAc or CTP provided CMP-NeuAc synthetase significant global protection from digestion by trypsin compared to the free enzyme. With these ligands bound, further degradation of the 15 and 17 kDa tryptic fragments were suppressed as well. Similarly, the sole addition of CMP-NeuAc or the nucleotide alone or

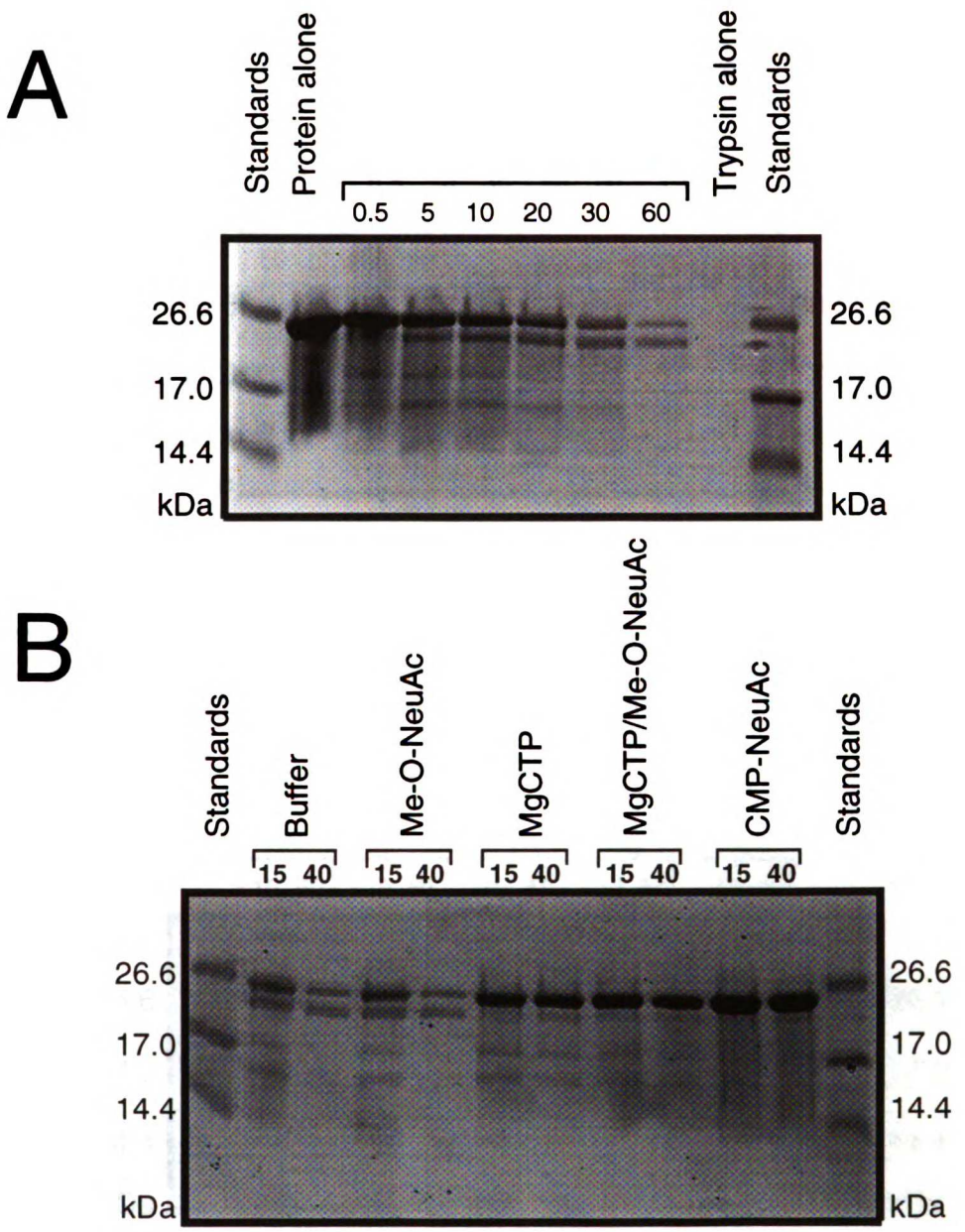

Figure 3.3 SDS-PAGE analysis of tryptic digests of CMP-NeuAc synthetase. (A) CMP-NeuAc synthetase (1.33 mg/mL) was digested with trypsin (27 µg/mL) at 25 °C over 60 minutes. (B) The enzyme digested in the presence of buffer alone (200 mM MOPS) or in the presence of buffer plus the following additives: 0.9 mM Me-O-NeuAc, 450 µM CTP/18 mM $MgCl_2$, 450 µM CTP/0.9 mM Me-O-NeuAc/18 mM $MgCl_2$ or 135 µM CMP-NeuAc for 15 and 40 minutes.

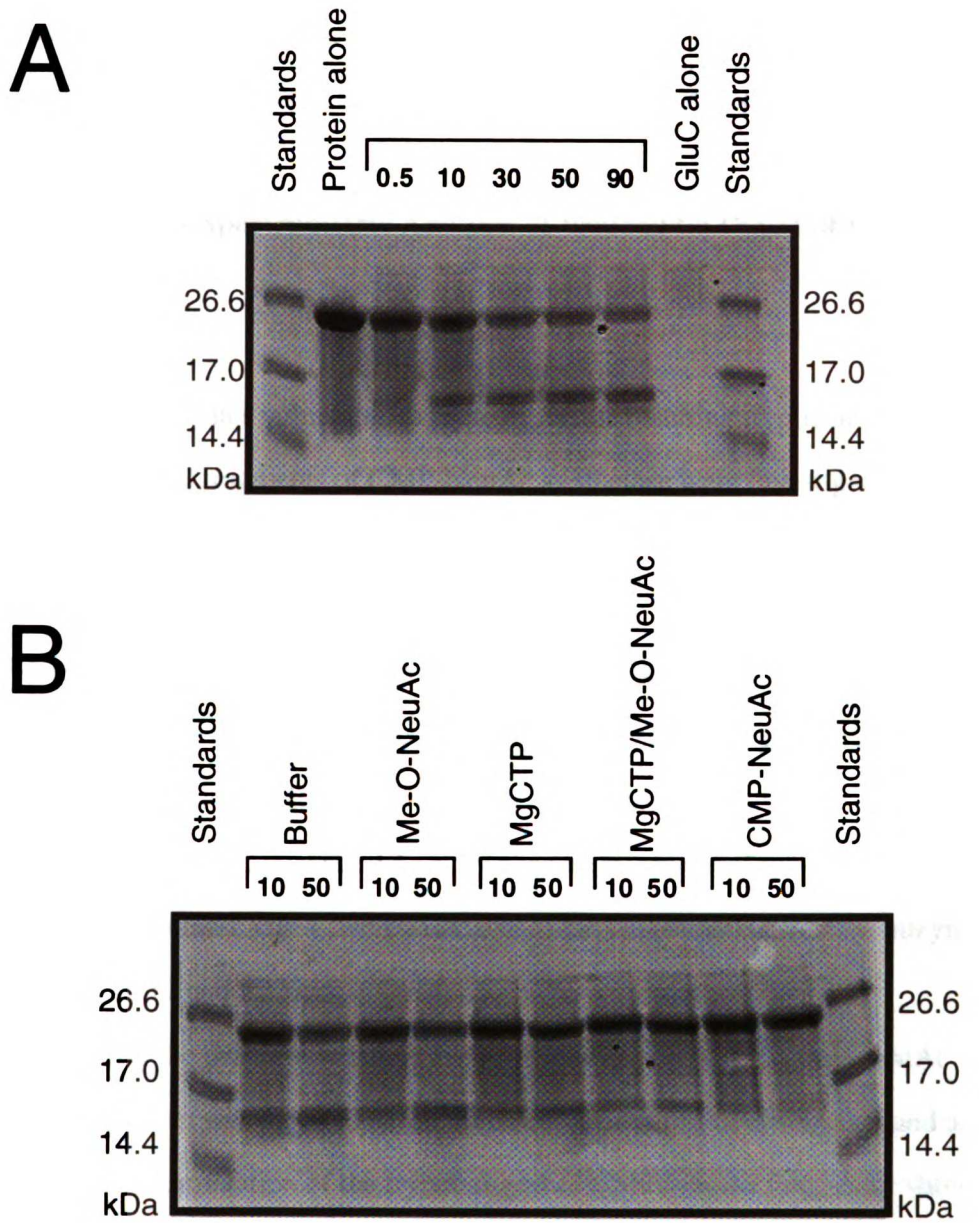

Figure 3.4 SDS-PAGE analysis of endoproteinase Glu-C digests of CMP-NeuAc synthetase. (A) CMP-NeuAc synthetase (1.33 mg/mL) was digested with endoproteinase Glu-C (111 μg/mL) at 25 °C over 90 minutes. (B) The enzyme digested in the presence of buffer alone (200 mM MOPS) or in the presence of buffer plus the following additives: 0.9 mM Me-O-NeuAc, 450 μM CTP/18 mM $MgCl_2$, 450 μM CTP/0.9 mM Me-O-NeuAc/18 mM $MgCl_2$ or 135 μM CMP-NeuAc for 10 and 50 minutes.

in conjunction with Me-O-NeuAc provided the enzyme some protection from endoproteinase Glu-C compared to the addition of sugar analog or buffer (Figure 3.4B).

3.3.2 MALDI Mass Spectrometric Analysis of Proteolytic Digest of CMP-NeuAc Synthetase

To identify all sites vulnerable to proteolysis, the resulting tryptic and endoproteinase Glu-C fragments of CMP-NeuAc synthetase were investigated by MALDI-MS. The analysis of the tryptic digest of the free enzyme led to the identification of 9 fragments (Figure 3.5), compared to 5 observed by SDS-PAGE analysis alone. Digestion of CMP-NeuAc synthetase with trypsin produced a total of 5 and 4 fragments resulting from single and double cleavages, respectively. The sites susceptible to cleavage by trypsin include K17, K19, K140 and R162. Conversely, the proteolysis of CMP-NeuAc synthetase with endoproteinase Glu-C generated 4 singly cleaved fragments (Figure3.6). The sites favored by endoproteinase Glu-C were exclusive to the C-terminal half of the enzyme and included E145, E217 and E223.

To identify the protease sensitive sites shielded in complexed CMP-NeuAc synthetase, the protein was digested in the presence of mixtures of the ligands and analyzed by MALDI-MS. Examination of the tryptic digest of CMP-NeuAc synthetase showed the binding of CTP with and without Me-O-NeuAc resulted in the disappearance of peaks A, B, D, E, G and H (Figure 3.5). Cleavage sites protected by the nucleotide alone or with the sugar analog corresponded to K17 and K19. However, the addition of CMP-NeuAc renders the enzyme completely resistant to proteolysis by trypsin. Analysis of the endoproteinase Glu-C digestion of CMP-NeuAc synthetase also revealed that addition of CTP with and without Me-O-NeuAc hampered proteolysis of the intact protein, significantly delaying the appearance of peaks A, B, C and D (Figure 3.6). Collectively, cleavage at E145, E217 and E223 by endoproteinase Glu-C was impeded when CMP-

Figure 3.5 MALDI-MS spectra of tryptic digest of CMP-NeuAc synthetase. (A) The enzyme digested with trypsin at 25 °C for 17 minutes in the presence of buffer alone (200 mM MOPS) or in the presence of buffer plus the following additives: 0.9 mM Me-O-NeuAc, 450 μM CTP/18 mM $MgCl_2$, 450 μM CTP/0.9 mM Me-O-NeuAc/18 mM $MgCl_2$ or 135 μM CMP-NeuAc. MH^+ and MH^{+2} represent the singly and doubly charged molecular ions for the intact protein. (B) Summary of all sites in CMP-NeuAc synthetase susceptible to cleavage by trypsin.

A

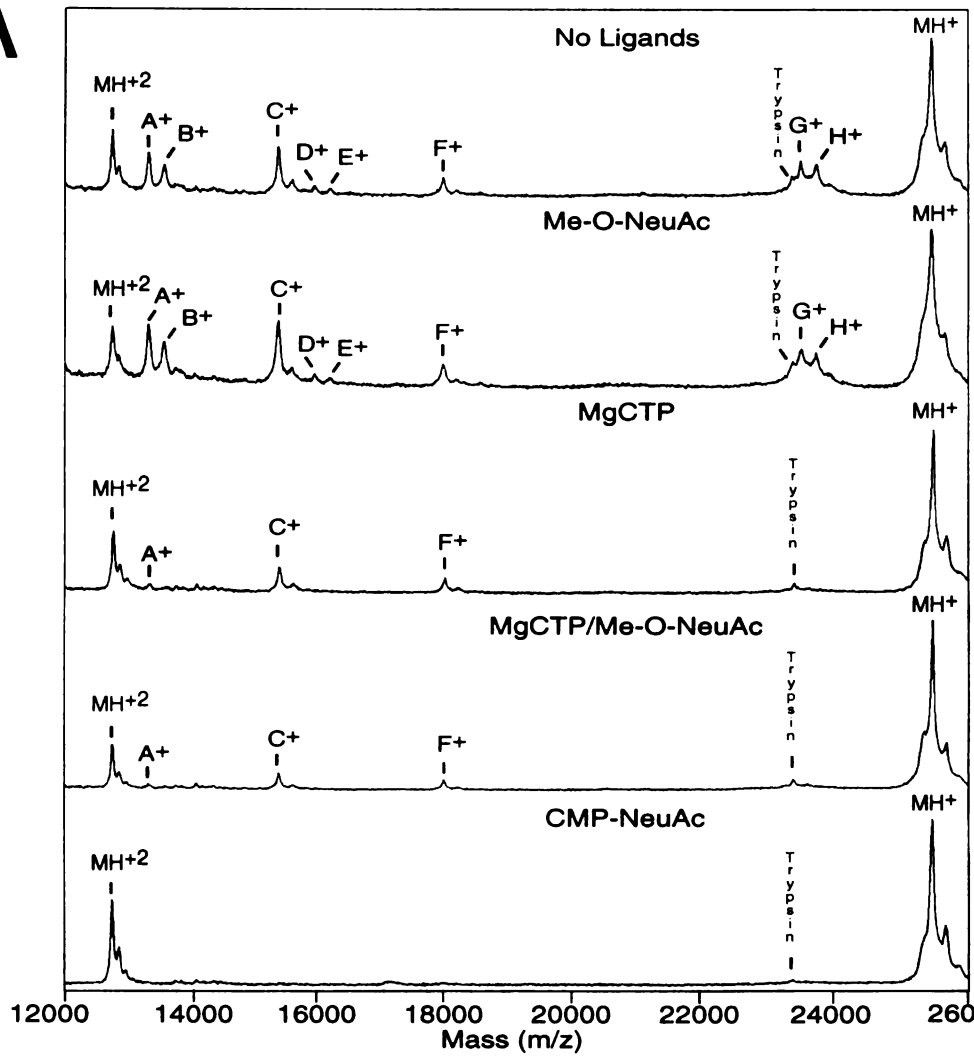

B

	Observed Fragments	M_r (average)
	141 — 227	10,172 *
A	20 — 140	13,279
B	18 — 140	13,523
C	1 — 140	15,287
D	20 — 162	15,850
E	18 — 162	16,093
F	1 — 162	17,858
G	20 — 227	23,433
H	18 — 227	23,676
	1 — 227	25,441

* Data not shown

Figure 3.6 MALDI-MS spectra of endoproteinase Glu-C digests of CMP-NeuAc synthetase. (A) The enzyme digested with endoproteinase GluC at 25 °C for 13 minutes in the presence of buffer alone (200 mM MOPS) or in the presence of buffer plus the following additives: 0.9 mM Me-O-NeuAc, 450 μM CTP/18 mM $MgCl_2$, 450 μM CTP/0.9 mM Me-O-NeuAc/18 mM $MgCl_2$ or 135 μM CMP-NeuAc. MH^+ and MH^{+2} represent the singly and doubly charged molecular ions for the intact protein. (B) Summary of all sites in CMP-NeuAc synthetase susceptible to cleavage by endoproteinase Glu-C.

A

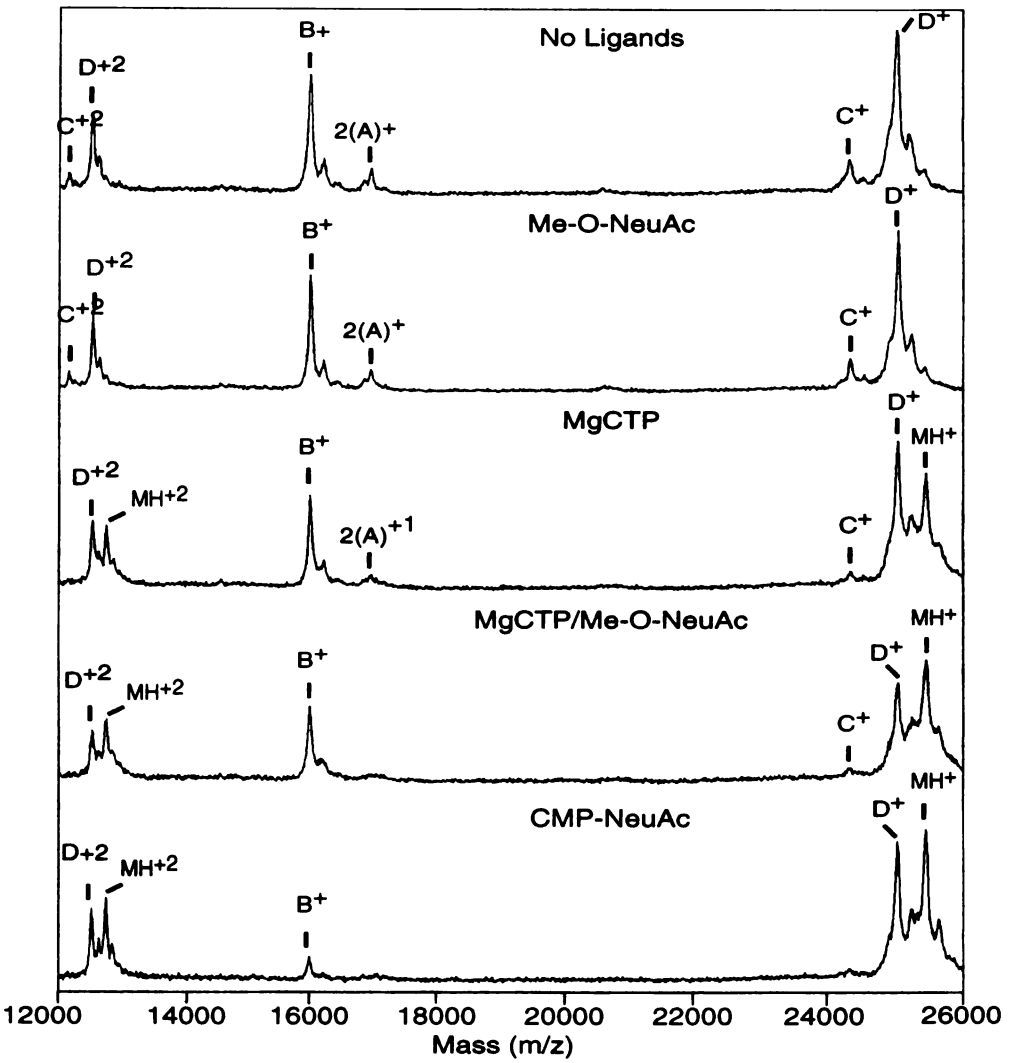

B

	Observed Fragments	M_r (average)
A	146 — 217	8,414
B	1 — 145	15,876
C	1 — 217	24,272
D	1 — 223	25006
	1 — 227	25,441

NeuAc and CTP alone or in conjunction with Me-O-NeuAc occupied the active site of the enzyme.

3.3.3 Global Exchange of CMP-NeuAc Synthetase

To probe the structure and dynamics of the *H. ducreyi* CMP-NeuAc synthetase, the isotopic exchange of the backbone amide hydrogens was investigated using mass spectrometry. First, the maximum number of hydrogens bonded to heteroatoms in CMP-NeuAc synthetase capable of isotopic exchange was determined under denaturing conditions at neutral pH (Figure 3.2). A total of 215 deuteriums ($N_{100\%}$) were incorporated into the enzyme and it had appeared that 99% of the non-proline amides had exchanged under these conditions (Figure 3.7). To assure the experimental conditions mostly survey the exchange of main chain amides of CMP-NeuAc synthetase, all hydrogens bonded to heteroatoms capable of exchange at low pH were measured in an in-exchange control study (Figure 3.2). In this experiment, an average of 59 deuteriums ($N_{In\text{-}Exchange}$) were found to incorporate into the enzyme exclusively during the acid quench and matrix mixing steps (Figures 3.7). Backbone amide hydrogen exchange rates are considerably suppressed under acidic conditions (pH 2-3), however, isotopic exchange of side chain groups remains considerable (Bai et al. 1993; Smith et al. 1997). Therefore, the increase in mass during the in-exchange control experiment results from the continued exchange of residue side chains, which are expected to rapidly reach an equilibrium with the solvent to reflect the final deuterium content. Following the subtraction of the background in-exchange of deuterium into side chain groups, a total of 156 deuteriums ($N_{observed}$) were determined to be solely retained in backbone amides, which represented 72% of all non-proline backbone amides in CMP-NeuAc synthetase (Figure 3.7). Since the amount of artifactual in-exchange is relatively modest, this value was not subtracted from subsequent measurements of deuterium incorporation (N_t) for the sake of simplicity.

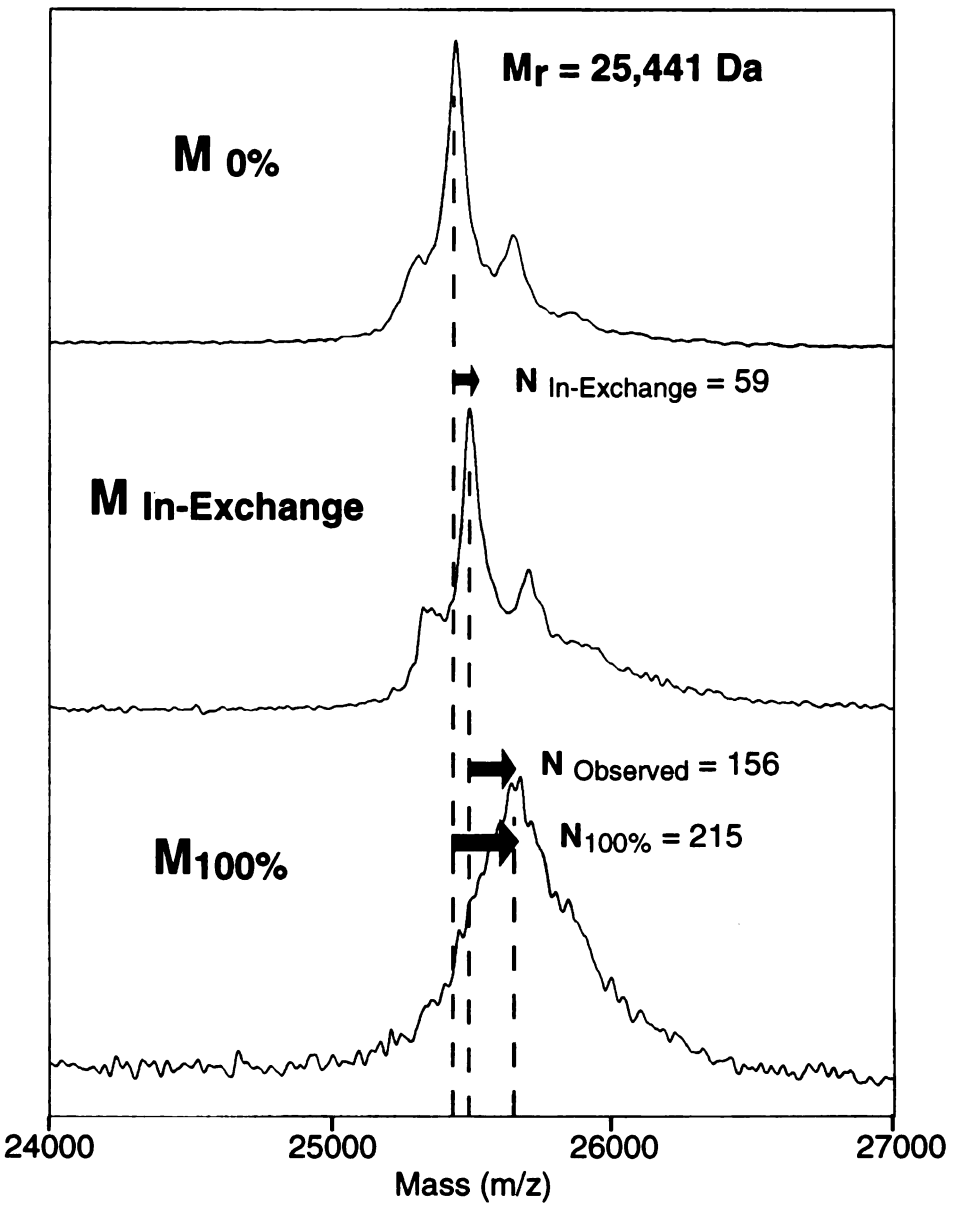

Figure 3.7 MALDI-MS spectra of CMP-NeuAc synthetase with varied isotopic distributions. The spectrum of CMP-NeuAc synthetase was recorded in solutions of natural isotopic abundance. The intact protein was analyzed following in-exchange and total exchange control experiments for the determination of $M_{in\text{-}exchange}$ and $M_{100\%}$.

To determine an adequate incubation time for the amide exchange studies, deuterium incorporation for the intact protein was measured as a function of time. Within one hour, the exchange reaction had reached an equilibrium, resulting in the exchange of an average of 145 amides ($N_{60\ minutes}$) (Figure 3.8). To quantitate the effects of ligand associations on changes in the overall solvent accessibility of backbone amides in CMP-NeuAc synthetase, the enzyme was pre-complexed with various ligands in water then exposed to D_2O for 1 hour. The average number of deuteriums incorporated into the enzyme with each combination of ligands was quantitated by mass spectrometry within 15 minutes of quenching the exchange reaction. Whether Me-O-NeuAc or CTP was bound to the enzyme, the percent deuterium incorporated into main chain amides was statistically unchanged compared to that for the apo-enzyme (Figure 3.9). However, the combination of CTP and Me-O-NeuAc protected an average of 16 backbone amides from exchange. Furthermore, when CMP-NeuAc was bound, an average of 24 backbone amides are protected from exchange.

3.3.4 Peptic Peptides from Exchanged CMP-NeuAc Synthetase

By virtue of the global protection of backbone amide hydrogens in CMP-NeuAc synthetase provided by bound ligands, we sought to identify the specific regions of the protein that experienced changes in isotopic content associated with the binding of different ligands. The spatial resolution of those amides shielded from bulk solvent was achieved by measuring deuterium incorporation for individual peptides generated from the digestion of exchanged CMP-NeuAc synthetase with pepsin. The digestion reaction was performed under acidic conditions (pH 2-3) at 0 °C, where amide back-exchange is extremely slow and pepsin activity is substantial. To minimize the duration of the proteolysis, an excess of pepsin was used to produce over 28 peptides in a 1 minute digest (Table 3.1, Figure 3.10). Since substrate specificity of pepsin is not restricted to just a couple of residues, the

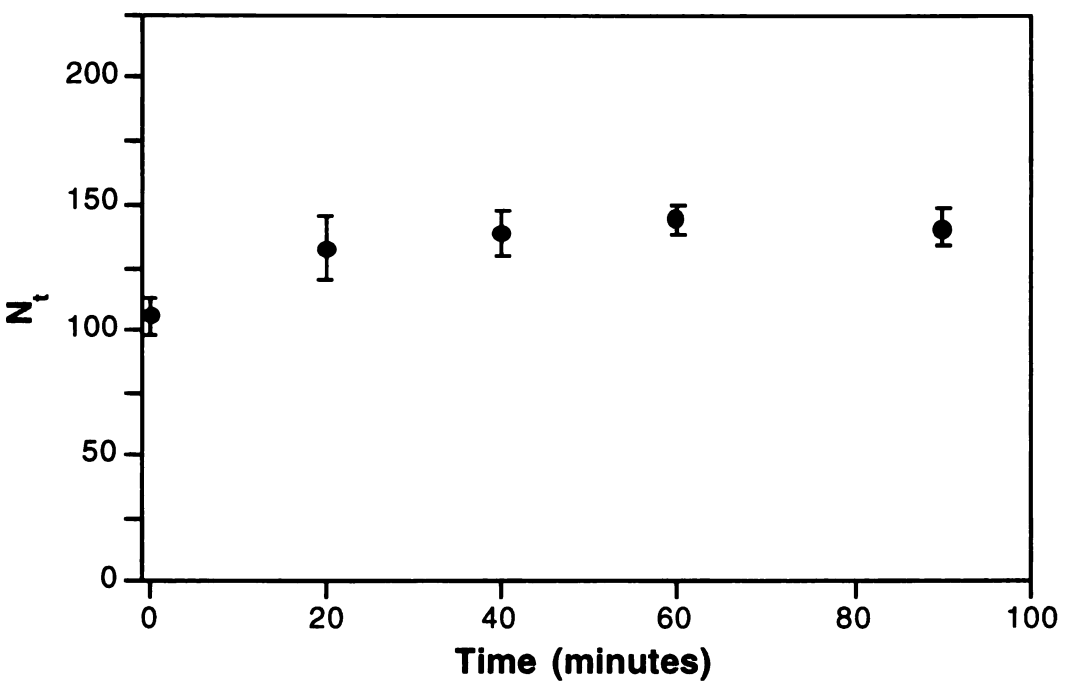

Figure 3.8 Deuterium exchange kinetics of CMP-NeuAc synthetase. The enzyme was exchanged alone in 90% D_2O at 25 °C and the total number of deuteriums incorporated into the protein for each time point measured (N_t). Each data point represents the average of 2-3 separate trials and error bars indicate standard deviation.

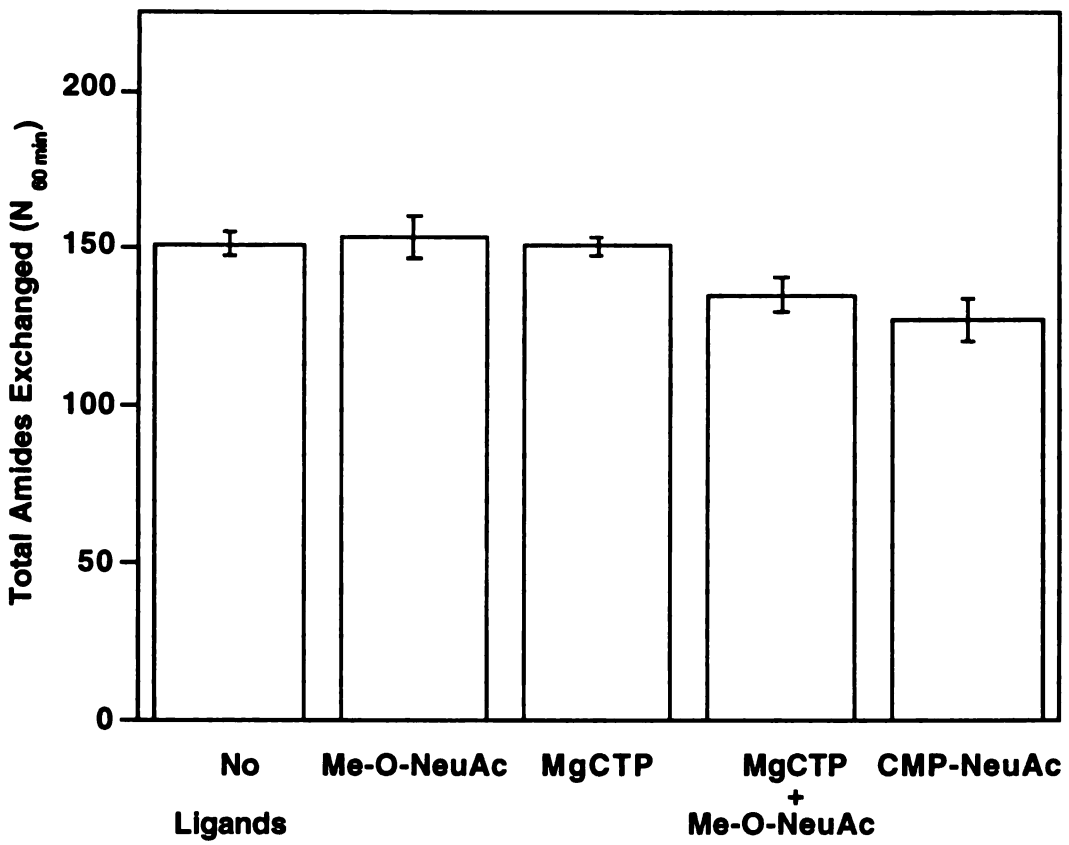

Figure 3.9 Deuterium exchange of CMP-NeuAc synthetase complexes. The enzyme (1.48 μg/μL) was incubated in 90% D_2O at 25 °C for 1 hour in the presence of buffer alone (200 mM MOPS) or in the presence of buffer plus the following additives: 1.0 mM Me-O-NeuAc, 500 μM CTP/20 mM $MgCl_2$, 500 μM CTP/1.0 mM Me-O-NeuAc/20 mM $MgCl_2$ or 150 μM CMP-NeuAc. Each value represents the average of 3-4 separate measurements of the total number of deuteriums incorporated into the protein (N_{60min}) bound with various ligands and standard deviations are indicated by error bars.

Table 3.1 Exchange parameters for peptic peptides of CMP-NeuAc synthetase

Peak	Location	PSD	$M_{r\ calculated}$ (average)	$M_{r\ measured}$ (average)	$N_{100\%}$	$N_{Theoretical}$
1	V(30-36)A		698.9	698.8	5.9	6
2	L(67-72)Y		762.9	762.9	4.5	4
3	I(184-189)F	X	819.0	819.0	5.3	5
4	V(83-90)A		865.0	865.0	[a]	7
5	L(67-73)L		876.1	876.0	5.4	5
6	L(183-189)F	X	932.1	932.1	6.3	6
7	A(59-66)T	X	967.0	967.0	7.6	7
8	Y(197-204)S	X	1009.1	1009.2	6.4	6
9	L(219-227)I	X	1073.3	1073.3	8.8	8
10	I(101-110)E	X	1127.3	1127.5	8.0	7
11	L(218-227)I		1186.4	1186.6	9.9	9
12	Y(197-206)D	X	1237.4	1237.4	8.8	8
13	C(132-143)L	X	1260.4	1260.7	[a]	10
14	I(101-112)D		1355.5	1355.8	9.9	9
15	V(30-43)F	X	1414.7	1414.7	12.6	13
16	F(120-132)C		1437.7	1436.7	11.9	12
17	Y(197-208)D	X	1465.6	1465.7	10.1	10
18	F(158-169)Y	X	1491.7	1491.4	9.7	9
19	Y(197-209)A	X	1536.7	1536.6	[a]	11
20	I(184-196)F	X	1698.0	1698.0	11.6	11
21	L(67-82)D		1836.1	1835.9	13.8	14
22	F(158-174)A	X	1961.2	1961.8	13.8	14
23	F(158-175)I	X	2074.4	2074.9	15.0	15
24	I(101-119)L	X	2097.5	2097.4	16.4	16
25	F(158-176)Y		2237.6	2238.1	16.2	16
26	M(1-23)L	X	2494.1	2494.1	21.8	21
27	D(44-66)T		2626.8	2627.0	24.2	22
28	M(1-29)L		3020.7	3020.8	[a]	26

[a] Unable to assign mass due to the lower intensity and broadness of the peaks after complete exchange.

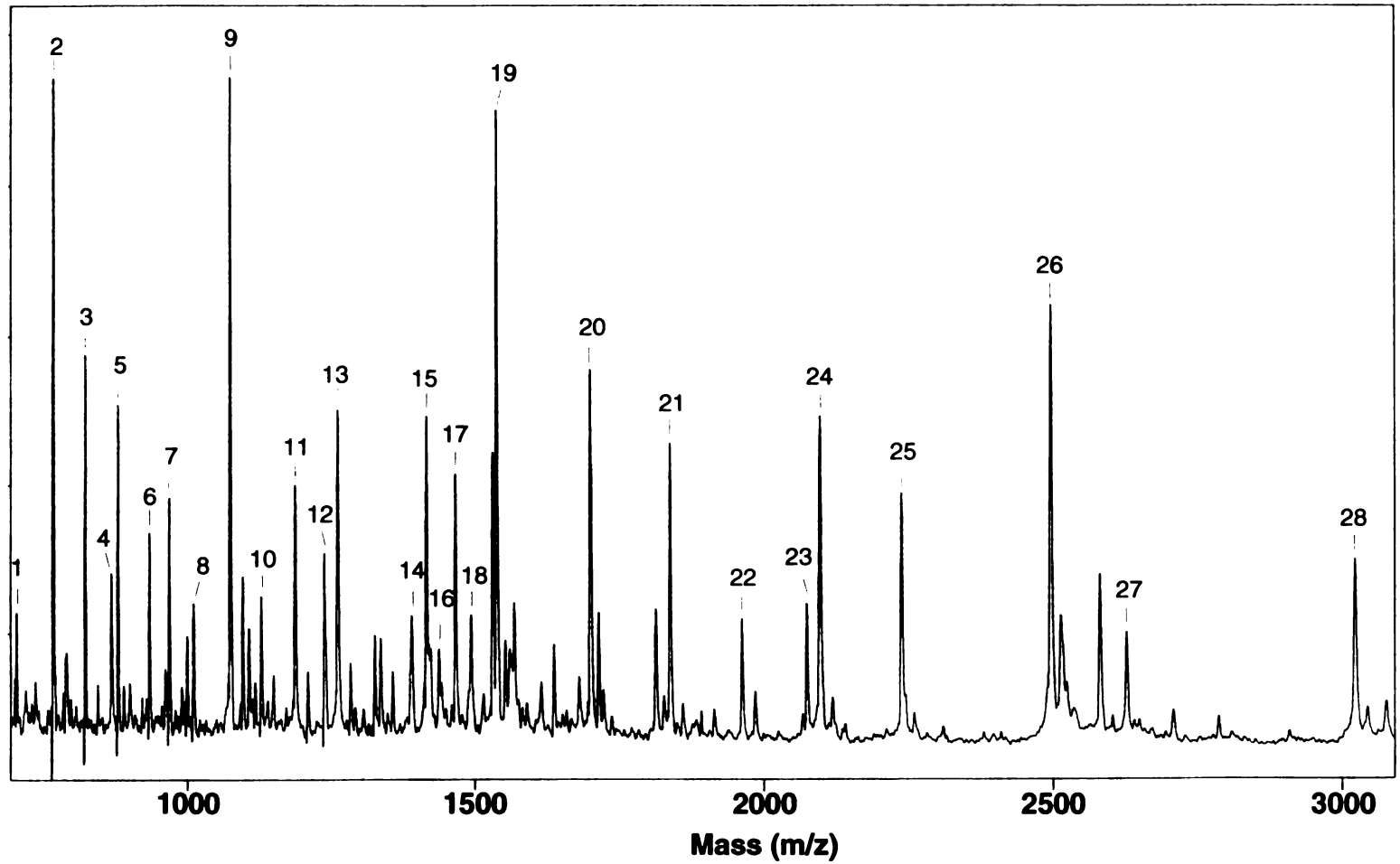

Figure 3.10 MALDI-MS spectrum of the peptic digest of CMP-NeuAc synthetase. The spectrum of the digest was recorded in solutions with natural isotopic distributions. Peptides identified in this study are numbered and have been summarized in Table 3.1.

identification of proteolytic products in some cases required direct sequencing by MALDI-PSD. However, some peptides were identified by a combination of the measured mass, knowledge of other flanking peptides and the experimentally observed specificity of pepsin. Despite the high ratio of pepsin:CMP-NeuAc synthetase (2.6:1, wt/wt), none of the peaks observed in the mass spectrum of the digest was attributed to autoproteolysis of pepsin. Although certain segments of CMP-NeuAc synthetase were represented in multiplicity, 84% of the sequence was covered by the entire population of peptides observed (Figure 3.11).

Once more, to guarantee our methods generally probe backbone amides, we first measured the exchange of all hydrogens bonded to heteroatoms capable of exchange in each peptide of the digest. Complete exchange of proteins in D_2O in many cases requires exposure to denaturants and/or elevated temperatures for extended periods of time. Considering the digestion of denatured CMP-NeuAc synthetase by pepsin was incomplete, it was necessary to instead exchange the pre-digested protein under harsh conditions. To measure the maximum number exchangeable sites for each peptide ($N_{100\%}$), CMP-NeuAc synthetase was digested with pepsin and batch eluted from a reversed phase column. The entire peptide pool was exchanged in D_2O for 6 hours at 83 °C near neutral pD and the number of deuteriums incorporated into each peptide was quantitated by MALDI-MS. In every instance, the total number of deuterons exchanged into the individual peptides was nearly equivalent to or slightly exceeded the number of non-proline backbone amides (Table 3.1). In-exchange control experiments revealed that a range of 1.8 to 6.6 deuteriums were incorporated into sites other than main chain amides over the entire population of peptides under the experimental conditions (data not shown). Once more, our methods mostly detect the exchange of backbone amides in the peptides and therefore, subsequent measurements were not corrected for deuterium incorporated into side chain groups during the pepsin digestion and matrix mixing steps under acidic conditions.

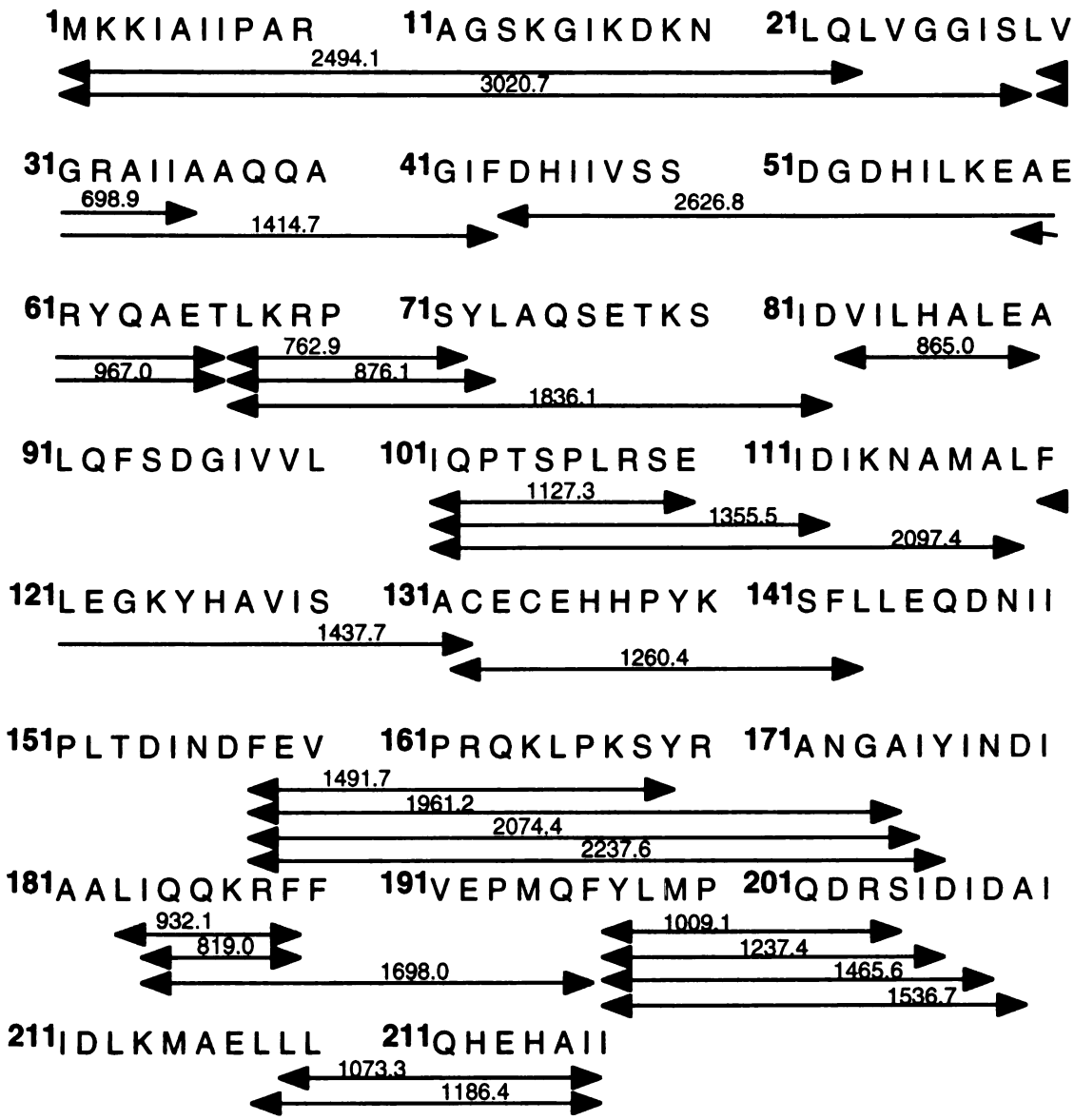

Figure 3.11 Amino acid sequence and location of peptic peptides of CMP-NeuAc synthetase. Peptic fragments used in this study are denoted by arrows along with the corresponding calculated average masses.

3.3.5 Localization of Regions Protected from Exchange in the Presence of Ligands

As the presence of CMP-NeuAc and the combination of CTP with Me-O-NeuAc were found to significantly effect the extent of amide exchange in CMP-NeuAc synthetase (Figure 3.9), we sought to localize the precise regions of the protein containing less deuterium when the ligands were bound (Figure 3.12). Although not observed at the protein level, the nucleotide alone was demonstrated to shield certain peptides from amide exchange. The highest degree of protection was observed in the peptide with an average mass of 2626.8 Da from region 1 (D44-T66) (Figure 3.12A). When CTP was bound to the enzyme, an average of 3.7 amide hydrogens were blocked from exchange compared to an average of 5.0 hydrogens when Me-O-NeuAc was also included. Moreover, an average of 6.1 amide hydrogens were shielded from the D_2O when CMP-NeuAc was bound. Similar decreases in deuterium incorporation were observed in the overlapping peptide with an average mass of 967.0 Da as well. A set of overlapping peptides from a second protected region (I101-L119) were also demonstrated to contain less deuterium when CMP-NeuAc or when CTP alone or in combination with Me-O-NeuAc were bound to CMP-NeuAc synthetase (Figure 3.12B). On the whole, a maximum of 1.9 amide hydrogens were protected from isotopic exchange in this particular segment of CMP-NeuAc synthetase. For any individual peptide from region 1 or 2, the presence of CMP-NeuAc alone, CTP alone or in combination the sialic acid analog provided comparable protection from amide exchange, which suggests these regions are primarily involved in the recognition of the CTP. In support of this hypothesis, several key amino acid residues contained within the shielded segments are conserved in both CMP-NeuAc and CMP-KDO synthetases and include D52, Q102 and P106 (Figure 3.13).

In a third region (F158-Y176), three overlapping peptides (M_r = 1961.2, 2074.4 and 2237.6 Da) were moderately protected from amide exchange in the presence of CTP and Me-O-NeuAc together (Figure 3.12C). This region of CMP-NeuAc synthetase amassed

Figure 3.12 Deuterium exchange of peptides derived from CMP-NeuAc synthetase complexes. Overlapping peptides significantly protected from amide exchange in CMP-NeuAc synthetase ligand-bound complexes are contained within one of three separate areas: (A) Region 1 (D44-T66), (B) Region 2 (I101-L119) or (C) Region 3 (F158-Y176). The individual peptides are denoted by their average calculated masses (Figure 3.11). CMP-NeuAc synthetase (1.48 μg/μL) was incubated in 90% D_2O at 25 °C for 1 hour in the presence of buffer alone (200 mM MOPS) or in the presence of buffer plus the following additives: 1.0 mM Me-O-NeuAc, 500 μM CTP/20 mM $MgCl_2$, 500 μM CTP/1.0 mM Me-O-NeuAc/20 mM $MgCl_2$ or 150 μM CMP-NeuAc. The exchanged enzyme complexes were digested and the amount of deuterium incorporated into individual peptides was quantitated (N_{60min}). Each value represents the average of 3-4 separate measurements and standard deviations are indicated by error bars.

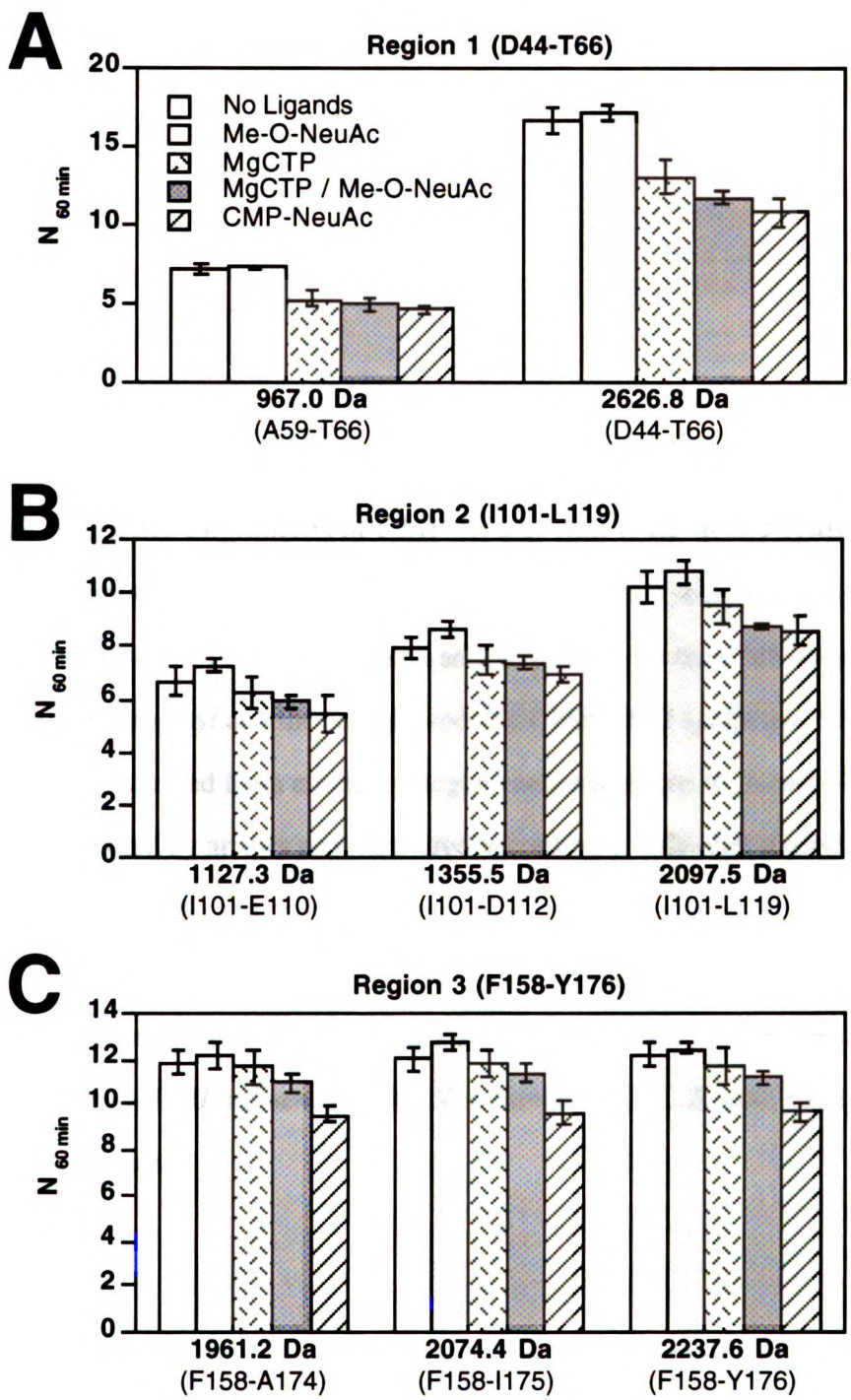
A
Region 1 (D44-T66)
No Ligands
Me-O-NeuAc
MgCTP
MgCTP / Me-O-NeuAc
CMP-NeuAc
N 60 min
20
15
10
5
0
967.0 Da
(A59-T66)
2626.8 Da
(D44-T66)
B
Region 2 (I101-L119)
N 60 min
12
10
8
6
4
2
0
1127.3 Da
(I101-E110)
1355.5 Da
(I101-D112)
2097.5 Da
(I101-L119)
C
Region 3 (F158-Y176)
N 60 min
14
12
10
8
6
4
2
0
1961.2 Da
(F158-A174)
2074.4 Da
(F158-I175)
2237.6 Da
(F158-Y176)

Figure 3.13 Sequence alignments of CMP-NeuAc and CMP-KDO synthetases. The top 5 sequences are CMP-NeuAc synthetases and the bottom 4 sequences are CMP-KDO synthetases (Tullius et al. 1996). The amino acid sequences for the CMP-NeuAc synthetase from *H. ducreyi* and the capsule-specific CMP-KDO synthetase from *E. coli* are in *bold*. Regions protected from amide hydrogen exchange in the *H. ducreyi* CMP-NeuAc synthetase are denoted by arrows and numbered accordingly. All sites susceptible to cleavage by trypsin (R, K) and endoproteinase Glu-C (E) are indicated by ▼. Residues conserved (7 or more identical) across both enzyme classes are *shaded*. *Boxes* indicate areas of a high percentage of identity among each class of enzymes. The abbreviations used are: HD, *H. ducreyi*; HI, *H. influenzae*; NM, *N. meningitidis*; EC, *E. coli*; SA, *S. agalactiae*; and CT, *C. trachomatis*.

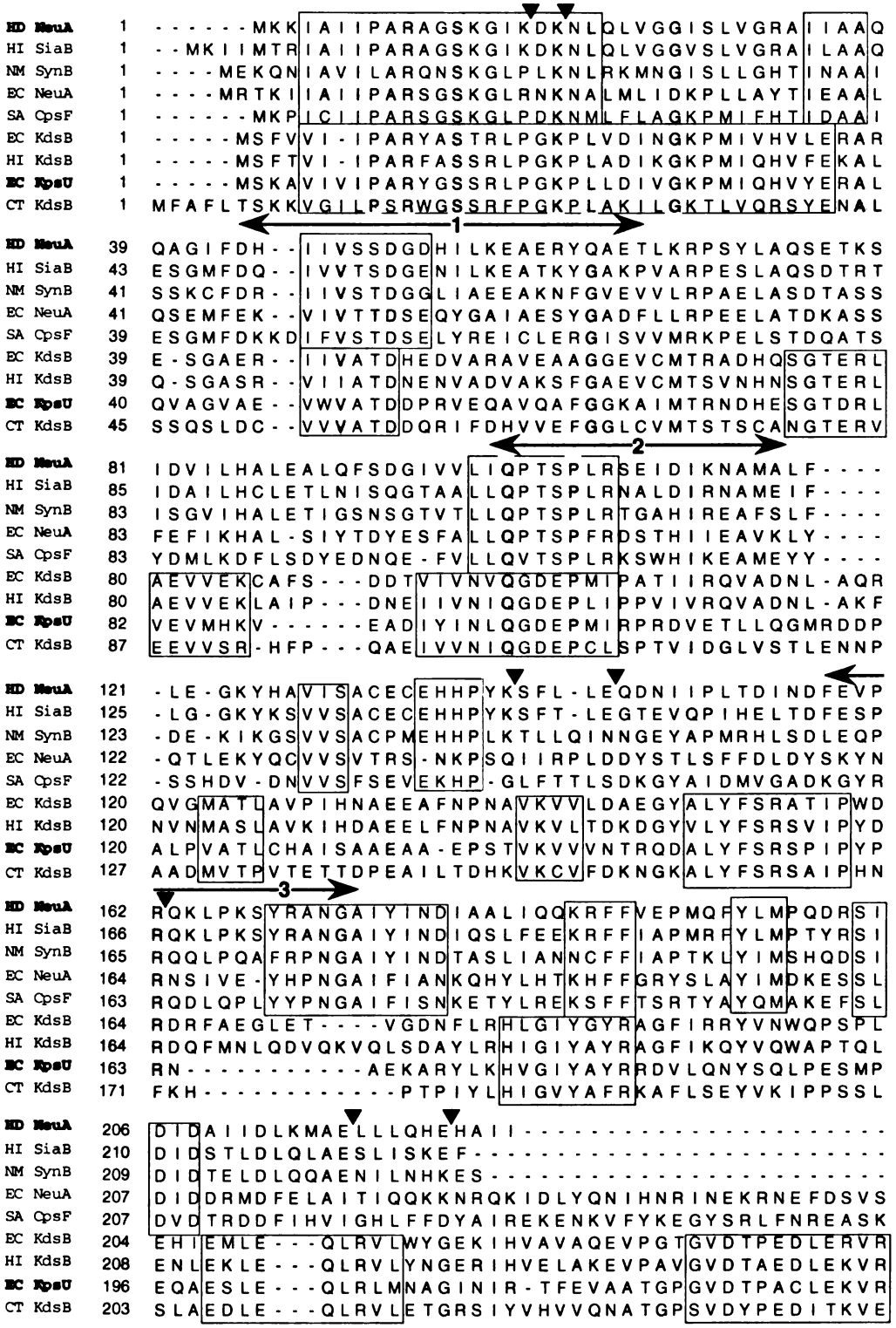
ND NeuA 1 ------MKKIAIIPARAGSKGIKDKNLQLVGGISLVGRAIIAAQ
HI SiaB 1 --MKIIMTRIAIIPARAGSKGIKDKNLQLVGGVSLVGRAILAAQ
NM SynB 1 ----MEKQNIAVILARQNSKGLPLKNLRKMNGISLLGHTINAAI
EC NeuA 1 ----MRTKIIAIIPARSGSKGLRNKNALMLIDKPLLAYTIEAAL
SA CpsF 1 ------MKPICIIPARSGSKGLPDKNMLFLAGKPMIFHTIDAAI
EC KdsB 1 -----MSFVVI-IPARYASTRLPGKPLVDINGKPMIVHVLERAR
HI KdsB 1 -----MSFTVI-IPARFASSRLPGKPLADIKGKPMIQHVFEKAL
EC KpsU 1 -----MSKAVIVIPARYGSSRLPGKPLLDIVGKPMIQHVYERAL
CT KdsB 1 MFAFLTSKKVGILPSRWGSSRFPGKPLAKILGKTLVQRSYENAL
1
ND NeuA 39 QAGIFDH--IIVSSDGDHILKEAERYQAETLKRPSYLAQSETKS
HI SiaB 43 ESGMFDQ--IVVTSDGENILKEATKYGAKPVARPESLAQSDTRT
NM SynB 41 SSKCFDR--IIVSTDGGLIAEEAKNFGVEVVLRPAELASDTASS
EC NeuA 41 QSEMFEK--VIVTTDSEQYGAIAESYGADFLLRPEELATDKASS
SA CpsF 39 ESGMFDKKDIFVSTDSELYREICLERGISVVMRKPELSTDQATS
EC KdsB 39 E-SGAER--IIVATDHEDVARAVEAAGGEVCMTRADHQSGTERL
HI KdsB 39 Q-SGASR--VIIATDNENVADVAKSFGAEVCMTSVNHNSGTERL
EC KpsU 40 QVAGVAE--VWVATDDPRVEQAVQAFGGKAIMTRNDHESGTDRL
CT KdsB 45 SSQSLDC--VVVATDDQRIFDHVVEFGGLCVMTSTSCANGTERV
2
ND NeuA 81 IDVILHALEALQFSDGIVVLIQPTSPLRSEIDIKNAMALF----
HI SiaB 85 IDAILHCLETLNISQGTAALLQPTSPLRNALDIRNAMEIF----
NM SynB 83 ISGVIHALETIGSNSGTVTLLQPTSPLRTGAHIREAFSLF----
EC NeuA 83 FEFIKHAL-SIYTDYESFALLQPTSPFRDSTHIIEAVKLY----
SA CpsF 83 YDMLKDFLSDYEDNQE-FVLLQVTSPLRKSWHIKEAMEYY----
EC KdsB 80 AEVVEKCAFS---DDTVIVNVQGDEPMIPATIIRQVADNL-AQR
HI KdsB 80 AEVVEKLAIP---DNEIIVNIQGDEPLIPPVIVRQVADNL-AKF
EC KpsU 82 VEVMHKV------EADIYINLQGDEPMIRPRDVETLLQGMRDDP
CT KdsB 87 EEVVSR-HFP---QAEIVVNIQGDEPCLSPTVIDGLVSTLENNP
ND NeuA 121 -LE-GKYHAVISACECEHHPYKSFL-LEQDNIIPLTDINDFEVP
HI SiaB 125 -LG-GKYKSVVSACECEHHPYKSFT-LEGTEVQPIHELTDFESP
NM SynB 123 -DE-KIKGSVVSACPMEHHPLKTLLQINNGEYAPMRHLSDLEQP
EC NeuA 122 -QTLEKYQCVVSVTRS-NKPSQIIRPLDDYSTLSFFDLDYSKYN
SA CpsF 122 -SSHDV-DNVVSFSEVEKHP-GLFTTLSDKGYAIDMVGADKGYR
EC KdsB 120 QVGMATLAVPIHNAEEAFNPNAVKVVLDAEGYALYFSRATIPWD
HI KdsB 120 NVNMASLAVKIHDAEELFNPNAVKVLTDKDGYVLYFSRSVIPYD
EC KpsU 120 ALPVATLCHAISAAEAA-EPSTVKVVVNTRQDALYFSRSPIPYP
CT KdsB 127 AADMVTPVTETTDPEAILTDHKVKCVFDKNGKALYFSRSAIPHN
3
ND NeuA 162 RQKLPKSYRANGAIYINDIAALIQQKRFFVEPMQFYLMPQDRSI
HI SiaB 166 RQKLPKSYRANGAIYINDIQSLFEEKRFFIAPMRFYLMPTYRSI
NM SynB 165 RQQLPQAFRPNGAIYINDTASLIANNCFFIAPTKLYIMSHQDSI
EC NeuA 164 RNSIVE-YHPNGAIFIANKQHYLHTKHFFGRYSLAYIMDKESSL
SA CpsF 163 RQDLQPLYYPNGAIFISNKETYLREKSFFTSRTYAYQMAKEFSL
EC KdsB 164 RDRFAEGLET----VGDNFLRHLGIYGYRAGFIRRYVNWQPSPL
HI KdsB 164 RDQFMNLQDVQKVQLSDAYLRHIGIYAYRAGFIKQYVQWAPTQL
EC KpsU 163 RN----------AEKARYLKHVGIYAYRRDVLQNYSQLPESMP
CT KdsB 171 FKH----------PTPIYLHIGVYAFRKAFLSEYVKIPPSSL
ND NeuA 206 DIDAIIDLKMAELLLQHEHAII--------------------
HI SiaB 210 DIDSTLDLQLAESLISKEF----------------------
NM SynB 209 DIDTELDLQQAENILNHKES----------------------
EC NeuA 207 DIDDRMDFELAITIQQKKNRQKIDLYQNIHNRINEKRNEFDSVS
SA CpsF 207 DVDTRDDFIHVIGHLFFDYAIREKENKVFYKEGYSRLFNREASK
EC KdsB 204 EHIEMLE---QLRVLWYGEKIHVAVAQEVPGTGVDTPEDLERVR
HI KdsB 208 ENLEKLE---QLRVLYNGERIHVELAKEVPAVGVDTAEDLEKVR
EC KpsU 196 EQAESLE---QLRLMNAGINIR-TFEVAATGPGVDTPACLEKVR
CT KdsB 203 SLAEDLE---QLRVLETGRSIYVHVVQNATGPSVDYPEDITKVE

even less deuterium upon the binding of CMP-NeuAc, an average of 2.3-2.4 deuteriums per peptide fewer than in the absence of ligands. We that concluded region 3 is sequestered from solvent in the event of a change in protein conformation concomitant with catalysis since the nucleotide alone does not significantly protect this region from amide exchange. As the degree of amide exchange for each peptide is similar in spite of length, the backbone amides shielded in the presence of the ligands appear to be concentrated within the segment spanning from F158 to A174. Region 3 contains a stretch of amino acids conserved in CMP-NeuAc synthetases only and an arginine (162) which is also conserved in CMP-KDO synthetases (Figure 3.13).

3.4 DISCUSSION

Lipooligosaccharide, the most abundant outer membrane component, is a virulence factor for a number of pathogenic bacteria, including members of the *Haemophilus* and *Neisseria* genera. In recent years, several genes have been shown to be involved in the biosynthesis of the amphipathic glycolipid (Gibson et al. 1997; Nichols et al. 1997; Phillips et al. 2000; Stevens et al. 1997; Sun et al. 2000) in particular, those required for the synthesis of LOS containing sialic acid (Bozue et al. 1999). In an effort to further our understanding of the enzymology of LOS sialylation in *H. ducreyi*, we have focused our studies on the *neuA* gene product, cytidine 5'-monophosphate N-acetylneuraminic acid (CMP-NeuAc) synthetase. CMP-NeuAc synthetase catalyzes the activation of the anomeric hydroxyl of sialic acid by a proposed in-line displacement of pyrophosphate from CTP to form the sialic acid donor substrate, CMP-NeuAc (Ambrose et al. 1992). As an enzyme family, CMP-NeuAc synthetases share an average of 32-65% identity and 50-79% similarity (Figure 3.13) (Tullius et al. 1996). Moreover, the sialic acid activating family of enzymes share significant sequence homology (11-18% similarity, 32-39% identity) with cytidine 5'-monophosphate 2-keto-3-deoxy-D-manno-octulosonic acid (CMP-KDO)

synthetases, another family of enzymes proposed to couple an α-keto acid monosaccharide to the nucleotide monophosphate via a nucleophilic displacement mechanism (Kohlbrenner et al. 1987). To gain more insight into the structure of CMP-NeuAc synthetase, we have investigated the surface topography of the enzyme by limited proteolysis and amide hydrogen exchange. Albeit a crystal structure is not available for any member of the CMP-NeuAc synthetase family, the structure of the CMP-KDO synthetase from *E. coli* (*kpsU* gene product) has been solved at 2.3 Å resolution (Figure 3.14) (Jelakovic et al. 1996) and should prove useful for interpreting results gained by the two independent methodologies.

The limited proteolysis of proteins in their native states is a powerful tool for probing higher order structure (Hubbard 1998). Although the primary structure of the substrate protein is an important factor for determining the potential for amide bond cleavage, the tertiary structure of the protein substrate ultimately dictates the probability of proteolysis. Numerous studies investigating proteins with known three dimensional structures by limited proteolysis have been conducted to ascertain the key factors influencing susceptibility to cleavage. Investigators quantifying the contributions of flexibility and exposure to limited proteolysis have shown that the incidence of enzymatic cleavage correlates with residue-average atomic temperature factors (B factors) and preferentially occurs in the highly exposed regions lacking secondary structural elements (Fontana et al. 1986; Vita et al. 1985). From collective observations, the investigators concluded segmental mobility in protein chains to be a significant factor governing limited proteolysis and therefore cleavage is anticipated to generally occur in surface exposed loops and turns rather than rigid segments of regular secondary structure. Limited proteolysis methods have increasingly been employed to probe the tertiary folds of proteins of unknown structure for the purpose of investigating protein surface accessibility, domain boundaries, unfolding/folding pathways and changes in protein conformation (Dieckmann et al. 1999; Fontana et al. 1997; Hubbard 1998; Krekel et al. 1999; Scaloni et al. 1999; Wyss et al. 1993). Herein we report the examination of the surface structure

Figure 3.14 Three dimensional structures of the capsule-specific CMP-KDO synthetase from *E. coli*. (A) Stereoview of the C_α backbone of dimeric CMP-KDO synthetase (Jelakovic et al. 1996) . (B) Ribbon diagram of one subunit of the CMP-KDO synthetase dimer. The molecular two-fold axes are denoted by dotted lines. Arg10 and Lys19 are shown coordinating an $IrCl_6^{-3}$ anion at the putative phosphate binding loop and are highlighted in *magenta*. The regions significantly protected from limited proteolysis and amide hydrogen exchange upon the binding of ligands to the CMP-NeuAc synthetase from *H. ducreyi* were mapped to the analogous segments of the CMP-KDO synthetase from *E. coli* based on sequence alignments (Figure 3.13). Areas of CMP-NeuAc synthetase protected from amide hydrogen exchange by the nucleotide, region 1 (45-67) and region 2 (96-114) are highlighted in blue and red respectively. Whereas the portion of the enzyme requiring elements of both the nucleotide and sugar for protection from amide exchange, region 3 (159-165), is labeled in green. The loop proposed to bind the phosphate of the CTP is represented in magenta. All sites cleaved by trypsin and Glu-C are numbered according to the sequence of the CMP-NeuAc synthetase from *H. ducreyi*.

A

B

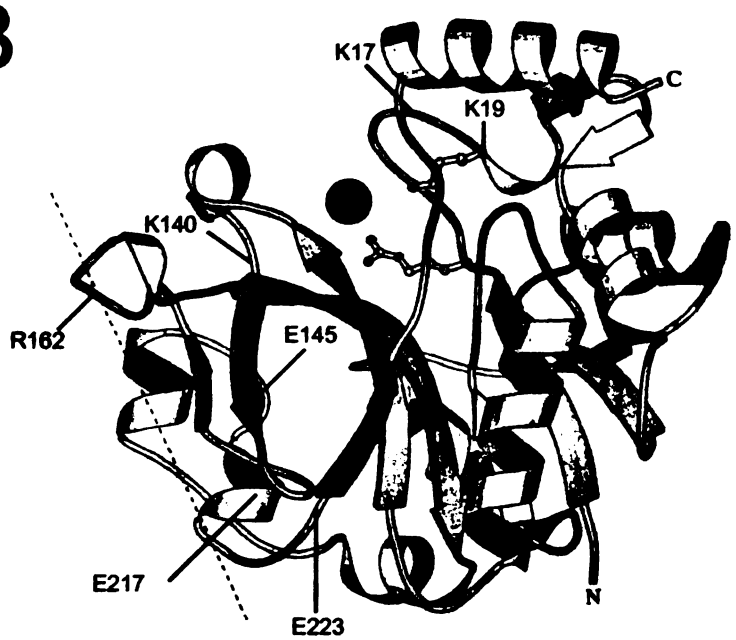

of the CMP-NeuAc synthetase as well as identification of protein determinants for binding the substrates in the native enzyme utilizing this powerful technique.

Initially, we surveyed the surface topography of CMP-NeuAc synthetase by controlled digestion of the free enzyme with two proteases of narrow substrate specificity requirements, trypsin and endoproteinase Glu-C. Analysis of the digestion products by MALDI-MS revealed the presence of additional fragments not observed by SDS-PAGE as well as permitted the quick identification of fragments based on observed masses and protease specificity (Figures 3.3-3.6). Between the two proteases, 7 cleavage sites were identified in CMP-NeuAc synthetase, altogether sampling the entire span of the protein. In the absence of any ligands, CMP-NeuAc synthetase was immediately cleaved at E223 by endoproteinase Glu-C followed by E217 and E145 whereas, tryptic digestion resulted in the fairly even cleavage of K17, K19, K140 and R162. Sequence alignments of CMP-NeuAc and CMP-KDO synthetases (Figure 3.13) were used to map the protease sensitive sites of the *H. ducreyi* CMP-NeuAc synthetase onto the corresponding regions of the CMP-KDO synthetase from *E. coli* (Figure 3.14) (Jelakovic et al. 1996; Tullius et al. 1996). Indeed, most of the protease susceptible sites were contained within surface loops or the exposed at the C-terminus of the CMP-KDO synthetase, suggesting that CMP-NeuAc synthetase has an analogous single domain containing fold.

To identify active site residues, we compared the proteolytic fragment fingerprints of free CMP-NeuAc synthetase to those derived from the enzyme bound with combinations of CTP, Me-O-NeuAc and CMP-NeuAc. Recent investigations demonstrated the *H. ducreyi* CMP-NeuAc synthetase to obey a sequential ordered Bi-Bi kinetic mechanism, where CTP is bound before NeuAc and pyrophosphate is released before CMP-NeuAc (Samuels et al. 1999). In accordance with the proposed mechanism, analyses of proteolytic digests by SDS-PAGE (Figures 3.3, 3.4) and MALDI-MS (Figures 3.5, 3.6) showed the addition of the sialic acid analog, Me-O-NeuAc, failed to affect the digestibility of the enzyme. However, CTP alone or in combination with Me-O-NeuAc equally provided CMP-NeuAc

synthetase overall protection from proteolysis by trypsin or endoproteinase Glu-C, which suggests the bound nucleotide alone sufficiently hinders access of the proteases to specific cleavage sites. Although the addition of the Me-O-NeuAc to the binary complex provided little if any additional protection from proteolysis by either protease, the product-bound enzyme complex was significantly more resistant to cleavage compared to the ternary complex, especially to trypsinolysis. These findings may indicate the occurrence of a change in protein conformation between substrate and product bound enzyme forms. Structural perturbations in certain segments of the backbone of CMP-NeuAc synthetase appear to be initiated upon the binding of the second substrate to the binary complex, a requisite interaction that may not be fully realized with the sialic acid analog. On the whole, the cleavage sites protected by bound ligands were classified as residing in one of two areas, segments involved in the recognition of the first substrate, CTP, or segments involved in the recognition of the second substrate and/or changes in conformation concomitant with catalysis.

In general, the binding of CTP hampered the proteolysis of all sites in CMP-NeuAc synthetase to various degrees. However, the nucleotide-sugar product dramatically inhibited cleavage of E145 and completely blocked cleavage of K140 and R162 (Figure 3.5). Inspection of the CMP-KDO synthetase structure revealed the residue corresponding to K140 to be located at the N terminal position of a β strand (β8) at the opening of the proposed substrate binding pocket, whereas E145 appears on the backside of the protein at a later position in the same strand (Figure 3.14) (Jelakovic et al. 1996). Despite residing in the middle of a large loop, the highly conserved R162 along with E145 appear in regions remote from the proposed active site, supporting the occurrence of conformational alterations in structure accompanying CMP-NeuAc binding as the origin of their protection from proteolysis. Conversely, the presence of CTP alone was enough to inhibit the cleavage of K17 and K19, which suggested the lysines are directly involved in the recognition of the nucleotide. These findings are in agreement with labeling experiments on the *H. ducreyi*

CMP-NeuAc synthetase that demonstrated the covalent modification of Lys19 by CTP 2,3' dialdehyde abolishes enzymatic activity (Tullius et al. 1999). Furthermore, site directed mutagenesis studies of the CMP-NeuAc synthetase from *E. coli* demonstrated the analogous residue (Lys21) is required for enzymatic activity (Stoughton et al. 1999). Total conservation of Lys19 across both the CMP-NeuAc and CMP-KDO synthetases, further suggests the basic residue plays a role in catalysis and or the binding of the common substrate, CTP. The structure of the unliganded CMP-KDO synthetase shows the residues equivalent to Lys17 and Lys19 are contained within a loop conserved in both enzyme families and postulated to bind phosphate of the nucleotide (Jelakovic et al. 1996).

To gain additional insight into the structure of CMP-NeuAc synthetase, the surface topography was surveyed by amide hydrogen exchange. Due to the dependence of main chain amide exchange rates upon solvent accessibility and degree of participation in secondary structure, stable isotopic exchange of amide hydrogens is a sensitive probe of protein structure and dynamics (Englander and Kallenbach 1983; Woodward et al. 1982). Nuclear magnetic resonance spectroscopy (NMR) has been the traditional method employed to measure amide hydrogen exchange rates, however, studies are typically restricted to the analysis of small, soluble proteins of the highest purity (Smith et al. 1997). In recent years, mass spectrometry has been routinely applied to such studies, while avoiding several of the foremost obstacles that have plagued NMR (Katta and Chait 1991; Smith et al. 1997; Zhang and Smith 1993). Perhaps the ability to spatially resolve regions of a protein experiencing variations in the levels of isotopic incorporation as a result of changes in protein conformation or ligand binding without any prior knowledge regarding structure other than amino acid sequence is the greatest advantage of employing mass spectrometry for isotopic exchange. This technique permits the assessment of the backbone amide hydrogens exclusively by exploiting differences between the pH dependencies of exchange for hydrogens of main chain amides and those bonded to heteroatoms of residue side chains (Bai et al. 1993). As the hydrogen exchange rates are influenced by changes in

solvent accessibility, amide hydrogen exchange mass spectrometry has been extended to the investigation of noncovalent interactions and ligand-induced changes in protein conformation (Mandell et al. 1998; Wang et al. 1997; Wang et al. 1998).

To further investigate the surface topography of CMP-NeuAc synthetase, all solvent accessible amides were probed by deuterium exchange coupled to MALDI-MS. Following total exchange under denaturing conditions, an average of 215 deuteriums ($N_{100\%}$) were retained in CMP-NeuAc synthetase, which contains a total of 216 backbone amide hydrogens in theory (Figure 3.7). However, a small portion of those protons exchanged are expected not to be bonded to main chain amide nitrogens due to the remaining D_2O (10%) in the final solutions analyzed by mass spectrometry. Under the conditions of the acidic quench (pH 2-3), backbone amide hydrogen exchange is suppressed by a factor of 10^4 and the reaction half-lives are on the order of 30 minutes or greater (Bai et al. 1993; Englander et al. 1985), however, the rates of isotopic exchange of side chain groups remain rapid relative to the time scale of analysis and therefore allow their immediate equilibration with isotopic content of the final solution analyzed (Smith et al. 1997). To determine the portion of incorporated deuterium not bound to main chain amides following the total exchange of the enzyme, in-exchange control experiments were performed where CMP-NeuAc synthetase was reconstituted in H_2O, and D_2O was introduced in the acid quench solution (Figure 3.2). An average of 59 deuteriums were incorporated into the enzyme solely during manipulations in acid, which for the most part represented deuterium trapped in side chain groups. Following the subtraction of background incorporation, a maximum of 72 % of all non-proline amides in CMP-NeuAc synthetase (156 backbone amides) could be detected by this protocol (Figure 3.7). This value is with reason based on the successful evaluation of amide hydrogen exchange in other proteins using LC-ESI-MS that have detected the exchange of at most 63% of all backbone amides following complete exchange (Wang et al. 1998). Later measurements were not corrected for in-exchange, especially since the focus

of this study was to assess changes in the extent of amide exchange in the enzyme bound with various ligands relative to isotopic exchange in the free enzyme.

After confirming that our methods monitor the exchange of most backbone amide hydrogens of CMP-NeuAc synthetase, we measured deuterium incorporation into the native enzyme as a function of time. Following an hour long exchange in 90% D_2O, the solvent accessible sites of CMP-NeuAc synthetase had reached an equilibrium, resulting in the incorporation of 151 deuteriums into the free protein (Figure 3.9). As expected only a fraction of all backbone amide hydrogens were substituted in the native protein due to the inaccessibility of protons bound in regular secondary elements. To further probe the structure of specific regions of CMP-NeuAc synthetase, the exchanged enzyme was proteolyzed and the levels of deuterium incorporation quantitated for each peptide. Although LC-ESI-MS is commonly used to monitor amide exchange, MALDI-MS is especially suitable for the direct analysis of protein digests since all information for a given condition is gained in a single spectrum without the need for purification steps. Despite the varying degrees of exchange for individual peptides in D_2O, the overall peak profile of the mass spectra remained relatively identical to that in water with the exception of peak broadening due to the wider distribution of isotopic states for the exchanged peptides. In control experiments analogous to those performed on the whole protein, the $M_{100\%}$ and $M_{in\text{-}exchange}$ values were determined for each peptide (Table 3.1). These studies demonstrated that the exchange protocol was capable of detecting 52-81 % of all backbone amides following subtraction of in-exchange background (data not shown). These values are also within reason based on reports from other groups monitoring 40-96 % using LC-ESI-MS methods (Ehring 1999; Resing and Ahn 1998; Wang et al. 1998; Wang et al. 1998).

To evaluate the global effects of non-covalent interactions on solvent accessibility of CMP-NeuAc synthetase, the quantity of deuterium incorporated into the enzyme complexed with various ligands was compared to that exchanged into the free enzyme (Figure 3.9). The saturation of the active site with either substrate had no effects on amide hydrogen

exchange. Although these findings were expected for an inhibitor not capable of binding to the free enzyme, the results suggest that the bound nucleotide alone is not sufficient to evoke a change in the solvent accessible surface of CMP-NeuAc synthetase large enough to be observed at the protein level. However, the combined presence of the nucleotide triphosphate and sugar analog produced a statistically significant decrease in the extent in amide exchange compared to the unliganded-enzyme, protecting an average of 16 amides from exchange. Moreover, the addition of CMP-NeuAc, instead of the substrate and the inhibitor, provided greater protection from isotopic exchange, shielding an average of 24 deuteriums. The gross decrease in deuterium incorporation may be in part due to the direct shielding provided by the ligands, however, the bulk of the effect may be attributed to a change in protein conformation following the binding of the second substrate since the unaccompanied nucleotide exerted very small or no detectable effects. To identify protein determinants involved in substrate recognition, the segments of the enzyme-ligand complexes containing less deuterium relative to the corresponding region in the free enzyme were spatially resolved by the proteolysis of the exchanged protein followed by analysis of the resulting peptides by MALDI-MS. Three different regions of CMP-NeuAc synthetase showed distinct decreases in deuterium incorporation upon ligand binding, each of which was represented by 2 or more overlapping peptide probes (Figure 3.12).

In the first protected region (D44-T66), two peptides displayed the highest decreases in the extent of amide exchange (Figure 3.12A). Although the effects of binding CTP to CMP-NeuAc synthetase were not detected at the protein level, decreases in the number of deuterons incorporated into region 1 were easily detected in the overlapping segments represented by peptides with a mass of 967.0 and 2626.8 Da. Within either segment of this region, the presence of CMP-NeuAc, CTP alone or CTP in combination with the sialic acid analog was found to hinder amide exchange nearly to the same degree and therefore, the bound nucleotide was concluded to directly shield backbone amides of the region spanning from Asp44 to Thr66 from bulk solvent. Sequence alignments revealed a

number of hydrophobic residues and an aspartic acid within this segment are conserved among both CMP-NeuAc and CMP-KDO synthetases, providing further support in favor of region 1 having an important role in the recognition of CTP (Figure 3.13) (Tullius et al. 1996). The analogous stretch of residues were mapped on the structure of the CMP-KDO synthetase from *E. coli* and found to span from β-strand4 to α-helix2 with the totally conserved aspartic acid (Asp52) placed directly behind the loop proposed to bind phosphate of CTP (Figure 3.14) (Jelakovic et al. 1996).

Similar effects were also observed for a set of overlapping peptides in a second protected region (I101-L119) of CMP-NeuAc synthetase (Figure 3.12B). Here, the presence of the nucleotide alone appeared to be the sole factor causing the decrease in the extent of amide exchange for the three peptides (M_r = 1127.3, 1335.5, and 2097.5 Da) of this region. Although this segment contained a stretch of residues (I101-R108) highly conserved in CMP-NeuAc synthetases, 3 amino acid residues were almost completely conserved throughout both CMP-NeuAc and CMP-KDO synthetases (Q102, P106 and I113) (Figure 3.13) (Tullius et al. 1996). The corresponding regions of CMP-KDO synthetase are mostly contained within α-helix4 and a loop lining the floor of the proposed binding pocket directly across from the putative phosphate binding loop (Figure 3.14) (Jelakovic et al. 1996). We therefore concluded that the second protected region spanning from I101 to L119 also participates in the binding of the nucleotide, CTP.

In the final protected segment (F158-176Y) of CMP-NeuAc synthetase, the extent of amide exchange was slightly suppressed upon the binding of CTP alone or in combination with Me-O-NeuAc (Figure 3.12C). However, the three overlapping peptides (M_r = 1961.2, 2074.4 and 2237.6 Da) of this region all showed significantly lower deuterium incorporation for the CMP-NeuAc-enzyme complex. Parallel effects of ligand binding were seen upon limited proteolysis of a highly conserved arginine (162) within this region where the presence of the product completely blocked proteolytic cleavage at this site. An inspection of the sequence alignment revealed that the third region protected from

amide exchange contains a large stretch of amino acids (Y169-D179) that are conserved within the CMP-NeuAc synthetase family, but are omitted from CMP-KDO synthetases (Figure 3.13) (Tullius et al. 1996). The absence of an analogous region in the CMP-KDO synthetase could suggest this segment participates in the recognition of the sialic acid. Since protection from limited proteolysis (R162) and amide exchange of region 3 are partially achieved in the ternary complex and full realized with CMP-NeuAc, the influence of the second substrate may extend beyond direct contact with residues of the active site to possibly include a change in conformation concomitant with catalysis.

In summary, we have shown that limited proteolysis and amide hydrogen isotopic exchange can be used to probe interactions between CMP-NeuAc synthetase and selected ligands. The coupling of these methods to MALDI mass spectrometry permitted the relatively easy assignment of proteolytic fragments as well as the efficient quantitation of deuterium incorporated into the intact protein and peptic peptides. These studies revealed that the presence of the first substrate, CTP, provided CMP-NeuAc synthetase partial protection from limited proteolysis, however, had no measurable effect on the global exchange of amide hydrogens. Yet, analysis of localized areas of the backbone revealed that the presence of CTP hindered proteolytic cleavage as well as amide exchange in certain regions of the enzyme. The sheltered segments were concluded to be directly involved in the binding of CTP, which is corroborated by results from mutagenesis and affinity labeling experiments on CMP-NeuAc synthetase (Stoughton et al. 1999; Tullius et al. 1999). Albeit, the addition of the sialic acid analog, Me-O-NeuAc, to the binary complex (E•MgCTP) provided little if any additional global protection from proteolysis by endoproteinase Glu-C or trypsin, the competitive inhibitor afforded greater protection from global amide exchange compared to that observed for the binary complex. However, no specific region of the enzyme appeared to be significantly protected from exchange in the ternary enzyme complex (E•MgCTP•Me-O-NeuAc) relative to exchange of the binary complex and may indicate that our methods are not detecting the binding of the sugar to localized regions of

the protein but rather, the occurrence of a change in protein conformation concomitant with catalysis leading to a structure with decreased solvent accessible surface. The advent of a change in protein conformation was further supported by the enhanced protection from both limited proteolysis and amide hydrogen exchange upon the binding of CMP-NeuAc to the enzyme beyond that observed in the ternary complex (E•MgCTP•Me-O-NeuAc). The ligand-induced change in protein conformation is presumed to be triggered by the presence of the second substrate and culminates with the release of the nucleotide sugar product, which may account for the dissociation of CMP-NeuAc from the enzyme as the rate-limiting step in k_{cat} (Samuels et al. 1999). Altogether, these studies highlight the complementary information extracted by limited proteolysis and amide hydrogen exchange techniques relevant to the nature of the active site and ligand-induced dynamics of the CMP-NeuAc synthetase from *H. ducreyi*.

CHAPTER 4.

Structural Analysis of Lipooligosaccharides (LOS) from Sialyltransferase Deficient Mutants of *Haemophilus influenzae*

4.1 INTRODUCTION

Studies surveying lipooligosaccharide (LOS) composition from encapsulated and non-encapsulated strains of *H. influenzae* revealed a high percentage contained sialic acid (NeuAc) (Hood et al. 1999; Mandrell et al. 1992). Considering that sialic acid contributes to the serum resistance of some members of the *Neisseria* and *Haemophilus* genera, we have focused our investigations towards understanding the role(s) of LOS sialylation as a virulence mechanism for the human pathogen responsible for invasive disease, *H. influenzae* type B (Hib). Over the years, LOS from a number of Hib strains have been characterized in an effort to correlate LOS structure with specific biological function(s). In this study, LOS glycoforms expressed by a clinical isolate and a transposon mutant, *H. influenzae* strains A2 and 276.4, respectively, have been reexamined using more sensitive techniques. Although previous investigations utilizing electrospray mass spectrometry (ESI-MS) detected the presence of two sialylated glycoforms in the A2 strain (Phillips et al. 1992), matrix assisted laser desorption ionization mass spectrometry (MALDI-MS) exposed 11 LOS glycoforms terminating with sialic acid, including poly-sialylated species never observed before. Examination of the LOS from the 276.4 strain by MALDI-MS showed the same major sialylated LOS glycoform observed in prior studies (Phillips et al. 1996), new minor sialylated species were also detected in the current study. To gain further insight into LOS structure, the oligosaccharide (OS) components of several larger glycoforms and the most abundant sialylated species were characterized by electrospray tandem mass

spectrometry (ESI-MS/MS). These investigations detailed the maturation of Hex-containing biosynthetic intermediates into acceptor glycoforms culminating with an N-acetyllactosamine, the substrates a LOS-specific sialyltransferase.

In a search for the putative sialyltransferase, a hypothetical protein encoded by HI0871 of the *H. influenzae* Rd genome was identified as having significant homology to a novel sialyltransferase (Lst) found in *H. ducreyi* (Bozue et al. 1999). To ascertain the function of the unknown gene product in the LOS biosynthesis, HI0871 (*siaA*) was inactivated by shuttle mutagenesis techniques in *H. influenzae* A2 and 276.4. MALDI-MS analysis of LOS from A2STF and 276.4STF strains showed the *siaA* mutants failed to produce the major sialylated species observed in the parental strains, leaving the non-reducing terminal N-acetyllactosamine of the asialo-LOS free. Surprisingly, the *siaA* mutant strains retained sialyltransferase activity, in both instances producing new minor species of higher molecular weight than those observed in their respective parental strains. Furthermore, species terminating with two or more sialic acids were detected in the *siaA* mutant strains as well as the parental strains including LOS species completely devoid of HexNAc. Collectively, these data implicate SiaA as a putative LOS specific sialyltransferase in *H. influenzae* and indicate the presence of at least a second sialyltransferase of dissimilar substrate specificity.

4.2 MATERIALS AND METHODS

4.2.1 Materials

Anhydrous hydrazine, neuraminidase (immobilized, *C. perfringens*), NAD, histidine, ribostamycin and chloramphenicol were from Sigma. Acetone (HPLC grade) and 2,5-dihydroxybenzoic acid were purchased from Aldrich. Nitrocellulose membranes (type VS, 0.025 μm) were obtained from Millipore. Brain heart infusion agar was purchased from

Difco and hemin from ICN. The original TA (thymidine adenosine) cloning kit was purchased from Invitrogen and pBluescript II SK- plasmid was from Stratagene.

4.2.2 Methods

The molecular biological manipulations, growth of bacterial cultures and isolation of lipooligosaccharides were performed in the laboratory of Professor Michael Apicella at the University of Iowa by Paul Jones.

4.2.2.1 *Construction of Putative Sialyltransferase Deficient Mutants of H. influenzae*

Plasmid pHS89-21 was constructed by TA (thymidine adenosine) cloning a 4.3 kb polymerase chain reaction product from *Haemophilus influenzae* strain 2019 with primers HSTR8 (CTGCAAAATACAGATAAAGCAACACTGGGG) and HSTR9 (CAGCGGCAAGAAATATAGGGTTAGAAAAAGC) into pCR2.1. The 4.3 kb DNA fragment containing the putative sialyltransferase (HI0871) was subcloned into the *EcoRI* site of pBluescript II SK-. pHS89-103K6 was constructed by ligating the kanamycin resistance gene cassette from pBSL86 (Alexeyev 1995) digested with *Pst*I into the *Nsi I* site of pHS89-103. The kanamycin resistance gene cassette lacks a transcriptional termination site and was inserted in the forward orientation with respect to the *siaA* gene (HI0871) (Seifert et al. 1986). pHS89-103K6 was digested with *Sca*I to linearize the construct and then transformed into the A2 and 276.4 strains using the MIV method (Herriott et al. 1970). The insertional mutation was integrated into the genomes of *H. influenzae* strains A2 and 276.4 by homologous recombination, forming the mutant strains A2STF and 276.4STF respectively. Transformants were selected on brain heart infusion agar plates containing ribostamycin.

4.2.2.2 *Growth of Haemophilus influenzae*

The organisms were grown on brain heart infusion agar supplemented with 10 μg/mL NAD and 10 μg/mL hemin. The 1 mg/mL hemin stock solution also contained 267 mM Tris and 6.4 mM histidine. Where appropriate, sialic acid (20 μg/mL), ribostamycin (15 μg/mL) and chloramphenicol (1 μg/mL) were added to the media. The organisms were grown for 16-48 hours at 37 °C.

4.2.2.3 *Isolation of Lipooligosaccharides (LOS)*

Lipooligosaccharides were isolated from *H. influenzae* using the proceeding proteinase K microextraction protocol (Apicella et al. 1994). A turbid solution of organisms grown on plates was added to a solution of PBS buffer in a 13X100 mm glass tube until an OD_{650} reading of 0.9 was reached. An aliquot of the turbid solution of bacteria (2 mL) was washed twice with PBS. The cells were resuspended in 200 μL of a solution of 60 mM Tris-HCl, 10 mM EDTA, 2.0% SDS pH 6.8 and incubated at 100 °C for 5 minutes. A 150 μL aliquot of the heated bacteria was transferred to a separate glass tube containing 30 μL of 2.5 mg/mL proteinase K in the same buffer and incubated at 37 °C overnight. The crude LOS was precipitated by adding 18 μL of 3 M sodium acetate and 360 μL of 95% ethanol and stored overnight at -20 °C. The crude LOS was pelleted at 16000 RCF for 2 minutes, washed twice with 70% ethanol and dried overnight or evaporated on a speed vacuum system.

4.2.2.4 *Preparation of O-deacylated Lipooligosaccharides (O-LOS) and Neuraminidase Treatment*

To make the LOS more amenable for mass spectrometric analysis, O-linked fatty acids were removed from the lipid A moiety, leaving the oligosaccharide and N-linked fatty acids of lipid A intact. The crude LOS (~90 ng, from a single plate) was incubated with anhydrous hydrazine (50 μL) at 37 °C for 25 minutes in a microcentrifuge tube, with

occasional sonication. Samples were cooled in the freezer (-10 °C) for 10 minutes prior to and after the addition of ice cold acetone (300 µL). The quenched reaction mixture was spun at 12000 RPM for 45 minutes in a chilled centrifuge. The supernatant was removed and the pelleted O-deacylated LOS (O-LOS) was dissolved in water (MilliQ) and evaporated on a speed vacuum system. To remove salts and other low molecular weight contaminants, the O-LOS (~1.8 µg/µL, 5 µL) was suspended on a nitrocellulose membrane over water (MilliQ) for 1 hour. Salt-free O-LOS was removed from the membrane, concentrated with a speed vacuum system and analyzed by MALDI-MS. For removal of neuraminic acid, the O-LOS (~0.45 µg/µL, 20 µL) was digested in 10 mM ammonium acetate pH 6.0 with immobilized neuraminidase (type VI, ~10 milliunits) for 7 hours at 30 °C. The enzyme was pelleted by centrifugation and the supernatant (15 µL)was transferred to a nitrocellulose membrane for drop dialysis (Gorisch 1988). The de-sialylated O-LOS was also concentrated and analyzed by MALDI-MS.

4.2.2.5 *Matrix Assisted Laser Desorption Ionization-Mass Spectrometry (MALDI-MS) of O-LOS*

An aliquot of the dialyzed O-LOS (~1.8 µg/µL) in water was mixed with an equal volume of a saturated solution of 2,5-dihydroxybenzoic acid in acetone on a stainless steel MALDI target. The O-LOS was analyzed on a Voyager-DE -TOF mass spectrometer (PerSeptive Biosystems) in the negative ion mode with 20,000 V accelerating voltage. Mass spectra were smoothed once by a 19 point Savitsky-Golay function and the masses assigned by centroiding the top 30% of the peak height. Mass spectra of O-LOS from *H. influenzae* A2 were calibrated internally with deprotonated molecular ions corresponding to glycoforms C_1 (m/z =2600.3), C_2 (m/z=2723.3), D_1 (m/z=2762.4), D_2 (m/z=2885.5) (summarized in Table 4.1) and the prompt fragment for lipid A (m/z=952.0). Whereas, the mass spectra of O-LOS from *H. influenzae* 276.4 were calibrated internally with deprotonated molecular ions corresponding to glycoforms B_1 (m/z =2438.1), B_2

(m/z=2561.2), C_1 (m/z=2600.3), C_2 (m/z=2723.3) (summarized in Table 4.1) and the prompt fragment for lipid A (m/z=952.0).

4.2.2.6 *Electrospray Ionization Tandem-Mass Spectrometry (ESI-MS/MS) of Oligosaccharide (OS) Components*

For more detailed structural analysis, the oligosaccharide (OS) was separated from the lipid A moiety by mild acid hydrolysis of the O-LOS from strains A2 and 276.4 grown in the presence of sialic acid. A solution of the O-LOS (~0.45 μg/μL, 20 μL) in 1% acetic acid was incubated in a microcentrifuge tube at 100 °C for 1 hour. The liberated lipid A was pelleted by centrifuging at 12,000 RPM at 4 °C for 20 minutes. The supernatant (15 μL) was transferred to a nitrocellulose membrane suspended over water and dialyzed for 1 hour. The desalted OS was transferred to a microcentrifuge tube, lyophilized and analyzed in the positive ion mode on a QSTAR hybrid quadrupole-TOF mass spectrometer (PE Sciex Instruments). The OS components (~0.1 μg/μL) were prepared in a solution of 40 mM ammonium acetate pH 4.5/50% acetonitrile/ H_2O and 5 μL of each sample was deposited into a Protana nanospray tip (medium). Tandem spectra were acquired with a 1100-1200 needle voltage and a quadrupole mass analyzer mass window of 1 m/z unit. Mass spectra were corrected by a two point calibration with the singly charged fragment ions (m/z = 187.0719 and 1285.5449) derived from the doubly charged parent ion (m/z = 785.8427) of the human [glu^1]-fibrinopeptide B.

4.3 RESULTS AND DISCUSSION

4.3.1 Identification of LOS Glycoforms in *H. influenzae* A2 and 276.4

Prior to investigating the effects of inactivating genes responsible for LOS biosynthesis in *H. influenzae*, the population of LOS glycoforms assembled by the A2

strain was assessed with MALDI-MS in the negative ion mode. All observed molecular ions and the proposed LOS compositions are summarized in Table 4.1. Alphabets represent individual glycoforms to which sialic acid (each denoted by an asterisk) and one or two phosphoethanolamines (denoted by subscript) are added. Analysis of the intact O-LOS confirmed the presence of a complex mixture of glycoforms, the majority of which represented extensions of the major species (C_1 and C_2) by up to 4 additional Hex (Figure 4.1). The most prominent glycoforms were also observed in prior investigations of *H. influenzae* A2 LOS by ESI-MS. However, the dominant species were found to contain either one or two phosphoethanolamine (PEA) moieties, as opposed to the solitary PEA observed in earlier studies. Discrepancies in PEA substitution may reflect the contrasting growth conditions, as the LOS in the current study were isolated from *H. influenzae* grown on solid as opposed to in liquid media. Furthermore, the MALDI-MS spectra of the A2 O-LOS included a species containing a HexNAc (N_1), a minor species which had not been observed in former investigations using ESI-MS on a triple quadrupole instrument (Phillips et al. 1992). More recent advances in the field of mass spectrometry, such as delayed ion extraction, have permitted the relatively quick and easy analysis of LOS, especially the evaluation of larger glycoforms in very low abundance (Gibson et al. 1997). However, delayed extraction methods also permitted the observation of ions arising from prompt (in-source) fragmentation of the O-LOS corresponding to the loss of HPO_3 (-80 Da) and H_3PO_4 (-98 Da) from the most abundant species. MALDI MS analysis of the O-LOS revealed the A2 strain expresses an even more complex mixture of glycoforms on its outer-membrane than previously thought.

To identify the glycoforms containing sialic acid (NeuAc), the O-LOS from the A2 strain was treated with neuraminidase and subsequently analyzed by MALDI-MS. In this experiment, a neuraminidase with broad substrate specificity from *C. perfringens* was chosen as the enzyme cleaves α2,3, α2,6 and α2,8 linked sialic acid from a variety of acceptor sugars. The mass spectra of the O-LOS after enzymatic hydrolysis showed the

Table 4.1 Summary of LOS glycoforms present in *H. influenzae* A2 and 276.4

Glycoform	Proposed Compositions (minimum structure includes 3Hep KDO(P) O-deacylated LipidA)				Calculated	A2	A2	276.4	276.4
$X_{1/2PEA}$	NeuAc	HexNAc	Hex	PEA	Mr (average)		+NeuAc		+NeuAc
A_1			2	1	2277.0			2277.2	2277.3
A_2			2	2	2400.0			2400.2	2400.0
B_1			3	1	2439.1	2439.4	2439.2	2439.2	2439.1
B_2			3	2	2562.2	2562.3	2562.2	2562.3	2562.2
C_1			4	1	2601.3	2601.2	2601.2	2601.1	2601.4
C_2			4	2	2724.3	2724.3	2724.2	2724.4	2724.3
D_1			5	1	2763.4	2763.4	2763.3		
D_2			5	2	2886.5	2886.7	3887.3		
E_1			6	1	2925.6	2925.6	2925.3		
E_2			6	2	3048.6	3048.7	3048.4		
F_1			7	1	3087.7	3087.6	3087.4		
F_2			7	2	3210.8	3210.7	3210.9		
G_1			8	1	3249.8	3250.4	3249.8		
G_2			8	2	3372.9	3273.6	3373.1		
H_1			9	1	3412.0				
H_2			9	2	3535.0				
I_1		1	3	1	2642.3				
I_2		1	3	2	2765.4				
J_1		1	4	1	2804.5			2804.3	2804.1
J_2		1	4	2	2927.5				
K_1		1	5	1	2966.6				
K_2		1	5	2	3089.7				
L_1		1	6	1	3128.8				
L_2		1	6	2	3251.8				
M_1		1	7	1	3290.9				
M_2		1	7	2	3414.0				

Glycoform	Proposed Compositions minimum structure includes 3Hep KDO(P) O-deacylated LipidA				Calculated	A2	A2	276.4	276.4
$X_{1/2}$	NeuAc	HexNAc	Hex	PEA	Mr (average)		+NeuAc		+NeuAc
N_1		1	8	1	3453.0	3451.3	3452.1		
N_2		1	8	2	3576.1				
O_1		1	9	1	3615.2				
O_2		1	9	2	3738.2				
P_1		1	10	1	3777.3				
P_2		1	10	2	3900.4				
Q_1		2	1	1	2521.3				
Q_2		2	1	2	2644.3				
R_1		2	5	1	3169.8				
R_2		2	5	2	3292.9				
A_1**	2		2	1	2859.5			2861.8	2860.7
C_2*	1		4	2	3015.6		3015.6		
E_1***	3		6	1	3799.3	3798.5	3797.8[a]		
E_2*	1		6	2	3339.9		3340.5		
F_1***	3		7	1	3961.5	3959.9	3960.7		
F_2*	1		7	2	3502.0		3502.3		
Q_2***	3	2	1	2	3518.1				3517.7
I_1***	3	1	3	1	3516.0				3517.7
K_1*	1	1	5	1	3257.9			3258.5	3258.3
K_2*	1	1	5	2	3380.9			3381.0	3380.8
R_1*	1	2	5	1	3461.1			3460.7	3460.3
L_1*	1	1	6	1	3420.0		3419.9		
L_2*	1	1	6	2	3543.1	3542.4	3542.7		
L_2**	2	1	6	2	3834.3	3835.0	3834.1		
M_1*	1	1	7	1	3582.2	3581.0	3582.2		
M_2*	1	1	7	2	3705.2	3705.5	3705.5		
P_1**	2	1	10	1	4359.8		4360.5[a]		

[a] Species observed after treatment of O-LOS with neuraminidase

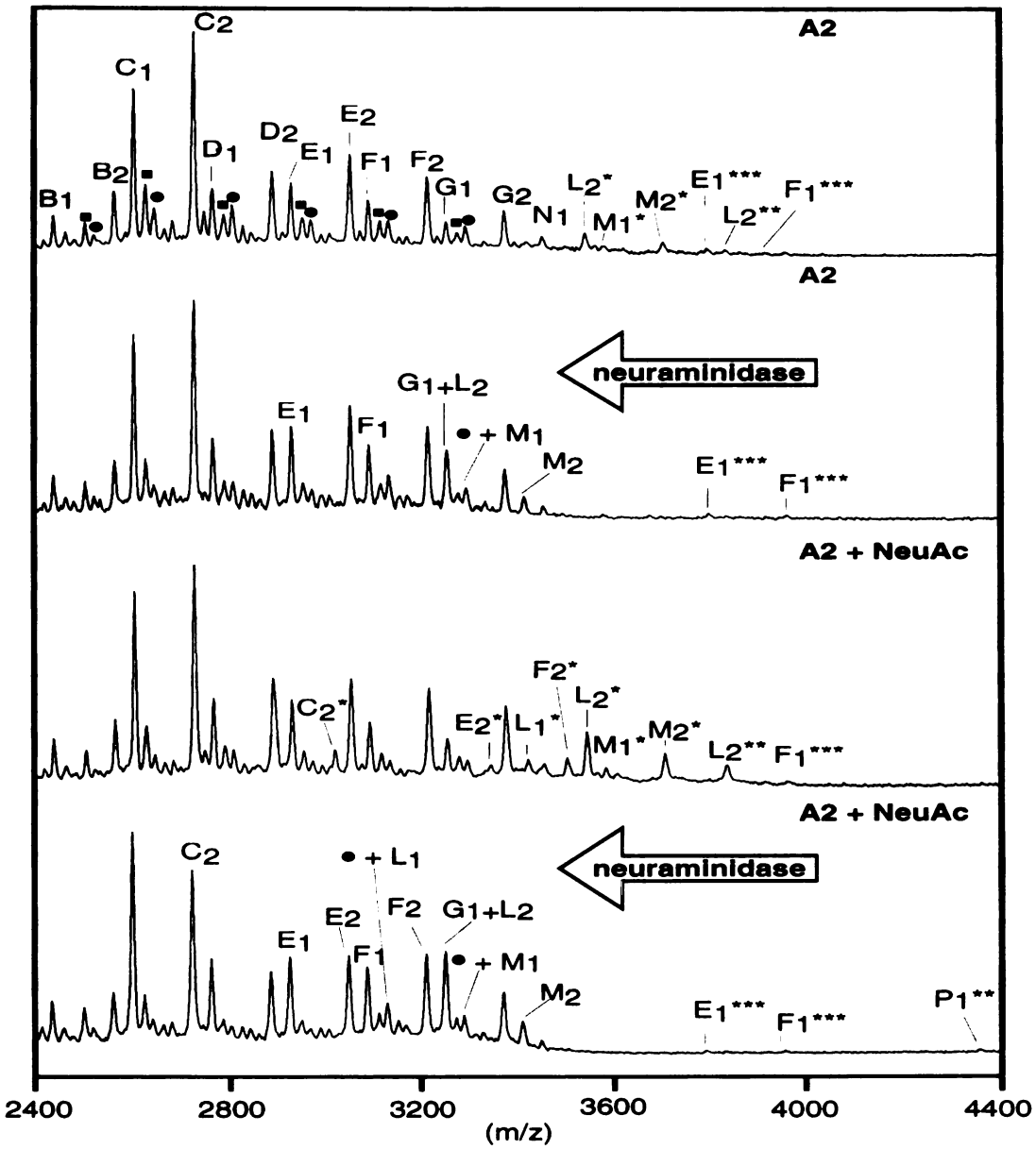

Figure 4.1 Negative ion MALDI-MS spectra of O-deacylated LOS from *H. influenzae* A2. Mass spectra compare LOS isolated from strain A2 grown in absence and presence of 20 μg/mL NeuAc before and after treatment with neuraminidase. See Table 4.1 for molecular weights and proposed compositions. Asterisks indicate the addition of sialic acid and the number of PEA moieties are denoted by subscript. Prompt fragments correspond to the loss of HPO_3 (●) and H_3PO_4 (■) from the most abundant species.

disappearance of 4 sialylated glycoforms (L_2*, L_2**, M_1* and M_2*), which in most cases, coincided with the appearance of lower molecular weight asialo-counterparts terminating with N-acetyllactosamine. To enhance the production of sialylated species, the bacteria were also cultured on solid media supplemented with sialic acid. As expected, the relative abundance of the sialylated species (L_2*, L_2**, M_1* and M_2*) increased without any noted alterations in the population of major glycoforms devoid of neuraminic acid. However, the appearance of several new sialylated glycoforms (L_1*, C_2*, E_2* and F_2*) were confirmed following treatment of the O-LOS with neuraminidase. In general, the most abundant LOS species terminating with sialic acid were glycoforms containing a single HexNAc and a total of 6 or 7 Hex. Interestingly, previous investigations of *H. influenzae* O-LOS revealed smaller sialylated glycoforms containing a single HexNAc and a total of 5 or 6 Hex, another discrepancy that may reflect altered growth conditions (Phillips et al. 1992). In the current study, other sialylated species were observed including several novel structures containing two or more sialic acids (E_1***, F_1***, L_2**, P_1**) and a single structure lacking HexNAc (F_2*) that was only observed when sialic acid was added to the culture media. Although the NTHi strain 375 was recently shown to synthesize a di-sialyllactose containing species (Hood et al. 1999), MALDI-MS proved a sensitive analytical tool for the analysis of an extremely heterogeneous mixture of LOS, having the capacity to detect minor poly-sialylated species in the A2 strain for the first time.

As the A2 strain expressed a complex mixture of LOS structures, a transposon mutant producing a smaller subset of the LOS structures was chosen for parallel studies aimed at identifying an LOS-specific sialyltransferase. The 276.4 isogenic mutant strain was constructed in the laboratory of Dr. Michael Apicella at the University of Iowa by shuttle mutagenesis of the lipooligosaccharide synthesis genes (*lsg*) loci of the parental strain, *H. influenzae* A2 (McLaughlin et al. 1992; Seifert et al. 1986). The minitransposon (m-Tn*3*Cm) was found to randomly insert into the fifth open reading frame (*lsgE*) encoding a putative galactosyltransferase (Phillips et al. 1996; Phillips et al. 2000). In the present

study, MALDI-MS analysis of the O-LOS isolated from the 276.4 strain showed the 3 and 4 Hex species (B_1, B_2, C_1 and C_2) as the major glycoforms (Figure 4.2). All observed LOS glycoforms present in 276.4 grown in the absence and presence of sialic acid and the proposed compositions are summarized in Table 4.1. As observed in previous investigations of the mutant strain, the relatively abundant glycoform containing a total of 5 Hex and a single HexNAc (K_2*) terminated with a single sialic acid residue. However, new sialylated glycoforms were observed in the 276.4 strain including a species containing 2 HexNAc (R_1*) and a di-sialylated structure lacking HexNAc (A_1**). The use of a mutant strain expressing fewer LOS glycoforms should facilitate the interpretation of the effects of gene mutation on LOS biosynthesis for subsequent experiments.

4.3.2 Structural Analysis of Oligosaccharide (OS) Components from *H. influenzae* A2 and 276.4

To obtain additional insight into the structures of higher molecular weight LOS glycoforms, the oligosaccharide components from *H. influenzae* A2 grown in the presence of sialic acid were analyzed by ESI-MS/MS in the positive ion mode. Chemical removal of the lipid A moiety from the intact O-LOS produced a smaller oligosaccharide (OS) component that more readily fragments in gas phase, therefore yielding more product ions for determining the sequential order of the linked sugars and branching patterns. As a consequence of the β-elimination of phosphate from the 4 position of KDO, all OS contain an anhydrous form of the acidic sugar at the reducing terminus. The tandem mass spectra of Hex containing OS were dominated by the typical series of Y-and B-fragment ions resulting from the cleavage of a glycosidic bond, where the charge is retained on the reducing and non-reducing termini, respectively (Figures 4.3 - 4.6). In general, the tandem mass spectra of 4 species (M_r = 1729.51, 1891.56, 2053.61, 2215.67 Da) revealed sets of Y-type ions corresponding to the successive loss of hexoses from the parent ions.

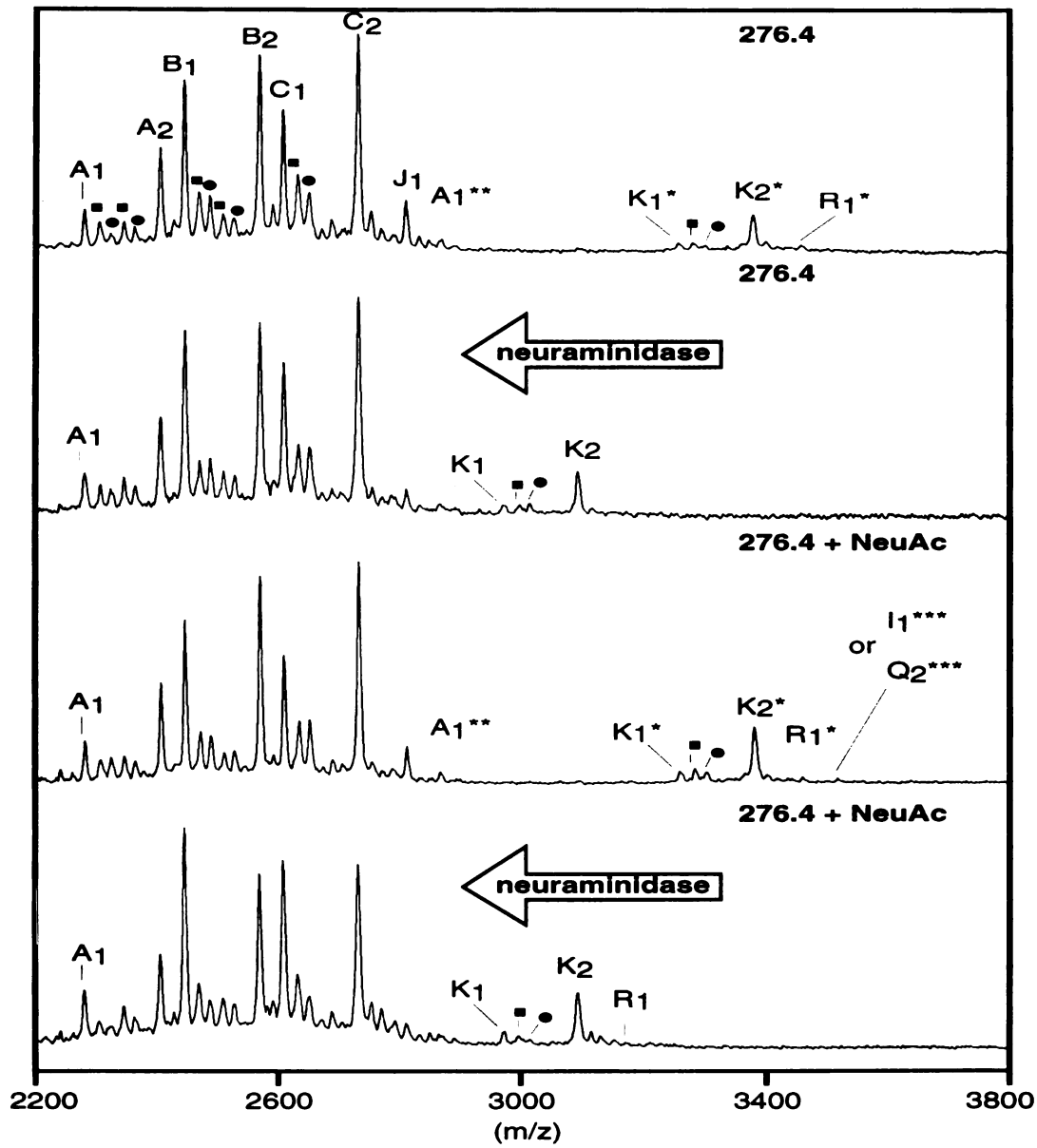

Figure 4.2 Negative ion MALDI-MS spectra of O-deacylated LOS from *H. influenzae* 276.4. Mass spectra compare LOS isolated from strain 276.4 grown in absence and presence of 20 μg/mL NeuAc before and after treatment with neuraminidase. See Table 4.1 for molecular weights and proposed compositions. Asterisks indicate the addition of sialic acid and the number of PEA moieties are denoted by subscript. Prompt fragments correspond to the loss of HPO_3 (●) and H_3PO_4 (■) from the most abundant species.

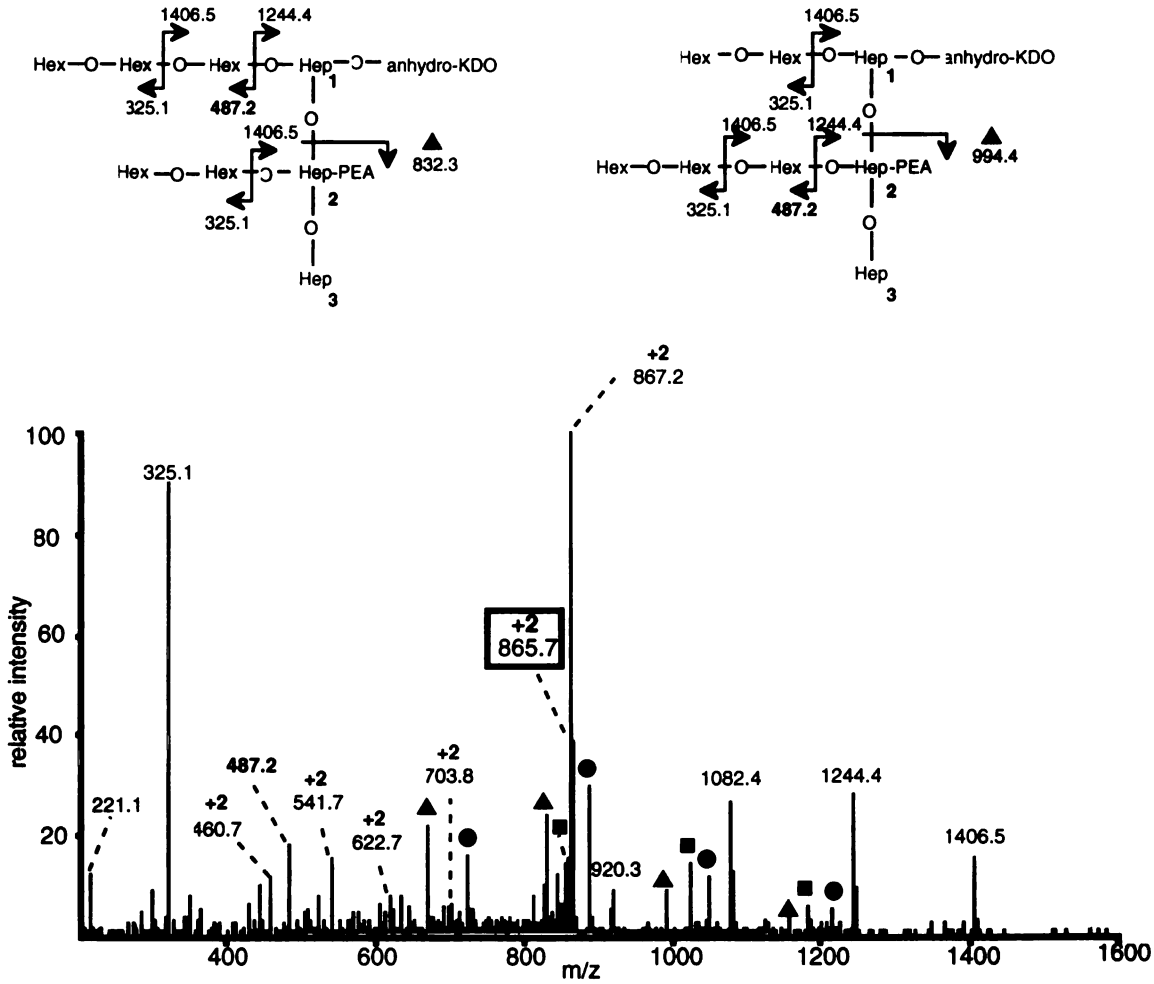

Figure 4.3 Positive ion ESI-MS/MS spectrum of $Hex_5PEA_1Hep_3$ anhydro-KDO oligosaccharide from *H. influenzae* A2. The doubly charged parent ion $(M+2H)^{+2}$ of the M_r 1729.51 Da species (monoisotopic mass) is indicated with a box. All product ions are singly charged unless otherwise noted. Families of fragment ions arise from the cleavage of bonds to Hex and KDO (● ions m/z= 728.3, 890.3, 1052.4, 1214.4), to Hex and Hep (■ ions m/z = 862.3, 1024.4, 1186.4) and to Hex, Hep and KDO (▲ ions m/z = 670.2, 832.3, 994.4, 1156.4).

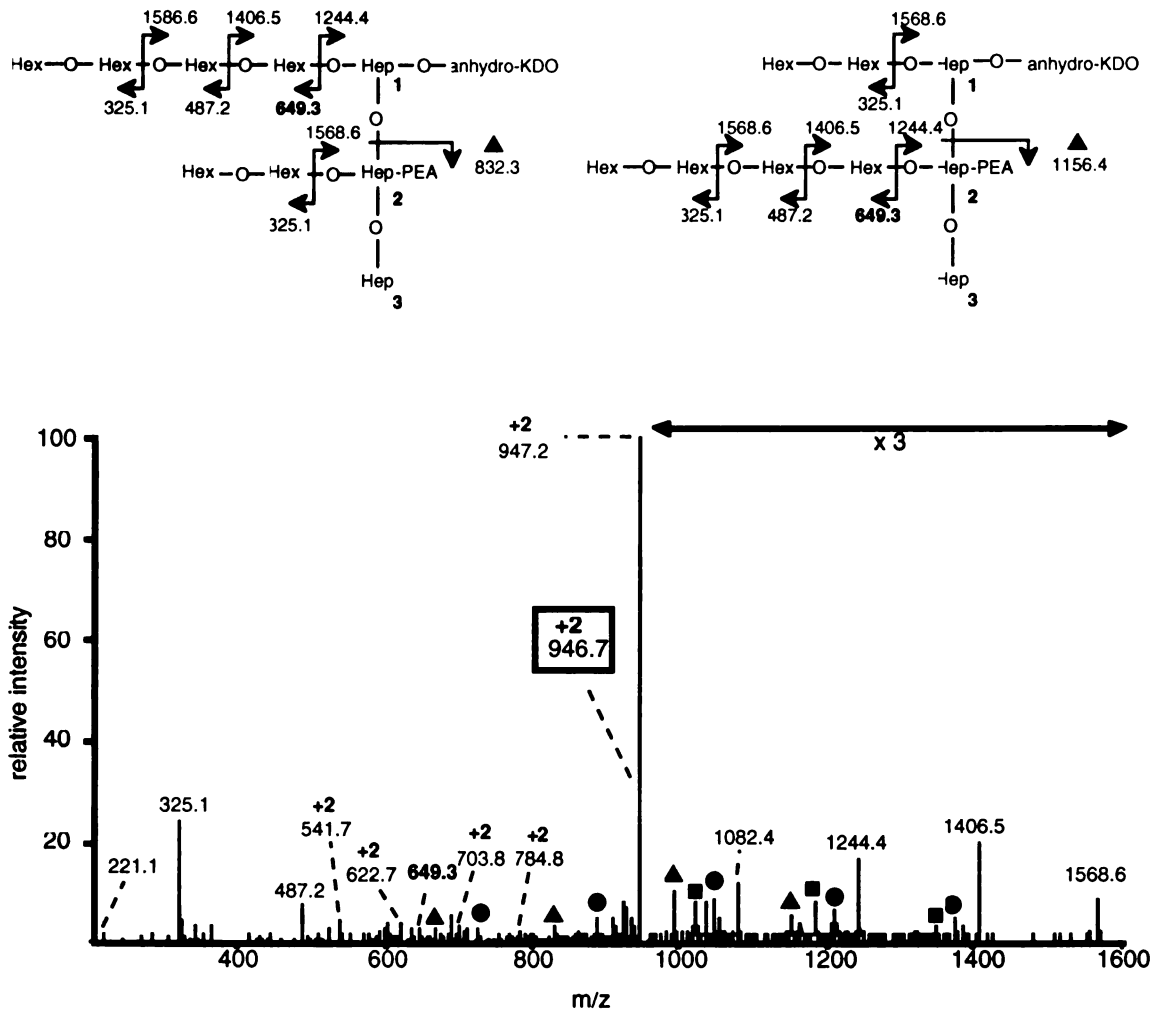

Figure 4.4 Positive ion ESI-MS/MS spectrum of $Hex_6PEA_1Hep_3$ anhydro-KDO oligosaccharide from *H. influenzae* A2. The doubly charged parent ion $(M+2H)^{+2}$ of the M_r 1891.56 Da species (monoisotopic mass) is indicated with a box. All product ions are singly charged unless otherwise noted. Families of fragment ions arise from the cleavage of bonds to Hex and KDO (● ions m/z= 728.3, 890.3, 1052.3, 1214.4, 1376.5), to Hex and Hep (■ ions m/z =1024.3, 1186.5, 1348.5) and to Hex, Hep and KDO (▲ ions m/z = 670.2, 832.3, 994.4, 1156.4).

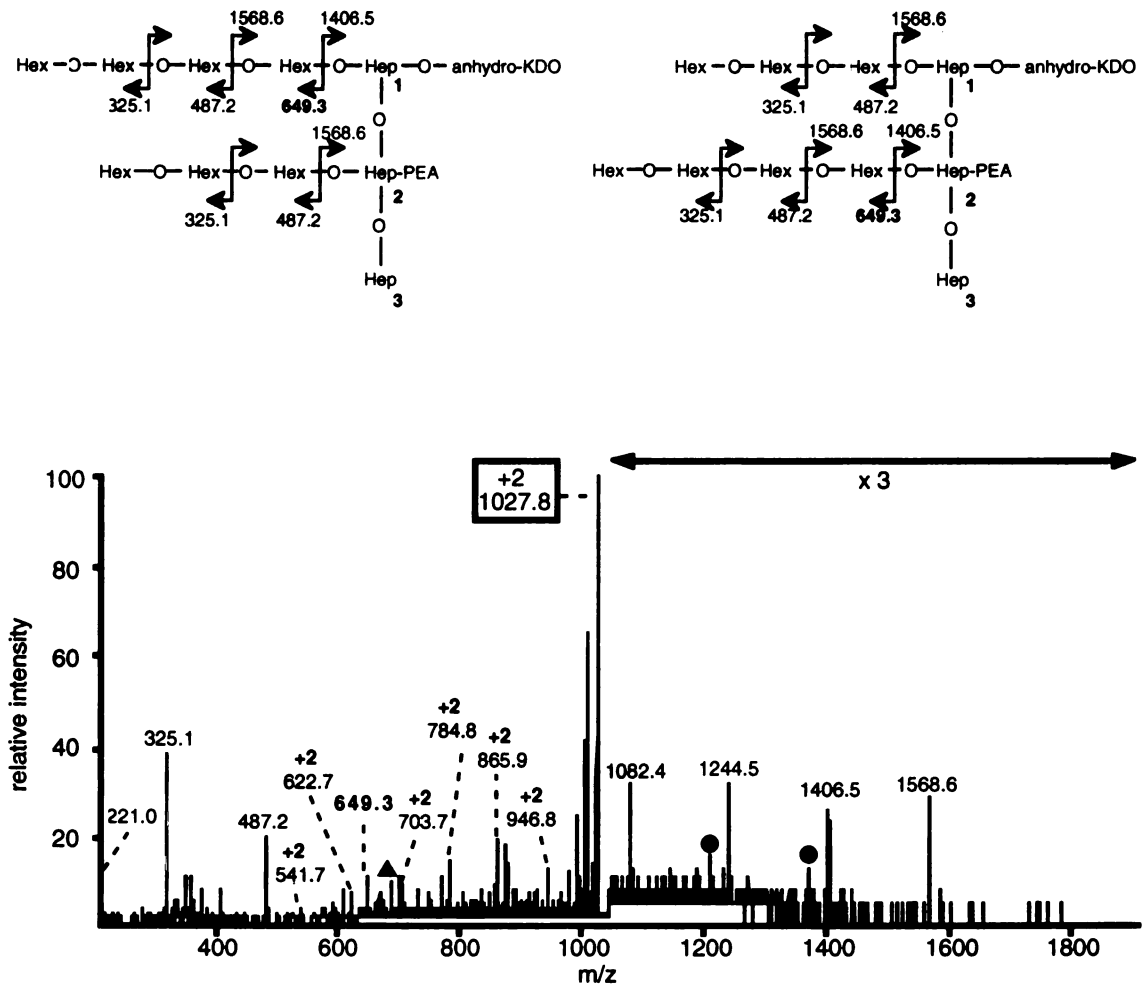

Figure 4.5 Positive ion ESI-MS/MS spectrum of $Hex_7PEA_1Hep_3$ anhydro-KDO oligosaccharide from *H. influenzae* A2. The doubly charged parent ion $(M+2H)^{+2}$ of the M_r 2053.61 Da species (monoisotopic mass) is indicated with a box. All product ions are singly charged unless otherwise noted. Families of fragment ions arise from the cleavage of bonds to Hex and KDO (● ions m/z= 1214.4, 1376.5) and to Hex, Hep and KDO (▲ ions m/z = 670.2).

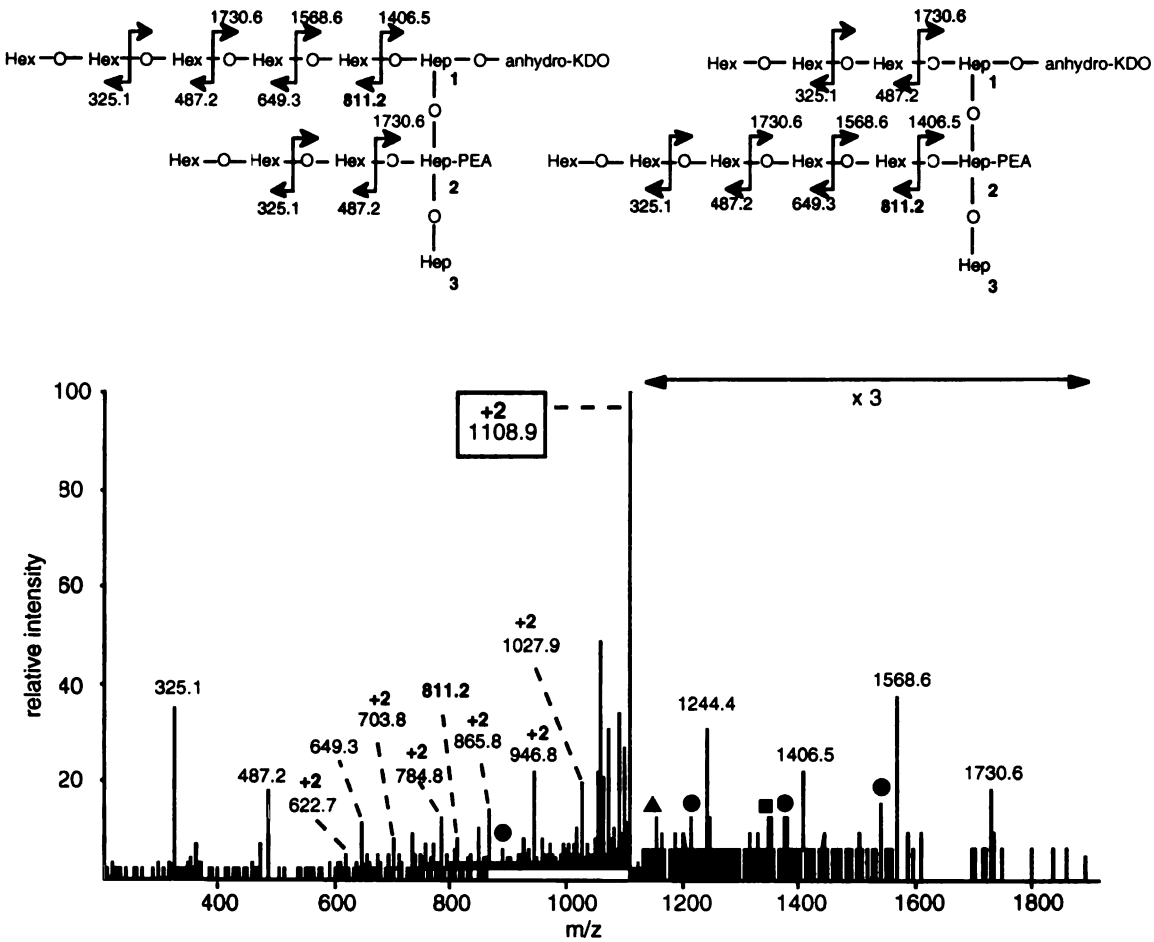

Figure 4.6 Positive ion ESI-MS/MS spectrum of $Hex_8PEA_1Hep_3$ anhydro-KDO oligosaccharide from *H. influenzae* A2. The doubly charged parent ion $(M+2H)^{+2}$ of the M_r 2215.67 Da species (monoisotopic mass) is indicated with a box. All product ions are singly charged unless otherwise noted. Families of fragment ions arise from the cleavage of bonds to Hex and KDO (● ions m/z= 890.3, 1214.4, 1376.5, 1538.5), to Hex and Hep (■ ion m/z =1348.4) and to Hex, Hep and KDO (▲ ion m/z = 1156.4).

Moreover, from well defined sets of B-type ions, the minimum size of at least one non-reducing terminal branch could be ascertained. For instance, MS/MS spectra of the M_r 1729.51 Da species showed the distinctive B-type product ion for the loss of 3 consecutively bonded hexoses (m/z = 487.2) from the parent ion (Figure 4.3). Likewise, product ions at m/z 649.3 established a nonreducing terminal branch of at least 4 consecutively bonded hexoses for the M_r 1891.56 and 2053.61 Da species (Figures 4.4 and 4.5), whereas the M_r 2215.67 Da species was found to contain at least 5 consecutively bonded hexoses based on the observation of the product ion at m/z 811.2 (Figure 4.6).

Various fragment ions arising from the simultaneous cleavage of multiple bonds were classified as belonging to one of three families of product ions (●, ■, ▲). For example, the MS/MS spectra of the M_r 1729.51 Da species (Figure 4.3) revealed the most abundant collection of product ions (●) resulting from the combined cleavage of glycosidic bonds to a Hex and Hep (Figure 4.3). Similarly, the second family of product ions (■) result from the cleavage of bonds to the KDO and a Hex from opposite ends of the same OS molecule. The preceding families of product ions (●, ■) are well represented in the mass spectra of larger OS containing Hex and especially highlight the susceptibility of glycosidic bonds to the KDO and non-reducing terminal Hep to collision induced dissociation in the highly efficient collision cell of the hybrid instrument.

These observations would prove useful for assigning the bonds cleaved to produce a third family of ions (▲) corresponding to the loss of KDO from the (●) doubly cleaved family of ions and a single bond cleavage between 2 core Hep. For example, the MS/MS spectra of the M_r 1729.51 Da species (Figure 4.3) showed two B-type product ions (▲ m/z = 832.3 and 994.4) that may have resulted from cleavage between the first and second core heptoses of the proposed LOS structure, where the middle Hep is substituted with either 2 or 3 Hex. However, a larger related ion (▲ m/z = 1156.4) is most likely the product of a three rather than a single cleavage event between the first and second Hep of the core, as more reliable ions in the current spectra and previous structural studies (Phillips et al. 1992)

exclude the possibility of any combination of 4 Hex extending from both the second and third Hep. In general, tandem MS analysis of OS containing a total of 6, 7 or 8 Hex yielded similar sets of ions resulting from multiple bond cleavages. In each case, the ions that unequivocally establish the minimum length of at least one non-reducing terminal branch are highlighted in bold and were consistent with two proposed structures. Collectively, structural elucidation of these sequential biosynthetic intermediates illustrate how the LOS specific-glycosyltransferases extend non-reducing branches from core Hep.

In an effort to assign the sequential linkages of sugars in the most abundant sialylated glycoforms, oligosaccharide components from both *H. influenzae* A2 and 276.4 grown in the presence of sialic acid were characterized by ESI-MS/MS. Hydrolysis of the O-LOS not only liberates the OS from the lipid A moiety, but also cleaves acid sensitive linkages to NeuAc, thus only permitting for the analysis of the acceptor glycoforms. The tandem-MS spectra of HexNAc containing acceptor glycoforms (M_r = 1932.59, 2094.64, 2256.69 Da) clearly showed an assortment of Y-type ions resulting from the initial loss of HexHexNAc and successive deductions of Hex, most likely indicating the presence of a non-reducing terminal N-acetyllactosamine (Figures 4.7-4.9). While, the opposite B-type product ion series retaining charge on the non-reducing terminal fragments (m/z = 366.2, 528.2, 690.3) was observed for all three acceptor molecules, regardless of molecular weight. These data indicate a non-reducing terminal branch contains a single HexNAc in addition to a minimum of 3 Hex and are consistent with two proposed structures where branches extending from the first and second Hep are interchangeable. The proposed structures of the HexNAc containing acceptor glycoforms (Figures 4.7-4.9) are also consistent with the proposed structures of their respective biosynthetic intermediates ($Hex_4 Hep_3 PEA_1$ anhydro-KDO, $Hex_5 Hep_3 PEA_1$ anhydro-KDO, $Hex_6 Hep_3 PEA_1$ anhydro-KDO), to which an N-acetyllactosamine is attached to form the substrate of the putative sialyltransferase.

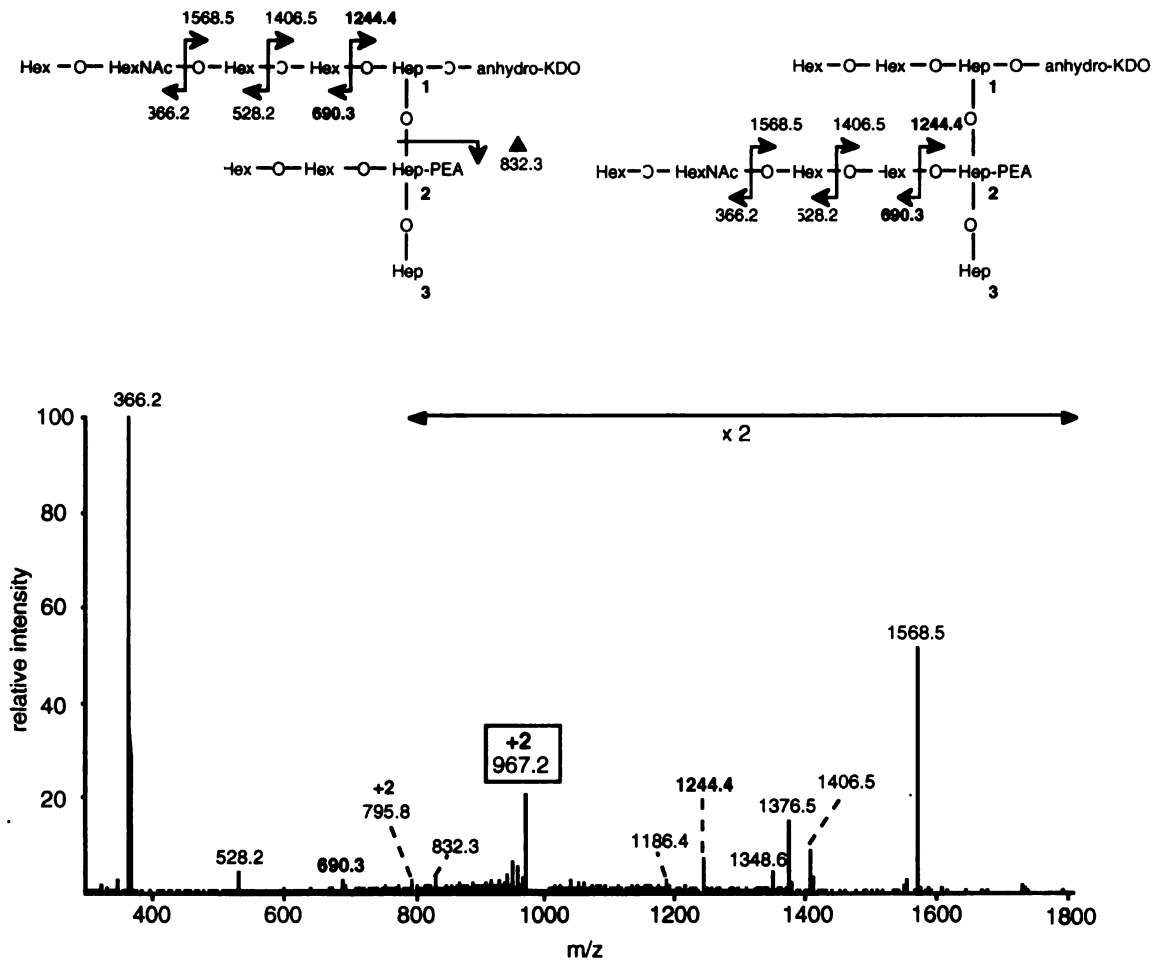

Figure 4.7 Positive ion ESI-MS/MS spectrum of $HexNAc_1 Hex_5 PEA_1 Hep_3$ anhydro-KDO oligosaccharide from *H. influenzae* 276.4. The doubly charged parent ion $(M+2H)^{+2}$ of the M_r 1932.59 Da species (monoisotopic mass) is indicated with a box. All product ions are singly charged unless otherwise noted. Families of fragment ions arise from the cleavage of bonds to Hex and Hep (■ ions m/z = 1186.4, 1348.6) and to Hex, Hep and KDO (▲ ion m/z = 832.3).

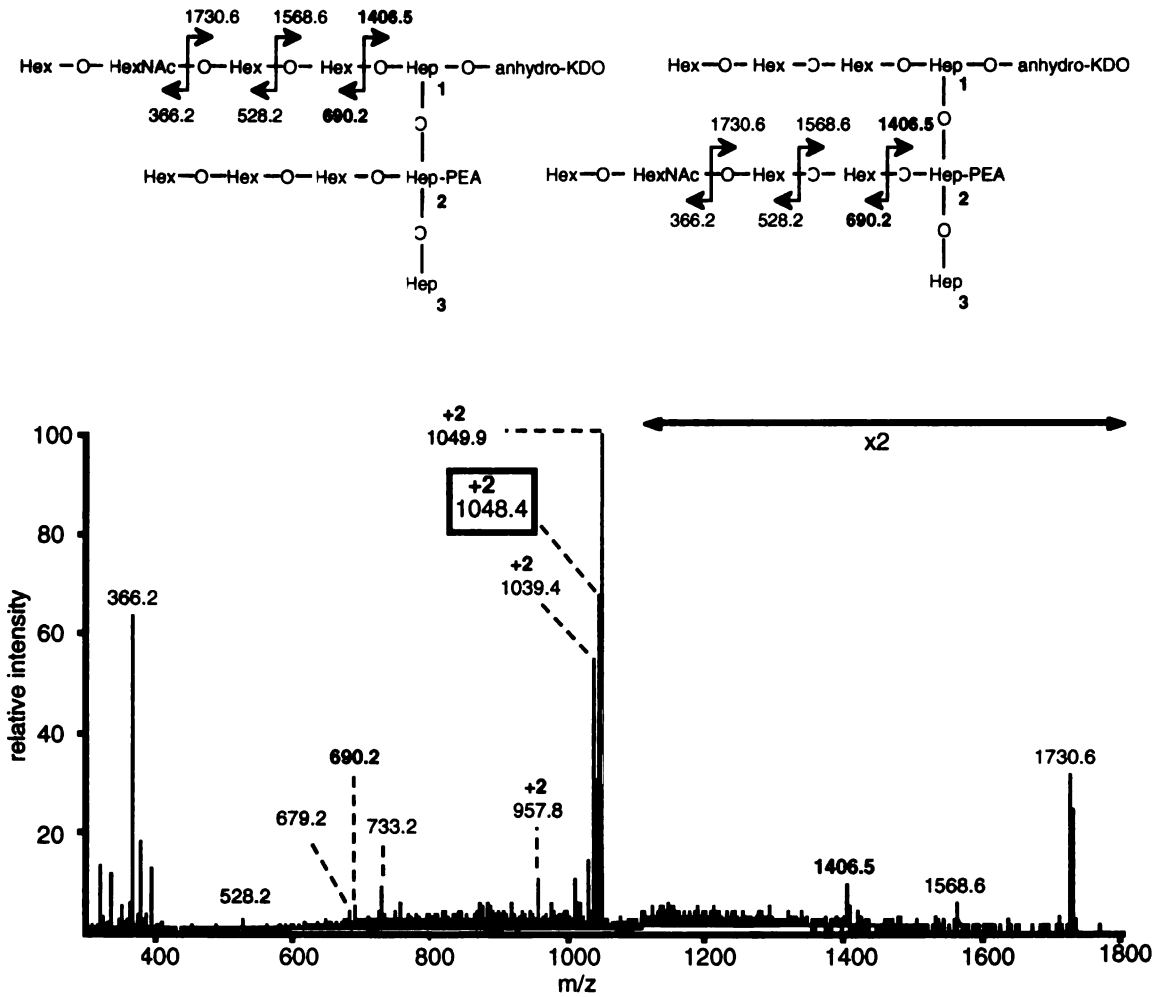

Figure 4.8 Positive ion ESI-MS/MS spectrum of $HexNAc_1Hex_6PEA_1Hep_3$ anhydro-KDO oligosaccharide from *H. influenzae* A2. The doubly charged parent ion $(M+2H)^{+2}$ of the M_r 2094.64 Da species (monoisotopic mass) is indicated with a box. All product ions are singly charged unless otherwise noted. Families of fragment ions arise from the cleavage of bonds to Hex and KDO (● ions m/z= 728.3, 890.3, 1052.4, 1214.4), to Hex and Hep (■ ions m/z = 862.3, 1024.4, 1186.4) and to Hex, Hep and KDO (▲ ions m/z = 670.2, 832.3, 994.4, 1156.4).

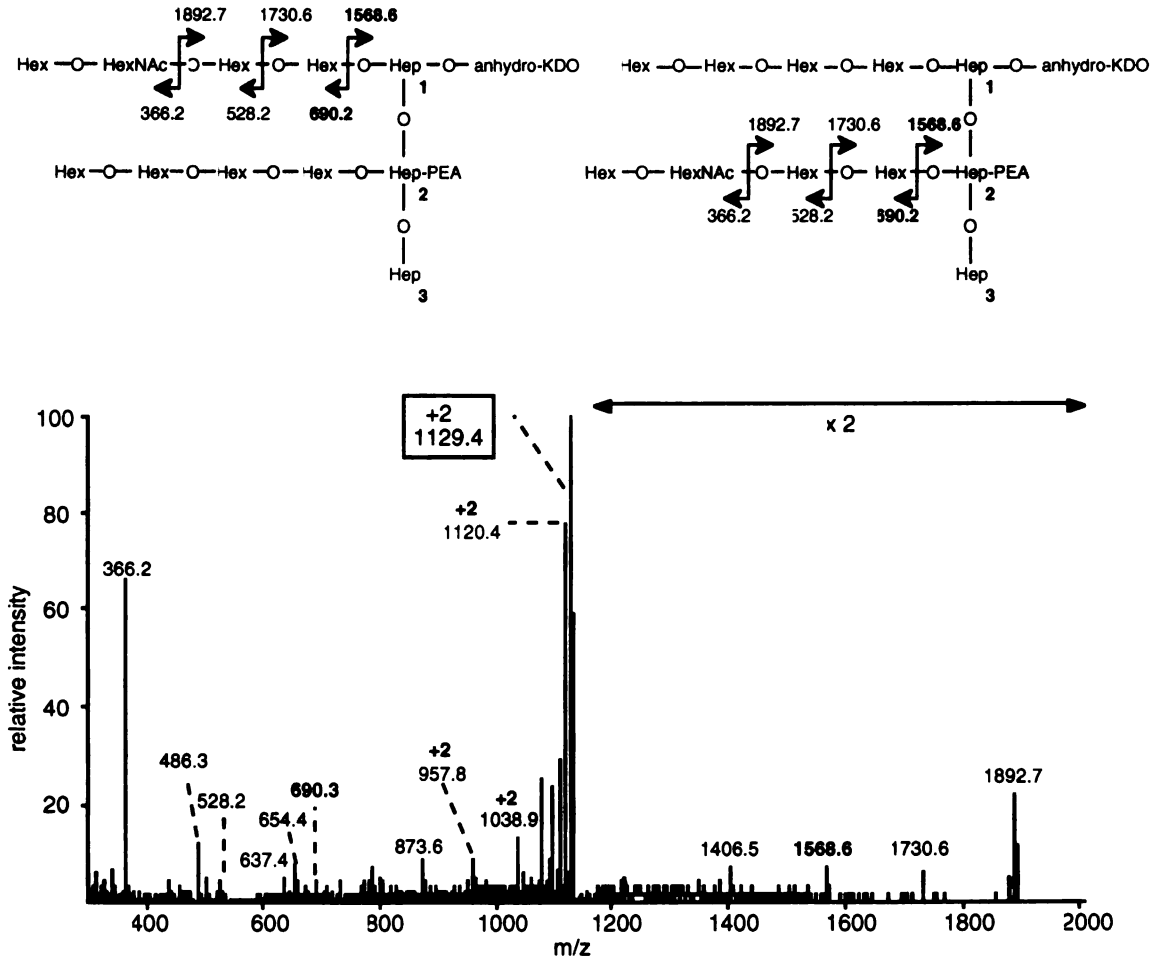

Figure 4.9 Positive ion ESI-MS/MS spectrum of $HexNAc_1 Hex_7 PEA_1 Hep_3$ anhydro-KDO oligosaccharide from *H. influenzae* A2. The doubly charged parent ion $(M+2H)^{+2}$ of the M_r 2256.59 Da species (monoisotopic mass) is indicated with a box. All product ions are singly charged unless otherwise noted. Families of fragment ions arise from the cleavage of bonds to Hex and KDO (● ions m/z= 728.3, 890.3, 1052.4, 1214.4), to Hex and Hep (■ ions m/z = 862.3, 1024.4, 1186.4) and to Hex, Hep and KDO (▲ ions m/z = 670.2, 832.3, 994.4, 1156.4).

4.3.3 Analysis of O-deacylated LOS (O-LOS) from Sialyltransferase Deficient Mutants of *H. influenzae* A2 and 274.4

In an investigation of LOS biosynthesis, a search of the complete *H. influenzae* strain Rd genome (Fleischmann et al. 1995; Hood et al. 1996) led to the identification of *orfY* (HI0871), a gene encoding a hypothetical protein having significant homology to a novel sialyltransferase (Lst) recently reported in *H. ducreyi* (Bozue et al. 1999). Investigators had previously mutated *orfY* in three typable strains of *H. influenzae* and monitored changes in LOS expression by SDS-PAGE (Hood et al. 1996). Although no detectable changes were reported for the RM7004 strain, very minor alterations in LOS structure were observed in strains RM153 and RM118. In an effort to resolve the function of the HI0871, designated *siaA*, the gene was inactivated in two well characterized strains of *H. influenzae* by shuttle mutagenesis in the laboratory of Dr. Michael Apicella. Mutant strains were constructed by the insertion of a kanamycin resistance cassette into *siaA*, followed by the integration of the nonfunctional gene into the genomes of *H. influenzae* strains A2 and 276.4 by homologous recombination. Alterations in LOS expression were assessed by comparing the glycoforms produced by the *siaA* mutant strains (A2STF and 276.4STF) to those produced by the parental strains (A2 and 276.4) employing MALDI-MS. Mass spectrometry of the LOS from the parental strain proved a sensitive method, allowing the confident assignment of glycoform compositions, as opposed to the sole use of SDS-PAGE.

Analysis of the LOS from the A2STF mutant strain revealed no gross changes in the expression of the major glycoforms found to be devoid of sialic acid in the parental strains (Figure 4.10). The mutant strain failed to produce major sialylated species (L_1*, L_2*, L_2**, M_1* and M_2*) observed in the parental strain, leaving the respective acceptor glycoforms free and unmodified (L_1, L_2, M_1 and M_2), the presumed substrate of SiaA. Unexpectedly, the A2STF mutant retained the capacity to produce minor sialylated LOS,

Figure 4.10 Negative ion MALDI-MS spectra comparing O-deacylated LOS from *H. influenzae* A2 and A2STF. Mass spectra comparing LOS isolated from strain A2STF grown in absence and presence of 20 μg/mL NeuAc before and after treatment with neuraminidase. See Table 4.2 for molecular weights and proposed compositions. The mass spectra of the O-LOS isolated from the parental strain A2 grown in the presence of 20 μg/mL sialic acid has been included for comparison. Asterisks indicate the addition of sialic acid and the number of PEA moieties are denoted by subscript. Prompt fragments correspond to the loss of HPO_3 (●) and H_3PO_4 (■) from the most abundant species.

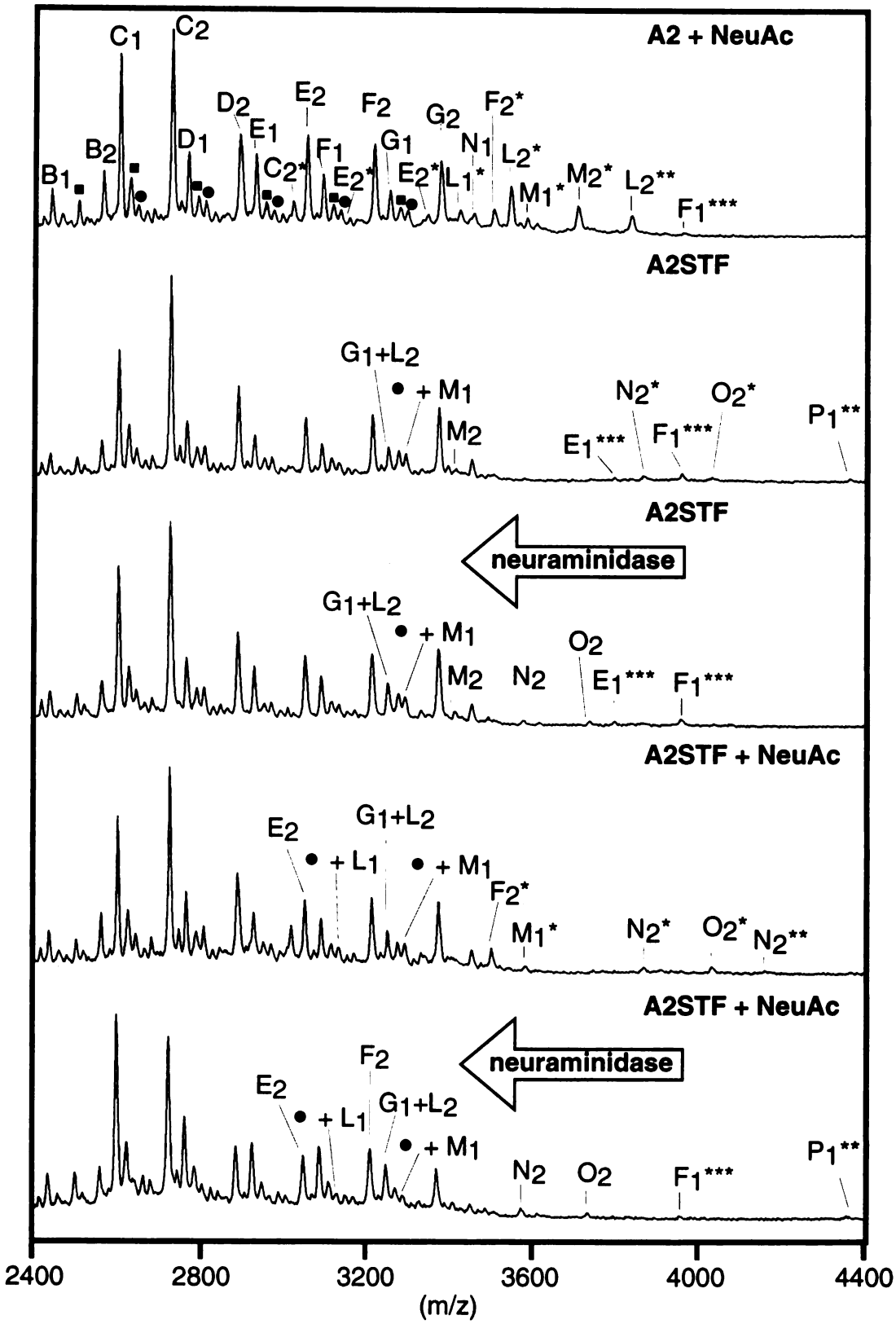
A2 + NeuAc
C1
C2
D2
E2
F2
G2
F2*
E1
D1
G1
N1
L2*
B2
B1
C2*
E2*
E2*
L1*
M2*
L2**
M1*
F1***
A2STF
G1+L2
+ M1
N2*
O2*
P1**
M2
E1***
F1***
A2STF
neuraminidase
G1+L2
+ M1
O2
M2
N2
E1***
F1***
A2STF + NeuAc
E2
G1+L2
+ L1
+ M1
F2*
M1*
N2*
O2*
N2**
A2STF + NeuAc
neuraminidase
F2
E2
G1+L2
+ L1
+ M1
P1**
N2
O2
F1***
2400
2800
3200
3600
4000
4400
(m/z)

which are summarized in Table 4.2. The appearance of the corresponding acceptor glycoforms upon treatment of the O-LOS with neuraminidase confirmed the expression of higher molecular weight species containing sialic acid and HexNAc (N_2*, O_2*), that were larger than the major SiaA products by 2 Hex and not observed in the parental strain. A major sialylated species lacking HexNAc (F_2*) was only observed in the A2STF mutant and parental strains when the bacteria were grown on solid media supplemented with sialic acid. The mutant strain also produced several structures extended by 2 or more sialic acids (N_2**, P_1***) including a pair completely lacking HexNAc (E_1***, F_1***). The expression of new sialylated glycoforms as a consequence of mutating *siaA* suggests a second sialyltransferase of dissimilar substrate specificity may function in *H. influenzae* as well.

In parallel studies, *siaA* was inactivated in the transposon mutant 276.4 and the LOS were evaluated with MALDI-MS (Figure 4.11). Overall, no gross alterations in the expression of dominant LOS glycoforms produced by 276.4STF compared to the parental strain were noted. As expected, the absence of the major sialylated species (K_1* and K_2*) coincided with the appearance of the acceptor glycoform (K_2) in A2STF. Although K_1 is altogether absent and K_2 appears in lower abundance compared to the parental strain following treatment with neuraminidase, these HexNAc-containing glycoforms were concluded to be the major substrates of SiaA in 276.4. Analogous to the findings for A2STF, the double mutant strain continued to assemble sialylated LOS (Table 4.3) including a species resembling the major wild type structure extended by 2 additional Hex (M_1* and M_2*). Furthermore, 276.4STF produced a minor species containing two Hex that was di-sialylated (A_1**). Once again, the observation of LOS containing sialic acid upon the deletion of *siaA* in 276.4, further supports the presence of at least a second sialyltransferase in *H. influenzae*.

In summary, to ascertain the function of *siaA* (HI0871) in *H. influenzae*, the gene was inactivated in two strains by insertional mutagenesis and the resulting LOS were

Table 4.2 Sialylated glycoforms observed in A2STF before and after neuraminidase treatment

Glycoform	Proposed Composition minimum structure includes 3Hep KDO(P) O-deacylated LipidA				calculated Mr	A2 + NeuAc	A2STF	A2STF	A2STF + NeuAc	A2STF + NeuAc
$X_{1/2PEA}$	NeuAc	HexNAc	Hex	PEA	(average)			neuraminidase		neuraminidase
C_2*	1		4	2	3015.6	3015.6			3015.3	
E_2*	1		6	2	3339.9	3340.5				
F_2*	1		7	2	3502.0	3502.3			3501.5	
E_1***	3		6	1	3799.3	3797.8[a]	3797.8	3798.2		
F_1***	3		7	1	3961.5	3960.1	3960.0	3959.2		3962.0
L_1*	1	1	6	1	3420.0	3419.9				
L_2*	1	1	6	2	3543.1	3542.7				
L_2**	2	1	6	2	3834.3	3834.1				
M_1*	1	1	7	1	3582.2	3582.2			3582.4	
M_2*	1	1	7	2	3705.2	3705.5				
N_2*	1	1	8	2	3867.4		3870.1		3868.4	
N_2**	2	1	8	2	4158.6				4159.1	
O_2*	1	1	9	2	4029.5		4032.0		4031.8	
P_1**	2	1	10	1	4359.8	4360.5[a]	4359.6			4359.6

[a] Species observed after treatment of O-LOS with neuraminidase

Figure 4.11 Negative ion MALDI-MS spectra comparing O-deacylated LOS from *H. influenzae* 276.4 and 276.4STF. Mass spectra comparing LOS isolated from strain 276.4STF grown in absence and presence of 20 μg/mL NeuAc before and after treatment with neuraminidase. See Table 4.3 for molecular weights and proposed compositions. The mass spectra of the O-LOS isolated from the parental strain 276.4 grown in the presence of 20 μg/mL sialic acid has been included for comparison. Asterisks indicate the addition of sialic acid and the number of PEA moieties are denoted by subscript. Prompt fragments correspond to the loss of HPO_3 (●) and H_3PO_4 (■) from the most abundant species.

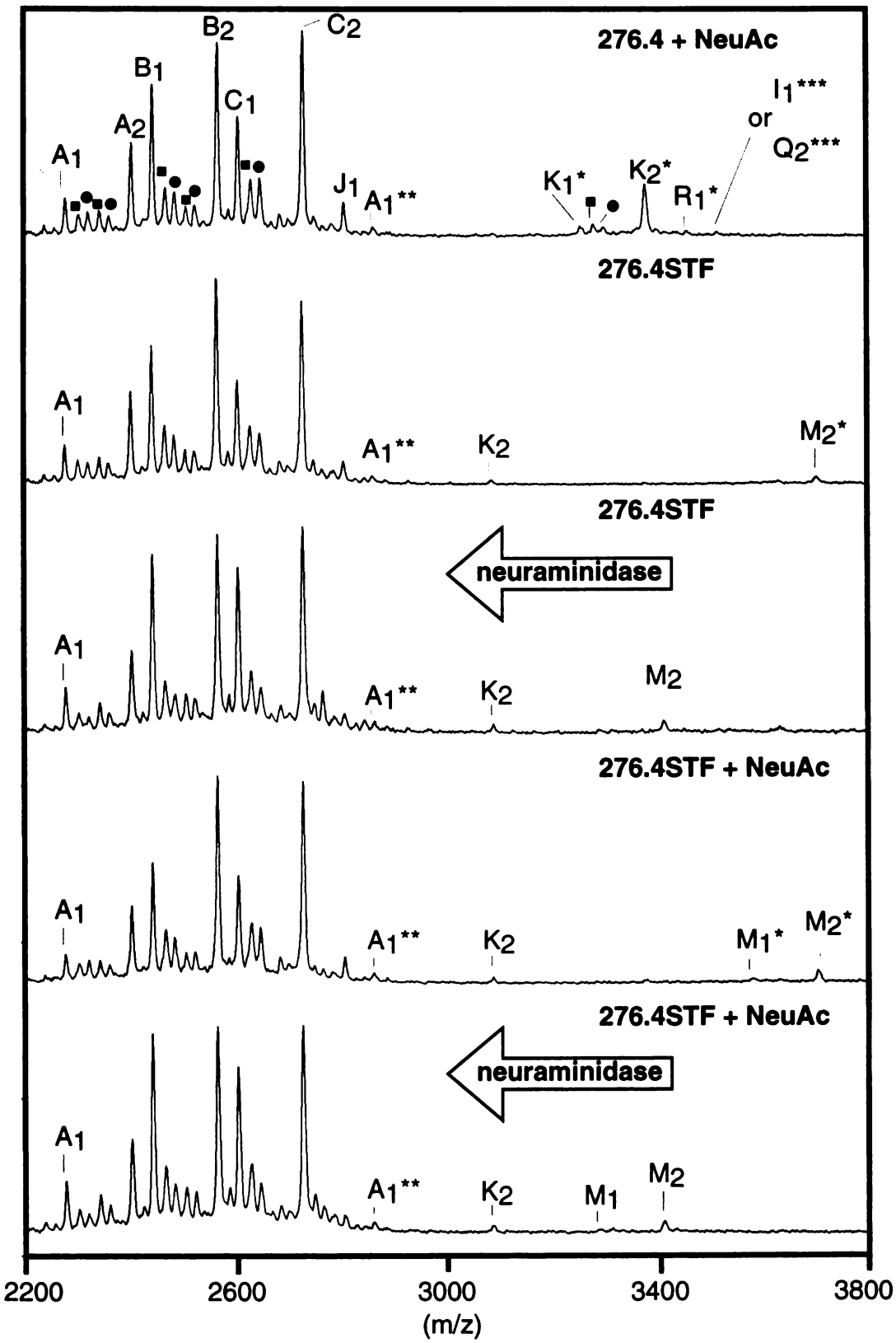
276.4 + NeuAc
B2
C2
B1
C1
A2
A1
J1
A1**
K1*
K2*
R1*
I1***
or
Q2***
276.4STF
A1
A1**
K2
M2*
276.4STF
neuraminidase
A1
A1**
K2
M2
276.4STF + NeuAc
A1
A1**
K2
M1*
M2*
276.4STF + NeuAc
neuraminidase
A1
A1**
K2
M1
M2
2200
2600
3000
3400
3800
(m/z)

Table 4.3 Sialylated glycoforms observed in 276.4STF before and after neuraminidase treatment

Glycoform	Proposed Composition minimum structure includes 3Hep KDO(P) O-deacylated LipidA				calculated Mr	276.4 + NeuAc	276.4STF	276.4STF	276.4STF + NeuAc	276.4STF + NeuAc
$X_{1/2PEA}$	NeuAc	HexNAc	Hex	PEA	(average)			neuraminidase		neuraminidase
A_1**	2		2	1	2859.5	2860.7	2860.9	2861.9	2860.5	2860.0
Q_2***	3	2	1	2	3518.1	3517.7				
I_1***	3	1	3	1	3516.0	3517.7				
K_1*	1	1	5	1	3257.9	3258.3				
K_2*	1	1	5	2	3380.9	3380.8				
M_1*	1	1	7	1	3582.2				3583.9	
M_2*	1	1	7	2	3705.2		3706.3		3704.4	
R_1*	1	2	5	1	3461.1	3460.3				

characterized by MALDI-MS. The hypothetical protein encoded by *siaA* was found to have significant homology to a sialyltransferase (Lst) recently identified in *H. ducreyi* (score 234, E value 1e-60) that is required for the transfer of sialic acid to the non-reducing terminal N-acetyllactosamine of the major LOS glycoform in vivo (Bozue et al. 1999). Subsequent to the deletion of *siaA*, both A2STF and 276.4STF were incapable of producing the major sialylated species observed in the parental strains. Instead, the respective free acceptor glycoforms remained unmodified in the mutant strains. Collectively, these data implicate SiaA as a putative sialyltransferase apparently responsible for the transfer of a single sialic acid to the non-reducing terminal N-acetyllactosamine of the LOS, in accordance with its homolog in *H. ducreyi*. Future studies complementing the defective gene in the mutant strains will be required to rule out potential polar effects on other biosynthetic genes as the source of alterations in the LOS expression.

In the absence of a functional SiaA, the STF mutant strains retained the capacity to manufacture minor species containing sialic acid. Most notably, both mutant strains apparently extended the SiaA acceptor species by 2 Hex, which in turn were sialylated by an unidentified sialyltransferase. Although the exact positions of sialylation have not been proven, it is conceivable that in lieu of sialylation by SiaA, two Hex are added directly to the free N-acetyllactosamine of remaining glycoforms to create a new acceptor site. The consumption of the remaining SiaA acceptor glycoforms by an alternative biosynthetic pathway may explain in part their decreased abundance compared to the neuraminidase treated parental strains. Moreover, LOS species lacking HexNAc and in some instances terminating with more than one sialic acid were found in both the mutant and parental strains, supporting the presence of another sialyltransferase with substrate specificity distinct from SiaA. In all, these data suggest the presence of a second putative sialyltransferase preferring LOS containing a Hex rather than a HexNAc as the penultimate non-reducing terminal sugar with the capacity to transfer sialic acid to a terminal Hex or sialic acid.

A candidate gene (GenBank accession number U32720, ORF HI0352) in the *H. influenzae* strain Rd genome was identified as having significant homology (39-40%) to 2 glycosyltransferases in *Campylobacter jejuni* OH4384, Cst-I and Cst-II (Gilbert et al. 2000). The 430 amino acid enzyme encoded by *cstI* was shown to have α2,3 sialyltransferase activity, transferring sialic acid to synthetic substrates terminating with lactose in vitro. Cst-II (291 amino acids), a truncated version of Cst-I, was also found to make α2,3 linkages between sialic acid and lactose derivatized substrates. However, Cst-II was shown have α2,8 activity as well, transferring sialic acid to a terminal sialyllactose or sialyl-N-acetyllactosamine of synthetic substrates in vitro. The discovery of the a gene encoding a 231 amino acid *cst-II/cst-II* homolog in *H. influenzae* warrants speculation that this unknown protein may account for mono- and poly-sialyltransferase activities in *H. influenzae* apart from SiaA, however the exact function of this gene product in LOS biosynthesis will need to be resolved in future studies employing isogenic mutants.

REFERENCES

Akkoyunlu, M., Ruan, M. and Forsgren, A. (1991). Distribution of protein D, an immunoglobulin D-binding protein, in *Haemophilus* strains. *Infect. Immun. 59(4)*, 1231-1238.

Alexeyev, M. F. (1995). Three kanamycin resistance gene cassettes with different polylinkers. *Biotechniques 18(1)*, 52, 54, 56.

Alfa, M. J. and DeGagne, P. (1997). Attachment of *Haemophilus ducreyi* to human foreskin fibroblasts involves LOS and fibronectin. *Microb. Pathogen. 22(1)*, 39-46.

Alfa, M. J., DeGagne, P. and Totten, P. A. (1996). *Haemophilus ducreyi* hemolysin acts as a contact cytotoxin and damages human foreskin fibroblasts in cell culture. *Infect. Immun. 64(6)*, 2349-2352.

Ambrose, M. G., Freese, S. J., Reinhold, M. S., Warner, T. G. and Vann, W. F. (1992). 13C NMR investigation of the anomeric specificity of CMP-N-acetylneuraminic acid synthetase from *Escherichia coli. Biochemistry 31(3)*, 775-780.

Apicella, M. A., Griffiss, J. M. and Schneider, H. (1994). *Methods Enzymol. 235*, 242-252.

Bai, Y., Milne, J. S., Mayne, L. and Englander, S. W. (1993). Primary structure effects on peptide group hydrogen exchange. *Proteins 17(1)*, 75-86.

Barenkamp, S. J. and St. Geme, J. W. (1996). Identification of a second family of high-molecular-weight adhesion proteins expressed by non-typable *Haemophilus influenzae*. *Mol. Microbiol. 19*(6), 1215-1223.

Barry, A. L., Phaller, M. A., Fuchs, P. C. and Packer, R. R. (1994). In vitro activities of 12 orally administered agents against 4 species of bacterial respiratory pathogens from US medical centers in 1992 and 1993. *Antimicrob. Agents Chemother. 38*, 2419-2425.

Bauer, B. A., Lumbley, S. R. and Hansen, E. J. (1999). Characterization of a WaaF (RfaF) homolog expressed by *Haemophilus ducreyi*. *Infect. Immun. 67*(2), 899-907.

Bauer, B. A., Stevens, M. K. and Hansen, E. J. (1998). Involvement of the *Haemophilus ducreyi* gmhA gene product in lipooligosaccharide expression and virulence. *Infect. Immun. 66*(9), 4290-4298.

Bauer, M. E. and Spinola, S. M. (1999). Binding of *Haemophilus ducreyi* to extracellular matrix proteins. *Infection and Immunity 67*(5), 2649-2652.

Bevington, P. R. (1969). Data reduction and error analysis for the physical sciences, McGraw-Hill, Inc.

Bitter-Suermann, D. (1993). Influence of bacterial polysialic capsules on host defenses: masquerade and mimikry. Polysialic acid: From microbes to man. Roth, J., Rutishauser, U., Troy, F. A. Basel, Birkhäuser Verlag: 11-24.

Bozue, J. L., Tullius, M. V., Wang, J., Gibson, B. W. and Musson, R. S. Jr. (1999). *Haemophilus ducreyi* produces a novel sialyltransferase: identification of the sialyltransferase gene and construction of mutants deficient in the production of the sialic acid-containing glycoform of the lipooligosaccharide. *J. Biol. Chem. 274(7)*, 4106-4114.

Bramley, J., Demarco de Hormaeche, R., Constantinidou, C., Nassif, X., Parsons, N., Jones, P., Smith, H. and Cole, J. (1995). A serum-sensitive, sialyltransferase-deficient mutant of *Neisseria gonorrhoeae* defective in conversion to serum resistance by CMP-NANA or blood cell extracts. *Microb. Pathogen. 18(3)*, 187-195.

Braun, V., Hobbie, S. and Ondraczek, R. (1992). *Serratia marcescens* forms a new type of cytolysin. *Fems Microbiol. Lett. 79(1-3)*, 299-305.

Brentjens, R. J., Ketterer, M., Apicella, M. A. and Spinola, S. M. (1996). Fine tangled pili expressed by *Haemophilus ducreyi* are a novel class of pili. *J. Bacteriol. 178(3)*, 808-816.

Brentjens, R. J., Spinola, S. M. and Campagnari, A. A. (1994). *Haemophilus ducreyi* adheres to human keratinocytes. *Microb. Pathogen. 16(3)*, 243-247.

Brown, T. J., Yen-Moore, A. and Tyring, S. K. (1999). An overview of sexually transmitted diseases. Part I. *Journal of the American Academy of Dermatology 41(4)*, 511-532.

Campagnari, A. A., Wild, L. M., Griffiths, G. E., Karalus, R. J., Wirth, M. A. and Spinola, S. M. (1991). Role of lipooligosaccharides in experimental dermal lesions caused by *Haemophilus ducreyi. Infect. Immun. 59(8)*, 2601-2608.

Cleland, W. W. (1963). The kinetics of enzyme-catalyzed reactions with two or more substrates or products. *Biochim. Biophys. Acta. 67*, 104-137.

Cope, L. D., Lumbley, S., Latimer, J., Klesney-Tait, J., Stevens, M. K., Johnson, L. S., Purven, M., Munson, R. S. J., Lagergard, T., Radolf, J. D. and Hansen, E. J. (1997). A diffusible cytotoxin of *Haemophilus ducreyi. Proc. Natl. Acad. Sci. USA* 94(8), 4056-4061.

Cotter, R. J., Honovich, J., Qureshi, N. and Takayama, K. (1987). Structural determination of lipid A from gram negative bacteria using laser desorption mass spectrometry. *Biomed. Environ. Mass Spectrom. 14(11)*, 591-598.

Datta, A. K. and Paulson, J. C. (1997). Sialylmotifs of sialyltransferases. *Indian Journal of Biochemistry and Biophysics 34(1-2)*, 157-165.

DeMaria, T. F., Apicella, M. A., Nichols, W. A. and Leake, E. R. (1997). Evaluation of the virulence of nontypeable *Haemophilus influenzae* lipooligosaccharide *htrB* and *rfaD* mutants in the chinchilla model of otitis media. *Infect. Immun.* 65(*11*), 4431-4435.

Dickerson, M. C., Johnston, J., Delea, T. E., White, A. and Andrews, E. (1996). The causal role for genital ulcer disease as a risk factor for transmission of human immunodeficiency virus. An application of the Bradford Hill criteria. *Sex Transm. Dis.* 23(*5*), 429-440.

Dieckmann, R., Pavela-Vrancic, M., Von Dohren, H. and Kleinkauf, H. (1999). Probing the domain structure and ligand-induced conformational changes by limited proteolysis of tyrocidine synthetase 1. *J. Mol. Biol.* 288(*1*), 129-140.

Ducreyi, A. (1889). Experimentelle Untersuchungen uber den Ansteckungsstoff des weichen Schankers und uber die Bubonen. *Monatsh. Prakt. Dermatol. 9*, 387-405.

Eagan, W. M., Tsui, F. P. and Zon, G. (1982). Structural studies of *Haemophilus influenzae* capsular polysaccharides. *Haemophilus influenzae*: epidemiology, immunology, prevention of disease. Sell, S. H. and Wright, P. F. New York, New York, Elsevier Science Publishing Co. INC: 185-196.

Ehring, H. (1999). Hydrogen exchange/electrospray ionization mass spectrometry studies of structural features of proteins and protein/protein interactions. *Anal. Biochem. 267(2)*, 252-529.

Englander, J. J., Rogero, J. R. and Englander, S. W. (1985). Protein hydrogen exchange studied by the fragment separation method. *Anal. Biochem. 147(1)*, 234-244.

Englander, S. W. and Kallenbach, N. R. (1983). Hydrogen exchange and structural dynamics of proteins and nucleic acids. *Quarterly Reviews of Biophysics 16(4)*, 521-655.

Ferrero, M. A., Reglero, A., Fernandez-Lopez, M., Ordas, R. and Rodriguez-Aparicio, L. B. (1996). N-acetyl-D-neuraminic acid lyase generates the sialic acid for colominic acid biosynthesis in *E. coli* K1. *Biochem. J. 317(1)*, 157-165.

Fleischmann, R. D., Adams, M. D., White, O., Clayton, R. A., Kirkness, E. F., Kerlavage, A. R., Bult, C. J., Tomb, J. F., Dougherty, B. A., Merrick, J. M., McKenney, K., Sutton, G., FitzHugh, W., Fields, C., Gocayne, J. D., Scott, J., Shirley, R., Liu, L.-I., Glodek, A., et al. (1995). Whole-genome random sequencing and assembly of *Haemophilus influenzae* Rd. *Science 269(5223)*, 496-512.

Fontana, A., Fassina, G., Vita, C., Dalzoppo, D., Zamai, M. and Zambonin, M. (1986). Correlation between sites of limited proteolysis and segmental mobility in thermolysin. *Biochemistry 25(8)*, 1847-1851.

Fontana, A., Polverino de Laureto, P., De Filippis, V., Scaramella, E. and Zambonin, M. (1997). Probing the partly folded states of proteins by limited proteolysis. *Folding and Design 2(2)*, R17-26.

Foxwell, A. R., Kyd, J. M. and Cripps, A. W. (1998). Nontypeable *Haemophilus influenzae*: pathogenesis and prevention. *Microbiology and Molecular Biology Reviews 62(2)*, 294-308.

Fromm, H. J. (1995). *Methods Enzymol. 249*, 123-143.

Ganguli, S., Zapata, G., Wallis, T., Reid, C., Boulnois, G., Vann, W. F. and Roberts, I. S. (1994). Molecular cloning and analysis of genes for sialic acid synthesis in *Neisseria meningitidis* group B and purifcation of the meningococcal CMP-NeuAc synthetase enzyme. *J. Bacteriol. 176(15)*, 4583-4589.

Gelfanova, V., Hansen, E. J. and Spinola, S. M. (1999). Cytolethal distending toxin of *Haemophilus ducreyi* induces apoptotic death of Jurkat T cells. *Infect. Immun. 67(12)*, 6394-6402.

Gibson, B. W., Campagnari, A. A., Melaugh, W., Phillips, N. J., Apicella, M. A., Grass, S., Wang, J., Palmer, K. L. and Munson, R. S., Jr. (1997). Characterization of a transposon Tn916-generated mutant of *Haemophilus ducreyi* 35000 defective in lipooligosaccharide biosynthesis. *J. Bacteriol. 179(16)*, 5062-5071.

Gibson, B. W., Engstrom, J. J., John, C. M., Hines, W. and Falick, A. M. (1997). Characterization of bacterial lipooligosaccharides by delayed extraction matrix-assisted laser desorption ionization time-of-flight mass spectrometry. *J. Am. Soc. Mass Spectrom. 8(6)*, 645-658.

Gibson, B. W., Melaugh, W., Phillips, N. J., Apicella, M. A., Campagnari, A. A. and Griffiss, J. M. (1993). Investigation of the structural heterogeneity of lipooligosaccharides from pathogenic *Haemophilus* and *Neisseria* and of R-type lipopolysaccharides from *Salmonella typhimurium* by electrospray mass spectrometry. *J. Bacteriol. 175(9)*, 2702-2712.

Giebink, G. S. (1989). The microbiology of otitis media. *Pediatric Infectious Disease Journal 8(Suppl. 1)*, S18-20.

Giebink, G. S. (1999). Otitis media: the chinchilla model. *Microbial Drug Resistance 5(1)*, 57-72.

Gilbert, M., Brisson, J. R., Karwaski, M. F., Michniewicz, J., Cunningham, A. M., Wu, Y., Young, N. M. and Wakarchuk, W. W. (2000). Biosynthesis of ganglioside mimics in *Campylobacter jejuni* OH4384. Identification of the glycosyltransferase genes, enzymatic synthesis of model compounds, and characterization of nanomole amounts by 600-mhz (1)H and (13)C NMR analysis. *J. Biol. Chem. 275(6)*, 3896-3906.

Gilbert, M., Cunningham, A. M., Watson, D. C., Martin, A., Richards, J. C. and Wakarchuk, W. W. (1997). Characterization of a recombinant *Neisseria meningitidis* alpha-2,3-sialyltransferase and its acceptor specificity. *Eur. J. Biochem. 249(1)*, 187-194.

Gilbert, M., Watson, D. C., Cunningham, A. M., Jennings, M. P., Young, N. M. and Wakarchuk, W. W. (1996). Cloning of the lipooligosaccharide alpha-2,3-sialyltransferase from the bacterial pathogens *Neisseria meningitidis* and *Neisseria gonorrhoeae*. *J. Biol. Chem. 271(45)*, 28271-28276.

Gilsdorf, J. R. and Ferrieri, P. (1986). Susceptibility of phenotypic variants of *Haemophilus influenzae* type b to serum bactericidal activity: relation to surface lipopolysaccharide. *J. Infect. Dis. 153(2)*, 223-231.

Gilsdorf, J. R., McCrea, K. W. and Marrs, C. F. (1997). Role of pili in *Haemophilus influenzae* adherence and colonization. *Infect. Immun. 65(8)*, 2997-3002.

Gilsdorf, J. R., Tucci, M. and Marrs, C. F. (1996). Role of pili in *Haemophilus influenzae* adherence to, and internalization by, respiratory cells. *Pediatric Research 39(2)*, 343-348.

Gorisch, H. (1988). Drop dialysis: time course of salt and protein exchange. *Anal. Biochem. 173(2)*, 393-398.

Green, B. A., Farley, J. E., Quinn-Dey, T., Deich, R. A. and Zlotnick, G. W. (1991). The e (P4) outer membrane protein of *Haemophilus influenzae*: biologic activity of anti-e serum and cloning and sequencing of the structural gene. *Infect. Immun. 59(9)*, 3191-3198.

Griffiss, J. M., Schneider, H., Mandrell, R. E., Yamasaki, R., Jarvis, G. A., Kim, J. J., Gibson, B. W., Hamadeh, R. and Apicella, M. A. (1988). Lipooligosaccharides: the principal glycolipids of the neisserial outer membrane. *Reviews of Infectious Diseases Suppl. 10*, S287-295.

Haft, R. F. and Wessels, M. R. (1994). Characterization of CMP-N-Acetylneuraminic acid synthetase of group B Streptococci. *J. Bacteriol. 176(23)*, 7372-7374.

Hammerschmidt, S., Birkholz, C., Zahringer, U., Robertson, B. D., Van Putten, J., Ebeling, O. and Frosch, M. (1994). Contribution of genes from the capsule gene complex (cps) to lipooligosaccharide biosynthesis and serum resistance in *Neisseria meningitidis. Mol. Microbiol. 11(5)*, 885-896.

Hammond, G. W., Lian, C. J., Wilt, J. C. and Ronald, A. R. (1978). Comparison of specimen collection and laboratory techniques for isolation of *Haemophilus ducreyi. J. Clin. Microbiol. 7(1)*, 39-43.

Hannah, P. and Greenwood, J. R. (1982). Isolation and rapid identification of *Haemophilus ducreyi. J. Clin. Microbiol. 16(5)*, 861-864.

Harada, T., Sakakura, Y. and Jin, C. S. (1990). Adherence of *Haemophilus influenzae* to nasal, nasopharyngeal and buccal epithelial cells from patients with otitis media. *European Archives of Oto-Rhino-laryngology 247(2)*, 122-124.

Herriott, R. M., Meyer, E. M. and Vogt, M. (1970). Defined nongrowth media for stage II development of competence in *Haemophilus influenzae. J. Bacteriol. 101(2)*, 517-524.

High, N. J., Deadman, M. E. and Moxon, E. R. (1993). The role of a repetitive DNA motif (5'-CAAT-3') in the variable expression of the *Haemophilus influenzae* lipopolysaccharide epitope alphaGal(1-4)beta Gal. *Mol. Microbiol. 9(6)*, 1275-1282.

Hiltke, T. J., Bauer, M. E., Klesney-Tait, J., Hansen, E. J., Munson, R. S. J. and Spinola, S. M. (1999). Effect of normal and immune sera on *Haemophilus ducreyi* 35000HP and its isogenic MOMP and LOS mutants. *Microb. Pathogen. 26(2)*, 93-102.

Hiltke, T. J., Campagnari, A. A. and Spinola, S. M. (1996). Characterization of a novel lipoprotein expressed by *Haemophilus ducreyi. Infect. Immun. 64(12)*, 5047-5052.

Holland, I. B., Blight, M. A. and Kenny, B. (1990). The mechanism of secretion of hemolysin and other polypeptides from gram-negative bacteria. *Journal of Bioenergetics and Biomembranes 22(3)*, 473-491.

Hood, D. W., Deadman, M. E., Allen, T., Masoud, H., Martin, A., Brisson, J. R., Fleischmann, R., Venter, J. C., Richards, J. C. and Moxon, E. R. (1996). Use of the complete genome sequence information of *Haemophilus influenzae* strain Rd to investigate lipopolysaccharide biosynthesis. *Mol. Microbiol. 22(5)*, 951-965.

Hood, D. W., Makepeace, K., Deadman, M. E., Rest, R. F., Thibault, P., Martin, A., Richards, J. C. and Moxon, E. R. (1999). Sialic acid in the lipopolysaccharide of *Haemophilus influenzae*: strain distribution, influence on serum resistance and structural characterization. *Mol. Microbiol. 33(4)*, 679-692.

Hood, D. W., Richards, J. C. and Moxon, E. R. (1999). *Haemophilus influenzae* lipopolysaccharide. *Biochemical Society Transactions 27(4)*, 493-498.

Hubbard, S. J. (1998). The structural aspects of limited proteolysis of native proteins. *Biochimica et Biophysica Acta 1382(2)*, 191-206.

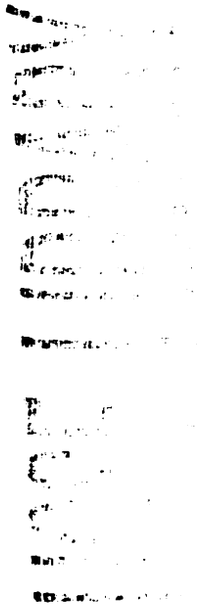

Jackson, A. D., Rayner, C. F., Dewar, A., Cole, P. J. and Wilson, R. (1996). A human respiratory-tissue organ culture incorporating an air interface. *American Journal of Respiratory and Critical Care Medicine 153(3)*, 1130-1135.

Jacques, M. and Paradis, S. (1998). Adhesin-receptor interactions in *Pasteurellaceae*. *FEMS Microbiol. Rev. 22(1)*, 45-59.

Jelakovic, S., Jann, K. and Schulz, G. E. (1996). The three-dimensional structure of capsule-specific CMP: 2-keto-3-deoxy-manno-octonic acid synthetase from *E. coli*. *FEBS Lett. 391(1-2)*, 157-161.

Jennings, H. J. (1983). Capsular polysaccharides as human vaccines. *Adv. Carbohydr. Chem. Biochem. 41(155-208)*

Jessamine, P. G. and Ronald, A. R. (1990). Chancroid and the role of genitial ulcer disease in the spread of human retroviruses. *Medical Clinics of North America 74(6)*, 1417-1430.

Kahler, C. M., Martin, L. E., Shih, G. C., Rahman, M. M., Carlson, R. W. and Stephens, D. S. (1998). The (alpha2-->8)-linked polysialic acid capsule and lipooligosaccharide structure both contribute to the ability of serogroup B *Neisseria meningitidis* to resist the bactericidal activity of normal human serum. *Infect. Immun. 66(12)*, 5939-5947.

Kahler, C. M. and Stephens, D. S. (1998). Genetic basis for biosynthesis, structure, and function of meningococcal lipooligosaccharide (endotoxin). *Critical Reviews in Microbiology 24(4)*, 281-334.

Katta, V. and Chait, B. T. (1991). Conformational changes in proteins probed by hydrogen-exchange electrospray-ionization mass spectrometry. *Rapid Commun. Mass Spectrom. 5(4)*, 214-217.

Kawakami, K., Ahmed, K., Utsunomiya, Y., Rikitomi, N., Hori, A., Oishi, K. and Nagatake, T. (1998). Attachment of nontypable *Haemophilus influenzae* to human pharyngeal epithelial cells mediated by a ganglioside receptor. *Microbiology and Immunology 42(10)*, 697-702.

Kean, E. L. (1991). Sialic acid activation. *Glycobiology 1(5)*, 441-447.

Kelm, S. and Schauer, R. (1997). Sialic acid in molecular and cellular interactions. *Int. Rev. Cytol. 175*, 137-240.

Kilian, M. (1985). *Haemophilus*. Manual of Clinical Microbiology. Lennette, E. H., Ballows, A., Hausler, W. J. J. and Shadomy, H. J. Washington, DC, American Society for Microbiology: 387-393.

Kimura, A. and Hansen, E. J. (1986). Antigenic and phenotypic variations of *Haemophilus influenzae* type lipopolysaccharide and their relationship to virulence. *Infect. Immun. 51(1)*, 69-79.

Klesney-Tait, J., Hiltke, T. J., Maciver, I., Spinola, S. M., Radolf, J. D. and Hansen, E. J. (1997). The major outer membrane protein of *Haemophilus ducreyi* consists of two OmpA homologs. *J. Bacteriol. 179(5)*, 1764-1773.

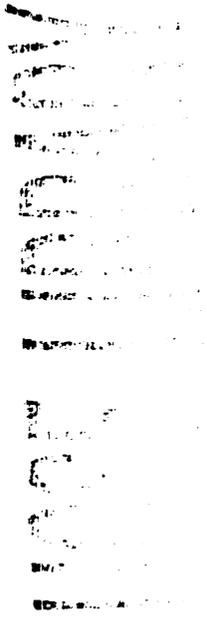

Klinman, J. P. and Matthews, R. G. (1985). Calculation of substrate dissociation constants from steady-state isotope effects in enzyme-catalyzed reactions. *J. Am. Chem. Soc. 107*, 1058-1060.

Koedel, U. and Pfister, H. W. (1999). Models of experimental bacterial meningitis. Role and limitations. *Infectious Disease Clinics of North America 13(3)*, 549-577.

Kohlbrenner, W. E., Nuss, M. M. and Fesik, S. W. (1987). 31P and 13C NMR studies of oxygen transfer during catalysis by 3-deoxy-D-manno-octulosonate cytidylyltransferase from *E. coli. J. Biol. Chem. 262(10)*, 4534-4537.

Kolberg, J., Hoiby, E. A. and Jantzen, E. (1997). Detection of the phosphorylcholine epitope in streptococci, *Haemophilus* and pathogenic *Neisseriae* by immunoblotting. *Microb. Pathogen. 22(6)*, 321-329.

Kreiss, J. K., Coombs, R., Plummer, F., Holmes, K. K., Nikora, B., Cameron, W., Ngugi, E., Ndinya Achola, J. O. and Corey, L. (1989). Isolation of human immunodeficiency virus from genital ulcers in Nairobi prostitutes. *J. Infect. Dis. 160(3)*, 380-384.

Krekel, F., Oecking, C., Amrhein, N. and Macheroux, P. (1999). Substrate and inhibitor-induced conformational changes in the structurally related enzymes UDP-N-acetylglucosamine enolpyruvyl transferase (MurA) and 5-enolpyruvylshikimate 3-phosphate synthase (EPSPS). *Biochemistry 38(28)*, 8864-8878.

Kroll, J. S. and Booy, R. (1996). *Haemophilus influenzae*: capsule vaccine and capsulation genetics. *Molecular Medicine Today 2(4)*, 160-165.

Kulshin, V. A., Zahringer, U., Lindner, B., Frasch, C. E., Tsai, C. M., Dmitriev, B. A. and Rietschel, E. T. (1992). Structural characterization of the lipid A component of pathogenic *Neisseria meningitidis*. *J. Bacteriol. 174(6)*, 1793-1800.

Kyd, J. and Cripps, A. (1999). Nontypeable *Haemophilus influenzae*: challenges in developing a vaccine. *Journal of Biotechnology 73((2-3))*, 103-108.

Kyd, J. M. and Cripps, A. W. (1998). Potential of a novel protein, OMP26, from nontypeable *Haemophilus influenzae* to enhance pulmonary clearance in a rat model. *Infect. Immun. 66(5)*, 2272-2278.

Lammel, C. J., Dekker, N. P., Palefsky, J. and Brooks, G. F. (1993). In vitro model of *Haemophilus ducreyi* adherence to and entry into eukaryotic cells of genital origin. *J. Infect. Dis. 167(3)*, 642-650.

Lee, C. J. (1987). Bacterial capsular polysaccharides--biochemistry, immunity and vaccine. *Mol. Immunol. 24(10)*, 1005-1019.

Lee, N. G., Sunshine, M. G., Engstrom, J. J., Gibson, B. W. and Apicella, M. A. (1995). Mutation of the htrB locus of *Haemophilus influenzae* nontypable strain 2019 is associated with modifications of lipid A and phosphorylation of the lipo-oligosaccharide. *J. Biol. Chem. 270(45)*, 27151-27159.

Linton, D., Karlyshev, A. V., Hitchen, P. G., Morris, H. R., Dell, A., Gregson, N. A. and Wren, B. W. (2000). Multiple N-acetyl neuraminic acid synthetase (neuB) genes in *Campylobacter jejuni*: identification and characterization of the gene involved in sialylation of lipo-oligosaccharide. *Mol. Microbiol. 35(5)*, 1120-1134.

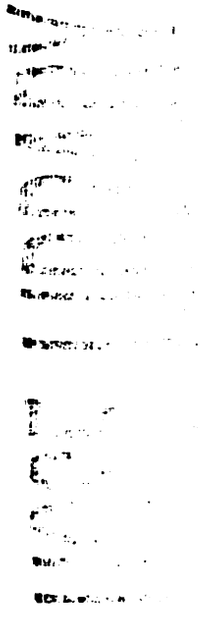

Liu, J. L.-C., Shen, G.-J., Ichikawa, Y., Rutan, J. F., Zapata, G., Vann, W. F. and Wong, C.-H. (1992). Overproduction of CMP-Sialic acid synthetase for organic synthesis. *J. Am. Chem. Soc. 114*, 3901-3910.

Mandell, J. G., Falick, A. M. and Komives, E. A. (1998). Identification of protein-protein interfaces by decreased amide proton solvent accessibility. *Proc. Natl. Acad. Sci. USA 95(25)*, 14705-14710.

Mandrell, R. E. and Apicella, M. A. (1993). Lipooligosaccharides (LOS) of mucosal pathogens: molecular mimcry and host-modification of LOS. *Immunobiol. 187*, 382-402.

Mandrell, R. E., Lesse, A. J., Sugai, J. V., Shero, M., Griffiss, J. M., Cole, J. A., Parsons, N. J., Smith, H., Morse, S. A. and Apicella, M. A. (1990). In vitro and in vivo modification of *Neisseria gonorrhoeae* lipooligosaccharide epitope structure by sialylation. *J. Exp. Med. 171(5)*, 1649-1664.

Mandrell, R. E., McLaughlin, R., Yousef, A. K., Lesse, A., Yamasaki, R., Gibson, B. W., Spinola, S. M. and Apicella, M. A. (1992). Lipooligosaccharides (LOS) of some *Haemophilus* species mimic human glycosphingolipids, and some LOS are sialylated. *Infect. Immun. 60(4)*, 1322-1328.

Masson, L. and Holbein, B. E. (1983). Physiology of sialic acid capsular polysaccharide synthesis in serogroup B *Neisseria meningitidis*. *J. Bacteriol. 154*(2), 728-736.

McLaughlin, R., Spinola, S. M. and Apicella, M. A. (1992). Generation of lipooligosaccharide mutants of *Haemophilus influenzae* type b. *J. Bacteriol. 174(20)*, 6455-6459.

Melaugh, W., Campagnari, A. A. and Gibson, B. W. (1996). The lipooliogosaccharides of *Haemophilus ducreyi* are highly sialylated. *J. Bacteriol. 187*, 564-570.

Melaugh, W., Phillips, N. J., Campagnari, A. A., Karalus, R. and Gibson, B. W. (1992). Partial characterization of the major lipooligosaccharide from a strain of *Haemophilus ducreyi*, the causative agent of chancroid, a genital ulcer disease. *J. Biol. Chem. 267(19)*, 13434-13439.

Melaugh, W., Phillips, N. J., Campagnari, A. A., Tullius, M. V. and Gibson, B. W. (1994). Structure of the major oligosaccharide from the lipooligosaccharide of *Haemophilus ducreyi* strain 35000 and evidence for additional glycoforms. *Biochemistry 33*, 13070-13078.

Monto, A. S. (1989). Acute respiratory infection in children of developing countries: challenge of the 1990s. *Reviews of Infectious Diseases 11(3)*, 498-505.

Moran, A. P., Prendergast, M. M. and Appelmelk, B. J. (1996). Molecular mimicry of host structures by bacterial lipopolysaccharides and its contribution to disease. *FEMS Immunol. Med. Microbiol. 16*(2), 105-115.

Morse, S. A. (1989). Chancroid and *Haemophilus ducreyi. Clinical Microbiology Reviews* 2(2), 137-157.

Moxon, E. R. and Kroll, J. S. (1990). The role of bacterial polysaccharide capsules as virulence factors. *Current Topics in Microbiology and Immunology 150*, 65-85.

Moxon, E. R., Rainey, P. B., Nowak, M. A. and Lenski, R. E. (1994). Adaptive evolution of highly mutable loci in pathogenic bacteria. *Current Biology 4(1)*, 24-33.

Moxon, E. R. and Vaughn, K. A. (1981). The type b capsular polysaccharide as a virulence determinant of *Haemophilus influenzae*: studies using clinical isolates and laboratory transformant. *J. Infect. Dis. 143(4)*, 517-524.

Münster, A. K., Eckhardt, M., Potvin, B., Muhlenhoff, M., Stanley, P. and Gerardy-Schahn, R. (1998). Mammalian cytidine 5'-monophosphate N-acetylneuraminic acid synthetase: A nuclear protein with evolutionarily conserved structural motifs. *Proc. Natl. Acad. Sci. USA 95*, 9140-9145.

Murphy, T. F. and Apicella, M. A. (1987). Nontypable *Haemophilus influenzae*: a review of clinical aspects, surface antigens, and the human immune response to infection. *Reviews of Infectious Diseases 9(1)*, 1-15.

Murphy, T. F. and Sethi, S. (1992). Bacterial infection in chronic obstructive pulmonary disease. *American Review of Respiratory Disease 146(4)*, 1067-1083.

Nelson, M. B., Munson, R. S. J., Apicella, M. A., Sikkema, D. J., Molleston, J. P. and Murphy, T. F. (1991). Molecular conservation of the P6 outer membrane protein among strains of *Haemophilus influenzae*: analysis of antigenic determinants, gene sequences, and restriction fragment length polymorphisms. *Infect. Immun. 59(8)*, 2658-2663.

Nichols, W. A., Gibson, B. W., Melaugh, W., Lee, N. G., Sunshine, M. and Apicella, M. A. (1997). Identification of the ADP-L-glycero-D-manno-heptose-6-epimerase (rfaD) and heptosyltransferase II (rfaF) biosynthesis genes from nontypeable *Haemophilus influenzae* 2019. *Infect. Immun. 65(4)*, 1377-1386.

Odumeru, J. A., Wiseman, G. M. and Ronald, A. R. (1985). Role of lipopolysaccharide and complement in susceptibility of *Haemophilus ducreyi* to human serum. *Infect. Immun. 50(2)*, 495-499.

Odumeru, J. A., Wiseman, G. M. and Ronald, A. R. (1987). Relationship between lipopolysaccharide composition and virulence of *Haemophilus ducreyi. J. Med. Microbiol. 23(2)*, 155-162.

Ortiz-Zepeda, C., Hernandez-Perez, E. and Marroquin-Burgos, R. (1994). Gross and microscopic features in chancroid: a study in 200 new culture-proven cases in San Salvador. *Sex Transm. Dis. 21(2)*, 112-117.

Palmer, K. L., Goldman, W. E. and Munson, R. S. J. (1996). An isogenic haemolysin-deficient mutant of *Haemophilus ducreyi* lacks the ability to produce cytopathic effects on human foreskin fibroblasts. *Mol. Microbiol. 21(1)*, 13-19.

Palmer, K. L., Grass, S. and Munson, R. S. J. (1994). Identification of a hemolytic activity elaborated by *Haemophilus ducreyi. Infect. Immun. 62(7)*, 3041-3043.

Palmer, K. L. and Munson, R. S. J. (1995). Cloning and characterization of the genes encoding the hemolysin of *Haemophilus ducreyi. Mol. Microbiol. 18(5)*, 821-830.

Palmer, K. L., Thornton, A. C., Fortney, K. R., Hood, A. F., Munson, R. S. J. and Spinola, S. M. (1998). Evaluation of an isogenic hemolysin-deficient mutant in the human model of *Haemophilus ducreyi* infection. *J. Infect. Dis. 178(1)*, 191-199.

Parke, J. C. J. (1987). Capsular polysaccharide of *Haemophilus influenzae* type b as a vaccine. *Pediatric Infectious Disease Journal 6(8)*, 795-798.

Passonneau, J. V. (1993). Enzymatic Analysis: A Practical Guide. Totowa, NJ, Humana Press.

Pavliak, V., Brisson, J. R., Michon, F., Uhrin, D. and Jennings, H. J. (1993). Structure of the sialylated L3 lipopolysaccharide of *Neisseria meningitidis. J. Biol. Chem. 268(19)*, 14146-14152.

Peltola, H. (2000). Worldwide *Haemophilus influenzae* type b disease at the beginning of the 21st century: global analysis of the disease burden 25 years after the use of the polysaccharide vaccine and a decade after the advent of conjugates. *Clin. Microbiol. Rev. 13(2)*, 302-317.

Phillips, N. J., Apicella, M. A., Griffiss, J. M. and Gibson, B. W. (1992). Structural characterization of the cell surface lipooligosaccharides from a nontypable strain of *Haemophilus influenzae. Biochemistry 31(18)*, 4515-4526.

Phillips, N. J., Apicella, M. A., Griffiss, J. M. and Gibson, B. W. (1993). Structural studies of the lipooligosaccharides from *Haemophilus influenzae* type b strain A2. *Biochemistry 32(8)*, 2003-2012.

Phillips, N. J., McLaughlin, R., Miller, T. J., Apicella, M. A. and Gibson, B. W. (1996). Characterization of two transposon mutants from *Haemophilus influenzae* type b with altered lipooligosaccharide biosynthesis. *Biochemistry 35(18)*, 5937-5947.

Phillips, N. J., Miller, T. J., Engstrom, J. J., Melaugh, W., McLaughlin, R., Apicella, M. A. and Gibson, B. W. (2000). Characterization of chimeric lipopolysaccharides from *E. coli* strain JM109 transformed with lipooligosaccharide synthesis genes (lsg) from *Haemophilus influenzae. J. Biol. Chem. 275(7)*, 4747-4758.

Plumbridge, J. and Vimr, E. (1999). Convergent pathways for utilization of the amino sugars N-acetylglucosamine, N-acetylmannosamine, and N-acetylneuraminic acid by *E. coli. J. Bacteriol. 181(1)*, 47-54.

Plummer, F. A., D'Costa, L. J., Nsanze, H., Karasira, P., MacLean, I. W., Piot, P. and Ronald, A. R. (1985). Clinical and microbiologic studies of genital ulcers in Kenyan women. *Sex Transm. Dis. 12(4)*, 193-197.

Plummer, F. A., Wainberg, M. A., Plourde, P., Jessamine, P., D'Costa, L. J., Wamola, I. A. and Ronald, A. R. (1990). Detection of human immunodeficiency virus type 1 (HIV-1) in genital ulcer exudate of HIV-1-infected men by culture and gene amplification. *J. Infect. Dis. 161(4)*, 810-811.

Preston, A., Mandrell, R. E., Gibson, B. W. and Apicella, M. A. (1996). The lipooligosaccharides of pathogenic gram-negative bacteria. *Crit. Rev. Microbiol. 22(3)*, 139-180.

Purcell, B. K., Richardson, J. A., Radolf, J. D. and Hansen, E. J. (1991). A temperature-dependent rabbit model for production of dermal lesions by *Haemophilus ducreyi*. *J. Infect. Dis. 164*(*2*), 359-367.

Purven, M. and Lagergard, T. (1992). *Haemophilus ducreyi*, a cytotoxin-producing bacterium. *Infect. Immun. 60*(*3*), 1156-1162.

Raetz, C. R. (1990). Biochemistry of endotoxins. *Annual Review of Biochemistry 59*, 129-170.

Rahman, M. M., Stephens, D. S., Kahler, C. M., Glushka, J. and Carlson, R. W. (1998). The lipooligosaccharide (LOS) of *Neisseria meningitidis* serogroup B strain NMB contains L2, L3, and novel oligosaccharides, and lacks the lipid-A 4'-phosphate substituent. *Carbohydr. Res. 307*(*3-4*), 311-324.

Rao, V. K., Krasan, G. P., Hendrixson, D. R., Dawid, S. and St Geme, J. W. (1999). Molecular determinants of the pathogenesis of disease due to non-typable *Haemophilus influenzae*. *FEMS Microbiol. Rev. 23*(*2*), 99-129.

Read, R. C., Wilson, R., Rutman, A., Lund, V., Todd, H. C., Brain, A. P., Jeffery, P. K. and Cole, P. J. (1991). Interaction of nontypable *Haemophilus influenzae* with human respiratory mucosa in vitro. *J. Infect. Dis. 163*(*3*), 549-558.

Reglero, A., Rodriguez-Aparicio, L. B. and Luengo, J. M. (1993). Polysialic acids. *International Journal of Biochemistry 25*(*11*), 1517-1527.

Resing, K. A. and Ahn, N. G. (1998). Deuterium exchange mass spectrometry as a probe of protein kinase activation. Analysis of wild-type and constitutively active mutants of MAP kinase kinase-1. *Biochemistry 37*(2), 463-475.

Rest, R. F. and Mandrell, R. E. (1995). *Neisseria* sialyltransferases and their role in pathogenesis. *Microb. Pathogen. 19*, 379-390.

Rietschel, E. T., Kirikae, T., Schade, F. U., Mamat, U., Schmidt, G., Loppnow, H., Ulmer, A. J., Zahringer, U., Seydel, U., Di-Padova, F., Schreir, M. and Brade, H. (1994). Bacterial endotoxin: molecular relationships of structure to activity and function. *Faseb J. 8*(2), 217-225.

Riise, G. C., Larsson, S. and Andersson, B. A. (1994). Bacterial adhesion to oropharyngeal and bronchial epithelial cells in smokers with chronic bronchitis and in healthy nonsmokers. *European Respiratory Journal 7*(*10*), 1759-1764.

Roberts, M. C., Bell, T. A., Sandstrom, K. I., Smith, A. L. and Holmes, K. K. (1986). Characterisation of *Haemophilus* spp. isolated from infant conjunctivitis. *J. Med. Microbiol. 21*(*3*), 219-224.

Rodriguez-Aparicio, L. B., Luengo, J. M., Gonzalez-Clemente, C. and Reglero, A. (1992). Purification and characterization of the nuclear cytidine 5'-monophosphate N-acetylneuraminic acid synthetase from rat liver. *J. Biol. Chem. 267*(*13*), 9257-9263.

Samuels, N. M., Gibson, B. W. and Miller, S. M. (1999). Investigation of the kinetic mechanism of cytidine 5'-monophosphate N-acetylneuraminic acid synthetase from *Haemophilus ducreyi* with new insights on rate-limiting steps from product inhibition analysis. *Biochemistry 38(19)*, 6195-6203.

Scaloni, A., Monti, M., Acquaviva, R., Tell, G., Damante, G., Formisano, S. and Pucci, P. (1999). Topology of the thyroid transcription factor 1 homeodomain-DNA complex. *Biochemistry 38(1)*, 64-72.

Schauer, R. (1982). Chemistry, metabolism, and biological functions of sialic acids. *Adv. Carbohydr. Chem. Biochem. 40*, 131-234.

Schauer, R., Haverkamp, J. and Ehrlich, K. (1980). Isolation and characterization of acylneuraminate cytidylyltransferase from frog liver. *Hoppe-Seyler's Z. Physiol. Chem. 361(5)*, 641-648.

Schauer, R., Kelm, S., Reuter, G., Roggentin, P. and Shaw, L. (1995). Biochemistry and role of sialic acids. Biology of the sialic acids. Rosenberg, A. New York, Plenum Press: 7-67.

Schilling, B., Samuels, N. M., Goon, S., Gaucher, S. P., Leary, J. A., Bertozzi, C. R. and Gibson, B. W. (2000). Incorporation of unnatural neuraminic acid derivatives into cell surface glycoforms of *Haemophilus ducreyi* - Biosynthetic pathways of lipooligosaccharides. *manuscript in preparation*

Schmelter, T., Ivanov, S., Wember, M., Stangier, P., Thiem, J. and Schauer, R. (1993). Partial purification and characterization of cytidine-5'-monophosphosphate N-acetylneuraminic acid synthase from rainbow trout liver. *Biol. Chem. Hoppe-Seyler 374(5)*, 337-342.

Schmid, G. P. (1997). Treatment of chancroid, 1997. *Clinical Infectious Diseases Suppl. 1*, S14-20.

Schmid, W., Christian, R. and Zbiral, E. (1988). Synthesis of both epimeric 2-deoxy-N-acetylneuraminic acids and their behaviour towards CMP-sialate synthetase: A comparison with 2-b-methylketoside of N-acetylneuraminic acid. *Tetrahedron Letters 29(30)*, 3643-3646.

Schweda, E. K., Jonasson, J. A. and Jansson, P. E. (1995). Structural studies of lipooligosaccharides from *Haemophilus ducreyi* ITM 5535, ITM 3147, and a fresh clinical isolate, ACY1: evidence for intrastrain heterogeneity with the production of mutually exclusive sialylated or elongated glycoforms. *J. Bacteriol. 177(18)*, 5316-5321.

Segel, I. H. (1975). Enzyme kinetics: behavior and analysis of rapid equilibrium and steady-state enzyme systems. New York, NY, John Wiley & Sons, Inc.

Seifert, H. S., Chen, E. Y., So, M. and Heffron, F. (1986). Shuttle mutagenesis: a method of transposon mutagenesis for *Saccharomyces cerevisiae. Proc. Natl. Acad. Sci. USA 83(3)*, 735-739.

Shames, S. L., Simon, E. S., Christopher, C. W., Schmid, W., Yang, L.-L. and Whitesides, G. M. (1991). CMP-N-acetylneuraminic acid synthetase of *E. coli*: high level expression, purification and use in the enzymatic synthesis of CMP-N-acetylneuraminic acid and CMP-neuraminic acid derivitives. *Glycobiology 1*(2), 187-191.

Smith, D. L., Deng, Y. Z. and Zhang, Z. Q. (1997). Probing the non-covalent structure of proteins by amide hydrogen exchange and mass spectrometry. *Journal of Mass Spectrometry 32*(2), 135-146.

Smith, H., Parsons, N. J. and Cole, J. A. (1995). Sialylation of Neisserial lipopolysaccharide: A major influence on pathogenicity. *Microb. Pathogen. 19*(6), 365-377.

Spinola, S. M., Griffiths, G. E., Shanks, K. L. and Blake, M. S. (1993). The major outer membrane protein of *Haemophilus ducreyi* is a member of the OmpA family of proteins. *Infect. Immun. 61*(4), 1346-1351.

Spinola, S. M., Hiltke, T. J., Fortney, K. and Shanks, K. (1996). The conserved 18,000-molecular-weight outer membrane protein of *Haemophilus ducreyi* has homology to PAL. *Infect. Immun. 64*(6), 1950-1955.

Spinola, S. M., Kwaik, Y. A., Lesse, A. J., Campagnari, A. A. and Apicella, M. A. (1990). Cloning and expression in *E.coli* of a *Haemophilus influenzae* type b lipooligosaccharide synthesis gene(s) that encodes a 2-keto-3-deoxyoctulosonic acid epitope. *Infect. Immun. 58*(6), 1558-1564.

Spinola, S. M., Orazi, A., Arno, J. N., Fortney, K., Kotylo, P., Chen, C. Y., Campagnari, A. A. and Hood, A. F. (1996). *Haemophilus ducreyi* elicits a cutaneous infiltrate of CD4 cells during experimental human infection. *J. Infect. Dis. 173*(2), 394-402.

Spinola, S. M., Wild, L. M., Apicella, M. A., Gaspari, A. A. and Campagnari, A. A. (1994). Experimental human infection with *Haemophilus ducreyi. J. Infect. Dis. 169*(5), 1146-1150.

St. Geme, J. W., Pinkner, J. S. r., Krasan, G. P., Heuser, J., Bullitt, E., Smith, A. L. and Hultgren, S. J. (1996). *Haemophilus influenzae* pili are composite structures assembled via the HifB chaperone. *Proc. Natl. Acad. Sci. USA 93*(21), 11913-11918.

Stevens, M. K., Klesney-Tait, J., Lumbley, S., Walters, K. A., Joffe, A. M., Radolf, J. D. and Hansen, E. J. (1997). Identification of tandem genes involved in lipooligosaccharide expression by *Haemophilus ducreyi. Infect. Immun. 65*(2), 651-660.

Stevens, M. K., Latimer, J. L., Lumbley, S. R., Ward, C. K., Cope, L. D., Lagergard, T. and Hansen, E. J. (1999). Characterization of a *Haemophilus ducreyi* mutant deficient in expression of cytolethal distending toxin. *Infect. Immun. 67*(8), 3900-3908.

Stoughton, D. M., Zapata, G., Picone, R. and Vann, W. F. (1999). Identification of Arg-12 in the active site of *E. coli* K1 CMP-sialic acid synthetase. *Biochem. J. 343*(2), 397-402.

Stull, T. L., Mendelman, P. M., Haas, J., E., Schoenborn, M. A., Mack, K. D. and Smith, A. L. (1984). Characterization of *Haemophilus influenzae* type b fimbriae. *Infect. Immun. 46*(3), 787-796.

Sun, S., Schilling, B., Tarantino, L., Tullius, M. V., Gibson, B. W. and Munson, R. S. J. (2000). Cloning and characterization of the lipooligosaccharide galactosyltransferase II gene of *Haemophilus ducreyi*. *J. Bacteriol. 182*(*8*), 2292-2298.

Throm, R. E., Al-Tawfiq, J. A., Fortney, K. R., Katz, B. P., Hood, A. F., Slaughter, C. A., Hansen, E. J. and Spinola, S. M. (2000). Evaluation of an isogenic major outer membrane protein-deficient mutant in the human model of *Haemophilus ducreyi* infection. *Infect. Immun. 68*(*5*), 2602-2607.

Totten, P. A., Lara, J. C., Norn, D. V. and Stamm, W. E. (1994). *Haemophilus ducreyi* attaches to and invades human epithelial cells in vitro. *Infect. Immun. 62*(*12*), 5632-5640.

Totten, P. A., Norn, D. V. and Stamm, W. E. (1995). Characterization of the hemolytic activity of *Haemophilus ducreyi*. *Infect. Immun. 63*(*11*), 4409-4416.

Trees, D. L. and Morse, S. A. (1995). Chancroid and *Haemophilus ducreyi*: an update. *Clin. Microbiol. Rev. 8*(*3*), 357-375.

Tsuji, S. (1996). Molecular cloning and functional analysis of sialyltransferases. *Journal of Biochemistry 120*(*1*), 1-13.

Tullius, M. V., Munson, R. S., Wang, J. and Gibson, B. W. (1996). Purification, cloning, and expression of a cytidine 5'-monophosphate N-acetylneuraminic acid synthetase from *Haemophilus ducreyi*. *J. Biol. Chem. 271*(*26*), 15373-15380.

Tullius, M. V., Vann, W. F. and Gibson, B. W. (1999). Covalent modification of Lys19 in the CTP binding site of cytidine 5'-monophosphate N-acetylneuraminic acid synthetase. *Protein Sci. 8(3)*, 666-675.

Van Alphen, L., Geelen-van den Broek, L., Blaas, L., Van Ham, M. and Dankert, J. (1991). Blocking of fimbria-mediated adherence of *Haemophilus influenzae* by sialyl gangliosides. *Infect. Immun. 59(12)*, 4473-4477.

Van Ham, S. M., Van Alphen, L., Mooi, F. R. and Van Putten, J. P. (1995). Contribution of the major and minor subunits to fimbria-mediated adherence of *Haemophilus influenzae* to human epithelial cells and erythrocytes. *Infect. Immun. 63(12)*, 4883-4889.

Van Schilfgaarde, M., Van Alphen, L., Eijk, P., Everts, V. and Dankert, J. (1995). Paracytosis of *Haemophilus influenzae* through cell layers of NCI-H292 lung epithelial cells. *Infect. Immun. 63 12(4729-4737)*

Vann, W. F., Silver, R. P., Abeijon, C., Chang, K., W., A., Sutton, A., Finn, C. W., Linder, W. and Kotsatos, M. (1987). Purification, properties, and genetic location of *E. coli* cytidine 5'-monophosphate N-acetylneuraminic acid synthetase. *J. Biol. Chem. 262(36)*, 17556-17562.

Vann, W. F., Tavarez, J. J., Crowley, J., Vimr, E. and Silver, R. P. (1997). Purification and characterization of the *E. coil* K1 neuB gene product N-acetylneuraminic acid synthetase. *Glycobiology 7(5)*, 697-701.

Vann, W. F., Zapata, G., Roberts, I. S., Boulnois, G. and Silver, R. P. (1993). Structure and function of enzymes in sialic acid metabolism in polysialic acid producing bacteria. Polysialic Acid: From Microbes to Man. Roth, J., Rutishauser, U., Troy, F. A. Basel, Birkhäuser Verlag: 125-136.

Vestweber, D. and Blanks, J. E. (1999). Mechanisms that regulate the function of the selectins and their ligands. *Physiological Reviews 79(1)*, 181-213.

Vimr, E. R. and Troy, F. A. (1985). Identification of an inducible catabolic system for sialic acids (nan) in *E. coli*. *J. Bacteriol. 164(2)*, 845-853.

Vita, C., Dalzoppo, D. and Fontana, A. (1985). Limited proteolysis of thermolysin by subtilisin: isolation and characterization of a partially active enzyme derivative. *Biochemistry 24(7)*, 1798-1806.

Wakarchuk, W. W., Gilbert, M., Martin, A., Wu, Y., Brisson, J. R., Thibault, P. and Richards, J. C. (1998). Structure of an alpha-2,6-sialylated lipooligosaccharide from *Neisseria meningitidis* immunotype L1. *Eur. J. Biochem. 254(3)*, 626-633.

Wang, F., Blanchard, J. S. and Tang, X. J. (1997). Hydrogen exchange/electrospray ionization mass spectrometry studies of substrate and inhibitor binding and conformational changes of *E. coli* dihydrodipicolinate reductase. *Biochemistry 36(13)*, 3755-3759.

Wang, F., Li, W., Emmett, M. R., Hendrickson, C. L., Marshall, A. G., Zhang, Y. L., Wu, L. and Zhang, Z. Y. (1998). Conformational and dynamic changes of Yersinia protein tyrosine phosphatase induced by ligand binding and active site mutation and revealed by H/D exchange and electrospray ionization Fourier transform ion cyclotron resonance mass spectrometry. *Biochemistry 37(44)*, 15289-15299.

Wang, F., Scapin, G., Blanchard, J. S. and Angeletti, R. H. (1998). Substrate binding and conformational changes of *Clostridium glutamicum* diaminopimelate dehydrogenase revealed by hydrogen/deuterium exchange and electrospray mass spectrometry. *Protein Sci. 7(2)*, 293-299.

Warren, L. and Blacklow, R. S. (1962). The biosynthesis of cytidine 5'-monophospho-N-acetylneuraminic acid by an enzyme from *Neisseria meningitidis. J. Biol. Chem. 237(11)*, 3527-3534.

Wasserheit, J. N. (1992). Epidemiological synergy. Interrelationships between human immunodeficiency virus infection and other sexually transmitted diseases. *Sex Transm. Dis. 19(2)*, 61-77.

Weber, A., Harris, K., Lohrke, S., Forney, L. and Smith, A. L. (1991). Inability to express fimbriae results in impaired ability of *Haemophilus influenzae* b to colonize the nasopharynx. *Infect. Immun. 59(12)*, 4724-4728.

Weiser, J. N. and Gotschlich, E. C. (1991). Outer membrane protein A (OmpA) contributes to serum resistance and pathogenicity of *E. coli* K-1. *Infect. Immun. 59(7)*, 2252-2258.

Weiser, J. N., Love, J. M. and Moxon, E. R. (1989). The molecular mechanism of phase variation of *H. influenzae* lipopolysaccharide. *Cell 59(4)*, 657-665.

Weiser, J. N., Maskell, D. J., Butler, P. D., Lindberg, A. A. and Moxon, E. R. (1990). Characterization of repetitive sequences controlling phase variation of *Haemophilus influenzae* lipopolysaccharide. *J. Bacteriol. 172(6)*, 3304-3309.

Weiser, J. N. and Pan, N. (1998). Adaptation of *Haemophilus influenzae* to acquired and innate humoral immunity based on phase variation of lipopolysaccharide. *Mol. Microbiol. 30(4)*, 767-775.

Weiser, J. N., Pan, N., McGowan, K. L., Musher, D., Martin, A. and Richards, J. (1998). Phosphorylcholine on the lipopolysaccharide of *Haemophilus influenzae* contributes to persistence in the respiratory tract and sensitivity to serum killing mediated by C-reactive protein. *J. Exp. Med. 187(4)*, 631-640.

Weiser, J. N., Shchepetov, M. and Chong, S. T. (1997). Decoration of lipopolysaccharide with phosphorylcholine: a phase-variable characteristic of *Haemophilus influenzae. Infect. Immun. 65(3)*, 943-950.

Weisgerber, C., Hansen, A. and Frosch, M. (1991). Complete nucleotide and deduced protein sequence of CMP-NeuAc: poly-alpha-2,8 sialosyl sialyltransferase of *E. coli* K1. *Glycobiology 1(4)*, 357-365.

Weller, P. F., Smith, A. L., Anderson, P. and Smith, D. H. (1977). The role of encapsulation and host age in the clearance of *Haemophilus influenzae* bacteremia. *J. Infect. Dis. 135(1)*, 34-41.

Westphal, O., Jann, K. and Himmelspach, K. (1983). Chemistry and immunochemistry of bacterial lipopolysaccharides as cell wall antigens and endotoxins. *Progress in Allerg 33*, 9-39.

Wood, G. E., Dutro, S. M. and Totten, P. A. (1999). Target cell range of *Haemophilus ducreyi* hemolysin and its involvement in invasion of human epithelial cells. *Infect. Immun. 67(8)*, 3740-3749.

Woodward, C., Simon, I. and Tuchsen, E. (1982). Hydrogen exchange and the dynamic structure of proteins. *Molecular and Cellular Biochemistry 48(3)*, 135-160.

Wyss, M., James, P., Schlegel, J. and Wallimann, T. (1993). Limited proteolysis of creatine kinase. Implications for three-dimensional structure and for conformational substrates. *Biochemistry 32(40)*, 10727-10735.

Yamasaki, R., Bacon, B. E., Nasholds, W., Schneider, H. and Griffiss, J. M. (1991). Structural determination of oligosaccharides derived from lipooligosaccharide of *Neisseria gonorrhoeae* F62 by chemical, enzymatic, and two-dimensional NMR methods. *Biochemistry 30(43)*, 10566-10575.

Yamasaki, R., Griffiss, J. M., Quinn, K. P. and Mandrell, R. E. (1993). Neuraminic acid is alpha 2-->3 linked in the lipooligosaccharide of *Neisseria meningitidis* serogroup B strain 6275. *J. Bacteriol. 175(14)*, 4565-4568.

Young, R. S., Fortney, K., Haley, J. C., Hood, A. F., Campagnari, A., Wang, J., Bozue, J. A., Munson, R. S. J. and Spinola, S. M. (1999). Expression of sialylated or paragloboside-like lipooligosaccharides are not required for pustule formation by *Haemophilus ducreyi* in human volunteers. *Infect. Immun. 67(12)*, 6335-6340.

Zhang, Z. and Smith, D. (1993). Determination of amide hydrogen exchange by mass spectrometry: a new tool for protein structure elucidation. *Protein Sci. 2(4)*, 522-531.

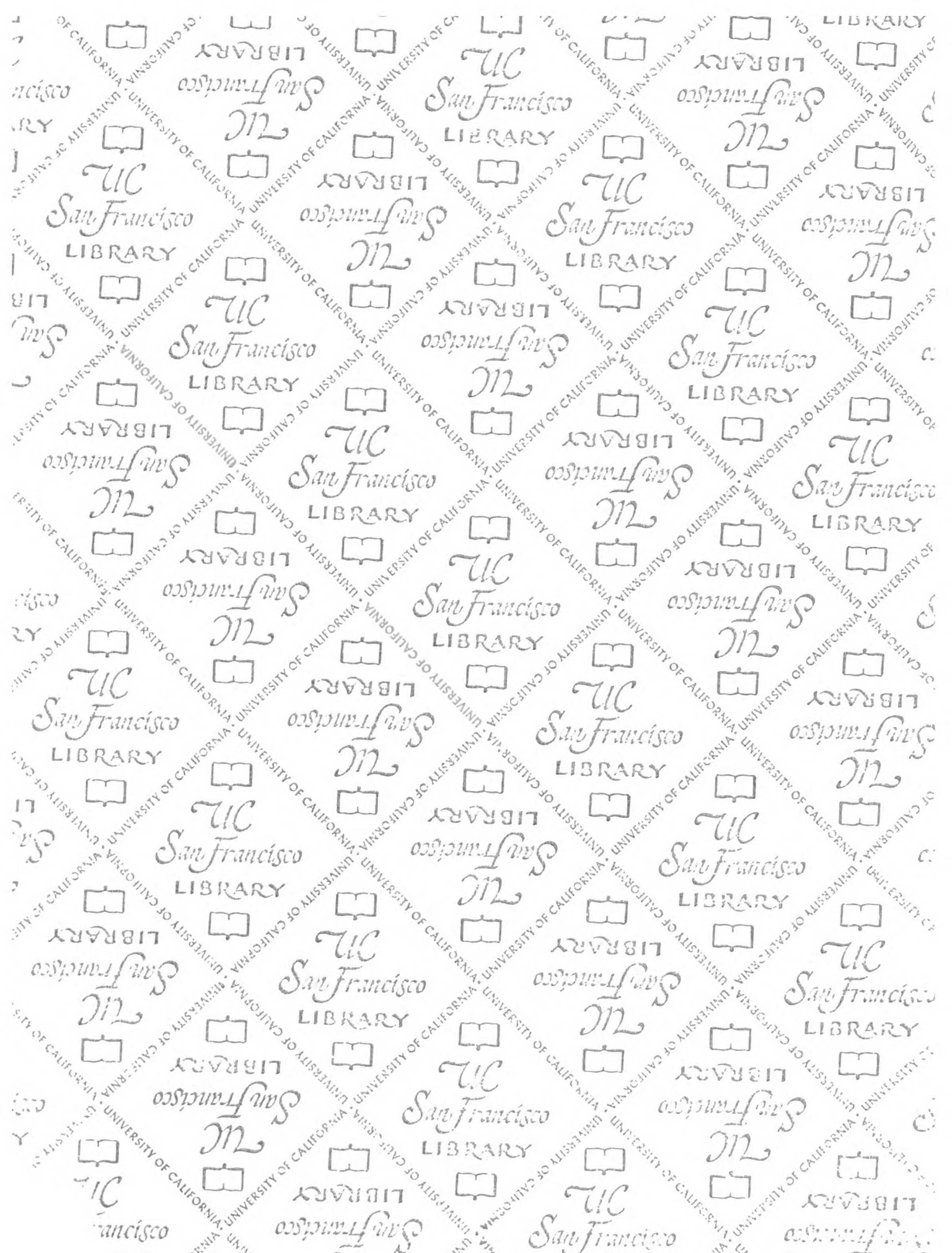
UC
San Francisco
LIBRARY
UNIVERSITY OF CALIFORNIA · UNIVERSITY OF CALIFORNIA